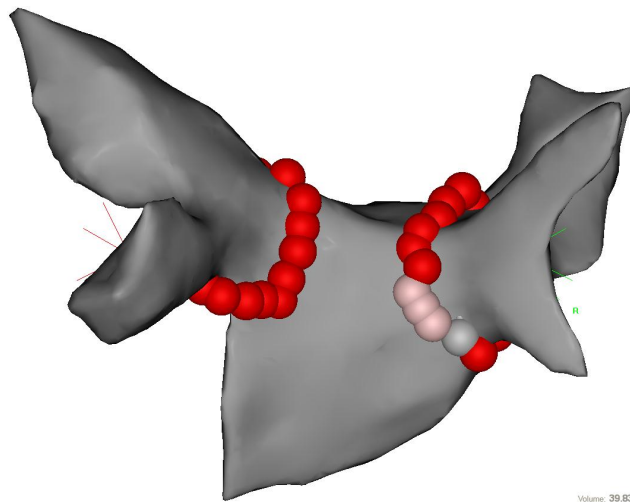


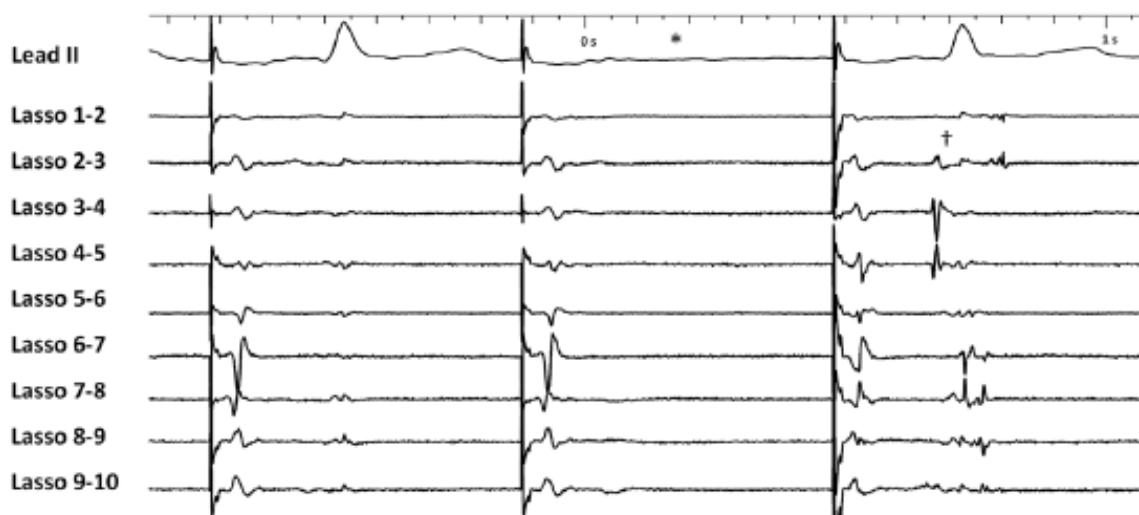
# International PhD program in Cardiovascular Pathophysiology and Therapeutics



## New perspectives in catheter ablation for atrial fibrillation Towards a better treatment to reach better outcomes



Volume: 39.83 LAO: 190°



PhD Thesis  
Teresa Strisciuglio MD



UNIVERSITÀ DEGLI STUDI DI NAPOLI  
**FEDERICO II**



**New perspectives in catheter ablation for atrial  
fibrillation**  
Towards a better treatment to reach better outcomes

PhD Thesis

Teresa Strisciuglio MD

21/09/1987 Naples (Italy)

Naples, XX/01/2021  
University Federico II of Naples, Faculty of Medicine,  
Via Pansini n. 5, 80131 Naples, Italy

*"Do not be like the cat who wanted a fish but was afraid to get his paws wet."*

William Shakespeare

# Contents

<b>Chapter 1</b>	General introduction	pag.7
	Aims and outline of the thesis	pag.14
<b>Chapter 2</b>	Methods	pag.16

## Part I: Reproducibility of the outcomes and generalizability of the standardized workflow

<b>Chapter 3</b>	The industrialization of ablation: a highly standardized and reproducible workflow for radiofrequency ablation of atrial fibrillation <i>Published in JACC Clin Electrophysiol. 2019 Mar;5(3):295-305.</i>	pag. 17
<b>Chapter 4</b>	Reproducibility of pulmonary vein isolation guided by the ablation index: 1-year outcome of the AIR registry <i>Published in J Cardiovasc Electrophysiol. 2020 Jul;31(7):1694-1701.</i>	pag.27

## Part II: The ablation outcomes: the effects on the burden and PVI durability

<b>Chapter 5</b>	Long-term impact of catheter ablation on arrhythmia burden in low-risk patients with paroxysmal atrial fibrillation: The CLOSE to CURE study <i>Published in Heart Rhythm. 2020 Apr; 17(4):535-543.</i>	pag.36
<b>Chapter 6</b>	Paroxysmal atrial fibrillation with high vs. low arrhythmia burden: atrial remodelling and ablation outcome <i>Published in Europace. 2020 Aug 1; 22(8):1189-1196.</i>	pag.44
<b>Chapter 7</b>	Pulmonary Vein Reconnection No Longer Occurs in the Majority of Patients After a	pag.56



Single Pulmonary Vein Isolation  
Procedure  
*Published in JACC Clin Electrophysiol. 2019  
Mar;5(3):295-305.*

Part III: What can we do better? Can we further improve the stability and/or increase the RF power?

- Chapter 8** Evaluation of a simple technique aiming at optimizing point-by-point isolation of the left pulmonary veins: a randomized study  
*Published in Europace. 2019 Aug 1;21(8):1185-1192.* pag.70
- Chapter 9** Evaluation of higher power delivery during RF pulmonary vein isolation using optimized and contiguous lesions  
*Published in J Cardiovasc Electrophysiol. 2020 May;31(5):1091-1098.* pag.78
- Chapter 10** Prospective Randomized Evaluation of High Power during CLOSE-guided Pulmonary Vein Isolation: The POWER-AF study  
*Under peer review* pag .88

Part IV: What about the safety?

- Chapter 11** Endoscopic evaluation of the esophagus after catheter ablation of atrial fibrillation using contiguous and optimized radiofrequency applications  
*Published in Heart Rhythm. 2019 Jul;16(7):1013-1020.* pag.91

Part V: How can we improve outcomes of ablation for persistent AF and atrial tachycardias? New technologies on the way

- Chapter 12** Identification of repetitive atrial activation patterns in persistent atrial fibrillation by direct contact high-density electrogram mapping pag.99

*Published in J Cardiovasc Electrophysiol. 2019  
Dec;30(12):2704-2712.*

<b>Chapter 13</b>	Activation Mapping With Integration of Vector and Velocity Information Improves the Ability to Identify the Mechanism and Location of Complex Scar-Related Atrial Tachycardias <i>Published in Circ Arrhythm Electrophysiol. 2018 Aug;11(8):e006536.</i>	pag.109
<b>Chapter 14</b>	Prospective evaluation of entrainment mapping as an adjunct to new-generation high-density activation mapping systems of left atrial tachycardias <i>Published in Heart Rhythm. 2020 Feb; 17(2):211-219.</i>	pag.130
<b>Chapter 15</b>	Directed Networks as a Novel Way to Describe and Analyze Cardiac Excitation: Directed Graph Mapping <i>Published in Front Physiol. 2019 Sep 10; 10:1138.</i>	pag.145
<b>Chapter 16</b>	Evaluation of Directed Graph-mapping in complex Atrial Tachycardias <i>Under peer review</i>	pag.159
<u>Part VI</u> General Discussion		pag.162
<u>Part VII</u> Conclusion		pag.181
List of abbreviations		pag.182
Bibliography		pag. 183
Curriculum vitae		pag.191
List of all publications		pag.195

# Chapter 1

## INTRODUCTION

Atrial fibrillation (AF) is the most common arrhythmia affecting millions of people worldwide and its incidence increases due to the ageing of population, representing a public health issue with significant economic consequences.

Catheter ablation of pulmonary veins (PV) represents a first line therapy, being recommended for symptomatic AF and for AF resistant to antiarrhythmic drugs [1]. Most triggers for paroxysmal atrial fibrillation come from the pulmonary veins, so the ablation involves creating circumferential lesions around the veins to electrically isolate them from the rest of the left atrium [2]. Pulmonary vein isolation (PVI) was demonstrated to be more effective than antiarrhythmic drugs especially for paroxysmal AF, whereas it is associated with less favourable outcomes for the persistent forms [3]. This difference in ablation efficiency in the persistent AF seems to be related to the presence, in addition to the PV trigger, of an atrial substrate that is responsible for the arrhythmia perpetuation.

Therefore, in patients with persistent AF, beyond the elimination of the PV trigger, more extensive ablation approaches may be preferred: linear ablations, ablation of complex fractionated atrial electrograms (CFAE) and the ablation of foci triggering AF including the coronary sinus, the left atrial appendage (LAA), the superior vena cava, the crista terminalis, and the ligament of Marshall [4]. However, so far no superiority of one approach over the other has been proved and their results are still far from enough [5]. Furthermore, another noteworthy aspect is that, especially when the ablation has created wide scar zones, the arrhythmia may recur as a complex atrial tachycardia that can be even more symptomatic than AF and may be difficult to ablate [6].

### *Catheter ablation: where are we now?*

Different sources of energy can be used to reach PVI [7], however so far the most used are the radiofrequency and the cryotherapy. The biophysics of lesion creation with these energies has been extensively studied and both have been demonstrated to be very effective but also safe during the PVI procedure [8]. The main difference between them is the energy and the mode of application: on one hand the radiofrequency ablation consists of a point-by-point lesion formation around the PV ostia (circumferential applications) by delivering energy from a linear catheter, whereas on the other hand the cryoablation is also defined “single-shot” ablation as the cryoenergy is delivered through a balloon that creates a circular lesion at the PV-left atrium junction with a single application.

To date, there are no clear evidences of the superiority of one technique over the other, as clearly demonstrated by the randomized trial FIRE and ICE [8]. The trial showed that irrespectively from the energy used the freedom from AF at 1 year was about 65%.

Nonetheless the study was conducted already 4 years ago and since then many improvements have been made in the ablation catheters and in the techniques.

For instance, the introduction of contact-force (CF) sensing catheters has improved ablation outcomes compared to non CF catheters [9].

During RF ablation only limited use of fluoroscopy is required, because catheter guidance is achieved with the use of an electroanatomical mapping system, however there is no certainty of the contact between the tip of the catheter and the atrial tissue, and thus no certainty of the effective heating needed to create the lesion. Before the advent of these CF sensors, the electrophysiologists had to rely on indirect signs of tip-tissue contact, such as the fall in local

impedance or the decrease in local EGM amplitude [10-11], that are poorly informative and not accurate [12].

In the FIRE and ICE only 2/3 of patients in the RF group were ablated with CF catheters, and this could explain the high rate of AF recurrence [13].

*PV reconnection is the issue: how to improve lesion creation?*

The electrical reconnection between the PV and the atrium is the major determinant of early and late AF recurrence, and the cause is represented by sub-optimal lesion creation [14-15].

The recovery of atrial oedema may reveal an area of irreversible damage, which is not wide and deep enough to dissociate the PVs from the rest of the atrium.

Creation of durable ablation lesions during PVI is thus of critical importance to ensure the short and long term success of the ablation procedure.

In the absence of real-time assessment of lesion development and transmuralty, surrogate measures of lesion quality are commonly utilized. The fall in local impedance during ablation, which has been shown to relate to lesion size, is widely used as a marker of the direct effect of ablation on cardiac tissue [10]. As for the RF ablation, with the advent of CF catheters the Force–Time Integral (FTI), which multiplies contact force by radiofrequency application duration, has been used as an index of creation of effective lesions and has been shown to be predictive of PVI segment reconnection at repeat electrophysiology study [11]. Prospective use of a minimum FTI target during each ablation application improved rates of durable PV isolation, but still the percentage of patients with reconnected veins was high [16-18]. Most probably this is because this parameter does not take into account the role of power delivery, and is derived from a simple multiplication of contact force by time, whereas it is likely that these factors along with power provide differing contributions to lesion formation.

Furthermore, using a single target FTI value for all segments of the circumferential PVI circle, assumes that tissue thickness, and therefore the ablation depth required, is the same for all areas of the left atrium. However, it is known from anatomical studies that tissue thickness varies considerably between different left atrial regions (the anterior wall is thicker than the posterior one) [19]. To overcome this issue a novel marker of lesion quality was needed. The ablation index (AI), which integrates CF, power, and ablation time in a logarithmic formula, has been shown to be predictive of lesion trans-murality in animal studies and therefore is now widely adopted as surrogate of lesion quality [20-21].

$$\text{Ablation Index} = \left( K * \int_0^t \text{CF}^a(\tau) P^b(\tau) d\tau \right)^c$$

*The CLOSE recipe and its “ingredients”*

In the era of CF catheters, the determinants of PV electrical reconnection have been investigated in the study by El Haddad [22], where forty-nine patients were ablated with a CF catheter and a mean CF of 10 grams, with a power of 25W for 30 sec at the posterior wall and 35 w for 60 sec at the anterior wall. For each delivered energy application, displayed by the electro-anatomical system as a tag, different parameters were analysed: power, time, delta impedance, force, FTI and furthermore the AI and the inter-tag distance (ITD) were calculated. At the sites of early (after adenosine administration) and late (at repeat ablation) reconnections the investigators found that the AI was lower and the ITD was higher compared to non-reconnected sites. In particular, the cut-off values that best predicted the absence of reconnection were 550-400 (anterior-posterior wall) for the AI and 6 mm for the ITD.

Therefore this study highlighted for the first time the weakest link in the ablation chain: the transmuralty of the lesions (AI) and the contiguity of the ablation line (ITD). Since then, a new ablation protocol, the so-called “CLOSE” protocol, has been developed, consisting of delivering RF energy at each site with a minimum AI of 400 at posterior wall and 550 at the anterior wall, and a maximum ITD of 6 mm, creating a “nephroid” shape encirclement of the left and right pulmonary veins. The CLOSE protocol in the setting of paroxysmal AF enables to reach excellent procedural (adenosine-proof isolation 98%) and 1-year outcomes (single-procedure freedom from any atrial tachy-arrhythmia 91%) [23]. The results of the CLOSE-guided ablation even outperform those of a conventional CF-guided ablation [24].

## References

1. Hindricks G, Potpara T, Dagres N et al. 2020 ESC Guidelines for the diagnosis and management of atrial fibrillation developed in collaboration with the European Association of Cardio-Thoracic Surgery (EACTS): The Task Force for the diagnosis and management of atrial fibrillation of the European Society of Cardiology (ESC) Developed with the special contribution of the European Heart Rhythm Association (EHRA) of the ESC
2. Haïssaguerre M, Jaïs P, Shah DC et al. Spontaneous initiation of atrial fibrillation by ectopic beats originating in the pulmonary veins. *N Engl J Med.* 1998 Sep 3;339(10):659-66.
3. Brooks AG, Stiles MK, Laborderie J, et al. Outcomes of long-standing persistent atrial fibrillation ablation: a systematic review. *Heart Rhythm* 2010; 7: 835-46.
4. Romero J, Gianni C, Di Biase L et al. Catheter Ablation for Long-Standing Persistent Atrial Fibrillation. *Methodist Debaquey Cardiovasc J.* 2015 Apr-Jun; 11(2): 87–93.
5. Verma A, Jiang CY, Betts TR, et al. Approaches to catheter ablation for persistent atrial fibrillation *N Engl J Med.* 2015 May 7;372(19):1812-22.
6. Knecht S, Veenhuyzen G, O'Neill MD et al. Atrial tachycardias encountered in the context of catheter ablation for atrial fibrillation part ii: mapping and ablation *Pacing Clin Electrophysiol.* 2009 Apr;32(4):528-38.
7. Rottner L, Bellmann B, Lin T et al. Catheter Ablation of Atrial Fibrillation: State of the Art and Future Perspectives *Cardiol Ther* (2020) 9:45–58
8. Kuck KH, Brugada J, Fürnkranz A et al. Cryoballoon or Radiofrequency Ablation for Paroxysmal Atrial Fibrillation *N Engl J Med.* 2016 Jun 9;374(23):2235-45
9. Afzal MR, Chatta J, Samanta A. et al. Use of contact force sensing technology during radiofrequency ablation reduces recurrence of atrial fibrillation: A systematic review and meta-analysis. *Heart Rhythm.* 2015;12(9): 1990–6.
10. Reichlin T, Lane C, Nagashima K, Nof E, Chopra N, Ng J et al. Feasibility, efficacy, and safety of radiofrequency ablation of atrial fibrillation guided by monitoring of the initial impedance decrease as a surrogate of catheter contact. *J Cardiovasc Electrophysiol* 2015;26:390–6.
11. le Polain de Waroux JB, Weerasooriya R, Anvardeen K, Barbraud C, Marchandise S, De Meester C et al. Low contact force and force-time integral predict early recovery and dormant conduction revealed by adenosine after pulmonary vein isolation. *Europace* 2015;17:877–83.
12. Nakagawa H, Kautzner J, Natale A, et al. Locations of high contact force during left atrial mapping in atrial fibrillation patients: electrogram amplitude and impedance are poor predictors of electrode-tissue contact force for ablation of atrial fibrillation. *Circ Arrhythm Electrophysiol.* 2013 Aug;6(4):746-53.



13. Kuck KH, Albenque JP, Chun KJ et al. Repeat Ablation for Atrial Fibrillation Recurrence Post Cryoballoon or Radiofrequency Ablation in the FIRE AND ICE Trial *Circ Arrhythm Electrophysiol.* 2019 May 22;12(6):e007247
14. Nery PB, Belliveau D, Nair GM, et al. Relationship between pulmonary vein reconnection and atrial fibrillation recurrence: a systematic review and meta-analysis. *J Am Coll Cardiol EP* 2016;2: 474–83.
15. Nanthakumar K, Plumb VJ, Epstein AE, Veenhuyzen GD, Link D, Kay GN. Resumption of electrical conduction in previously isolated pulmonary veins: rationale for a different strategy? *Circulation* 2004;109:1226–9.
16. Ouyang F, Antz M, Ernst S, et al. Recovered pulmonary vein conduction as a dominant factor for recurrent atrial tachyarrhythmias after complete circular isolation of the pulmonary veins: lessons from double Lasso technique. *Circulation* 2005;111:127–35.
17. Neuzil P, Reddy VY, Kautzner J, Petru J, Wichterle D, Shah D et al. Electrical reconnection after pulmonary vein isolation is contingent on contact force during initial treatment: results from the EFFICAS I study. *Circ Arrhythm Electrophysiol* 2013;6: 327–33.
18. Kautzner J, Neuzil P, Lambert H, Peichl P, Petru J, Cihak R et al. EFFICAS II: optimization of catheter contact force improves outcome of pulmonary vein isolation for paroxysmal atrial fibrillation. *Europace* 2015;17:1229–35.
19. Ho SY, Cabrera JA, Sanchez-Quintana D. Left atrial anatomy revisited. *Circ Arrhythm Electrophysiol* 2012;5:220–8.
20. Nakagawa H, Ikeda A, Govari A, et al. Prospective study to test the ability to create RF lesions at predicted depths of 3, 5, 7 and 9 mm using a new formula incorporating contact force, radiofrequency power and application time (Force-Power-Time Index) in the beating canine heart. *Heart Rhythm* 2013;10:S481 (abstr).
21. Das M, Loveday JJ, Wynn GJ et al. Ablation index, a novel marker of ablation lesion quality: prediction of pulmonary vein reconnection at repeat electrophysiology study and regional differences in target values. *Europace* 2017 May 1;19(5):775-783.
22. El Haddad M, Taghji P, Philips T et al. Determinants of Acute and Late Pulmonary Vein Reconnection in Contact Force-Guided Pulmonary Vein Isolation: Identifying the Weakest Link in the Ablation Chain *Circ Arrhythm Electrophysiol.* 2017 Apr;10(4):e004867.
23. Taghji P, El Haddad M, Philips T, et al. Evaluation of a strategy aiming to enclose the pulmonary veins with contiguous and optimized radiofrequency lesions in paroxysmal atrial fibrillation: a pilot study. *J Am Coll Cardiol EP* 2018;4:99–108.
24. Philips T, Taghji P, El Haddad M, et al. Improving procedural and one-year outcome after contact force-guided pulmonary vein isolation: the role of interlesion distance, ablation index, and contact force variability in the 'CLOSE'-protocol. *Europace* 2018;20:f419–27.

## AIMS AND OUTLINES OF THE THESIS

The overall aim of the studies presented in this thesis is to elucidate whether there is still room for improvement in the field of catheter ablation for AF either paroxysmal and persistent, and the following chapters will guide the reader in a virtual path that addresses this issue.

*Chapter 3 and 4* answer to the question whether the excellent outcomes for paroxysmal AF ablation obtained with the CLOSE protocol, that have been reported in many single centre experiences, are reproducible with larger numbers and also in multicentre studies.

*Chapters 5 and 6* are focused on the arrhythmia burden reduction, that is an important endpoint of an efficient ablation procedure

*Chapter 7* evaluates the PVI durability at repeat ablation for recurrence of AF

*Chapter 8, 9 and 10* drive the reader's attention to some technical aspects of the CLOSE guided ablation procedure that could be ameliorated to improve its efficacy. In particular, they a) elucidate how to reduce the instability of the ablation catheter, responsible of dislocations and insufficient lesions formation and thus of the lengthening of the ablation time, b) investigate the effects of increasing the RF power

*Chapter 11* has the purpose of investigating the safety of the CLOSE protocol. Beyond being effective the optimal ablation strategy aims to be also safe for the patients. One of the most dangerous complications of the RF ablation is the damage to the esophagus, and in particular

the atrio-esophageal fistula. The study hereby described evaluated the effects of this ablation protocol on the esophagus. This is the last chapter focused on ablation of paroxysmal AF.

*Chapter 12* is a turning point with the main topic being represented by the persistent AF. This chapter investigated a new mapping technology (Pentaray+CARTOFINDER, Biosense Inc.) and the related ablation outcomes

*Chapters 13, 14, 15 and 16* are built around the atrial tachycardias (AT) that occur frequently after extensive ablation for persistent AF. In particular, they describe the newest algorithms developed for the identification of their mechanisms and whether these novelties are associated with better ablation outcomes

## Chapter 2

### METHODOLOGY

The study presented in chapters 3 enrolled patients of the Department of Cardiology of the Heart Centre in Aalst, Belgium. Patients in chapter 4 were recruited from a multicentre registry involving 25 European centres, with the majority of them being in Italy. The data analysis was performed in the Clinica Montevergine of Mercogliano, Avellino.

The patients enrolled in chapters from 5 to 16 were all recruited at the Department of Cardiology of the AZ Sint-Jan in Bruges, Belgium.

All studies analysed the procedural and long-term outcomes of the ablations for paroxysmal/persistent AF or for AT. All the patients recruited signed the informed consent.

These studies were approved by the local ethical boards.


Detailed methodology of each study is specified separately within each chapter.

## Chapter 3

Journal of Interventional Cardiac Electrophysiology  
<https://doi.org/10.1007/s10840-019-00622-y>

---

### **The industrialization of ablation: a highly standardized and reproducible workflow for radiofrequency ablation of atrial fibrillation**

Tom De Potter<sup>1</sup>  • Tina D. Hunter<sup>2</sup> • Lee Ming Boo<sup>3</sup> • Sofia Chatzikyriakou<sup>1,4</sup> • Teresa Strisciuglio<sup>1,5</sup> • Etel Silva<sup>1</sup> • Peter Geelen<sup>1</sup>

## **Introduction**

Real-time contact force (CF)-sensing catheters have been shown to improve ablation outcomes when compared to non-CF technologies in atrial fibrillation (AF) ablation. Ablation Index (AI), which integrates CF, power, and ablation time in a logarithmic formula, was shown to be an independent predictor of pulmonary vein (PV) reconnection. Further, a recent study in 100 patients showed that a standardized AI-guided workflow improved 1-year outcomes compared to non-standardized CF ablation. Use of these combined technologies allows for standardization of PV ablation workflow, leading to increased predictability. The objective of this study was to assess whether the use of a highly standardized workflow, combining CF-sensing technology with AI and visualization of lesion durability, positively impacts the procedural efficiency and effectiveness of radiofrequency (RF) ablation in large real-world paroxysmal AF (PAF) and persistent AF (PsAF) populations. This study reports on improvements in the levels and variability of procedural efficiency measures—procedural duration and fluoroscopy use in particular— as well as freedom from atrial arrhythmia recurrence rates through the 12-month visit.

## **Methods**

Consecutive AF ablations from 2014 to 2015 at a high-volume site in Belgium were included. All procedures used a 3D anatomic model generated from real-time 3D rotational angiography (3DRA) integrated automatically in the mapping system, with no additional catheter-based geometry reconstruction (figure 1), followed by radiofrequency encircling of the pulmonary veins (25 W posterior wall, 35 W anterior wall) with a THERMOCOOL SMARTTOUCH® Catheter guided by CARTO VISITAG™ Module (2.5 mm/5 s stability, 50% > 7

g) and ablation index (targets: 550 anterior wall, 400 posterior wall). Efficiency endpoints were procedure time, fluoroscopy time, and radiation dose. The primary effectiveness endpoint was freedom from atrial arrhythmia recurrence.

Follow-up visits typically occurred at 3, 6, and 12 months post-ablation, at which time patients were monitored for atrial arrhythmia recurrence via questionnaire and ECG recording, with a 24-h Holter monitor at the end of follow-up. Atrial arrhythmia recurrence included AF, atrial tachycardia, or atrial flutter. Arrhythmia events occurring in the first month after ablation were blanked from the analysis and no repeat ablations were performed within the first 3 months. Additional unscheduled Holter monitoring was performed in cases of undocumented / unexplained symptoms.

## **Results**

A total of 787 patients underwent catheter ablation for AF (605 PAF, 182 PsAF), and approximately half of these procedures were re-ablations (PAF: 46.8%, PsAF: 47.3%). There was a higher percentage of males in the PsAF group than in the PAF group (76.4% vs. 65.6%), and the PsAF patients were slightly older, at  $65.4 \pm 9.8$  years vs.  $62.7 \pm 11.1$  years (Table 1). Hypertension was the most prevalent comorbidity among both groups (PAF: 46.6%, PsAF: 52.8%) followed by mitral insufficiency (PAF: 31.1%, PsAF: 42.9%), which was primarily grade 1. Baseline patient characteristics are summarized in Table 1.

### *Procedural detail*

Procedural efficiency measures are shown in Table 2. Mean procedure times, which included 20 min of waiting time post- PVI, were short (PAF:  $96.1 \pm 26.2$  min; PsAF:  $109.2 \pm 35.6$  min). The majority of procedures were performed in 120 min or less (PAF: 90.6%; PsAF: 81.3%).

Mean fluoroscopy times were minimal in both the PAF ( $6.1 \pm 3.8$  min) and PsAF groups ( $6.9 \pm 4.7$  min), with corresponding radiation doses of  $5.9 \pm 3.4$  Gy\*cm<sup>2</sup> and  $7.4 \pm 4.9$  Gy\*cm<sup>2</sup>, respectively. Acute PVI was achieved in all patients.

Though the collection of detailed components of the total procedure time was not performed as a part of this study for all patients, a separate study collected this detail on a subset of 20 patients from the PAF cohort. A summary of the times for each step through the conclusion of the initial PV isolation is summarized in Table 3 as a point of reference for the reader. Serious procedure-related complications were infrequent, occurring in only 1.8% (8/435) of the patients with ablations in 2015, after the structured reporting of these events began (Table 2). These consisted of seven pericardial effusion (four requiring pericardiocentesis) and one bleeding complication. There were no stroke or cardiac tamponade events, and no deaths.

### *Effectiveness*

Rates of freedom from atrial arrhythmia recurrence through the latest follow-up visit were significantly higher for PAF patients than for PsAF patients (OR: 2.0, 95% CI: 1.4–2.9,  $p = 0.0003$ , Table 4). Adjusted rate estimates were  $81.0 \pm 1.6\%$  for PAF vs.  $67.9 \pm 3.5\%$  for PsAF (Fig. 2). Patients having de novo ablations had higher rates of freedom from recurrence versus those with prior ablations (OR: 1.9, 95% CI: 1.3–2.7  $p = 0.0004$ ,  $80.5 \pm 2.2\%$  vs.  $68.6 \pm 2.7\%$ ). The only additional statistically significant predictor of freedom from recurrence was lower age ( $p = 0.0410$ ), which was standardized to 65 years for calculating the adjusted mean recurrence rates. In the subset of 418 patients (322 PAF, 96 PsAF) with de novo ablations, first procedure freedom from recurrence rate estimates were higher in both cohorts than those seen in the respective full population cohort (PAF:  $85.7 \pm 2.0\%$ , PsAF:  $74.0 \pm 4.5\%$ , Fig. 2).



Re-ablation rates were 9.6% and 9.9% over mean followup times of  $438 \pm 201$  days and  $430 \pm 190$  days in the PAF and PsAF cohorts, respectively. AAD utilization was ongoing in 34.7% and 40.1% of the PAF and PsAF cohorts as of their last follow-up visit.

## **Conclusion**

A highly standardized workflow for AF ablation greatly reduced procedural variability by using 3D rotational angiography and image integration for the mapping phase, and Visitag- AI guided ablation enabled by the ST CF-sensing catheter for the ablation phase. This workflow led to predictably low procedure and fluoroscopy times, with good clinical outcomes as seen in the high rates of freedom from atrial arrhythmia recurrence in both PAF and PsAF populations.

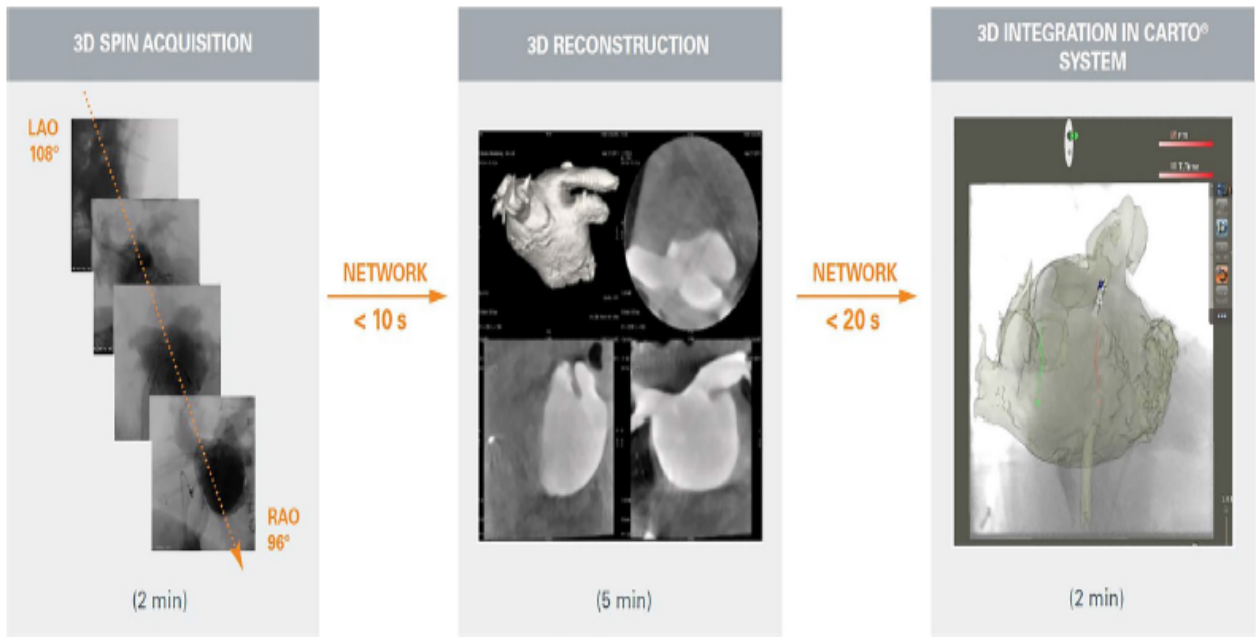


**Fig. 1** Ablation workflow schematic. \*Segmentation could also be done with CARTO® “image integration” tool. In that case, the output of the 3D reconstruction can be directly retrieved from CARTO®

**Fig. 2** Adjusted mean rates of freedom from atrial arrhythmia recurrence. Error bars represent the standard error of the adjusted mean. Rates were calculated at 65 years of age. PAF: paroxysmal atrial fibrillation, PsAF: persistent atrial fibrillation

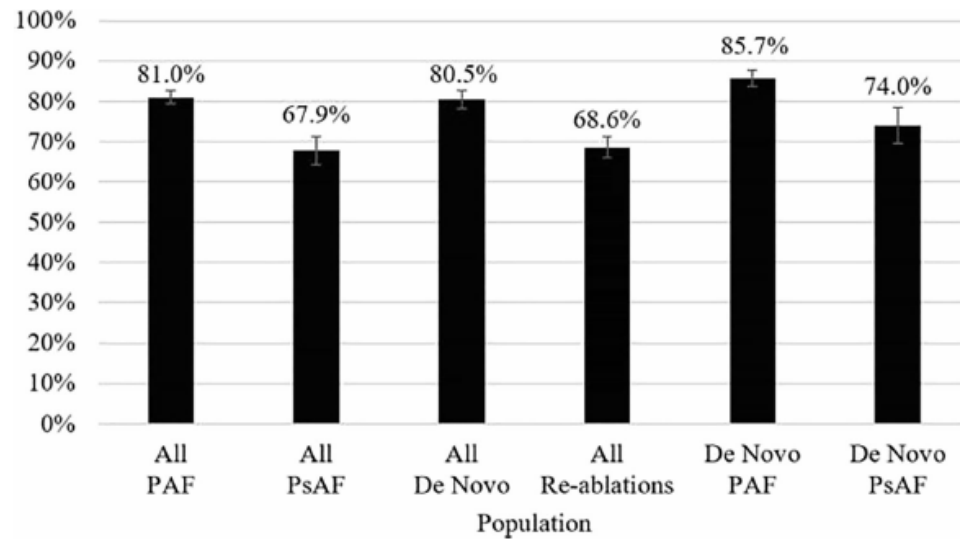


**Table 1** Baseline patient characteristics

	PAF ( <i>N</i> = 605)	PsAF ( <i>N</i> = 182)
Age, years	62.7 ± 11.1	65.4 ± 9.8
Less than 65	309 (51.1)	76 (41.8)
65–74	219 (36.2)	74 (40.7)
75 and older	77 (12.7)	32 (17.6)
Male	397 (65.6)	139 (76.4)
Body mass index kg/m <sup>2</sup>	27.1 ± 4.2	28.3 ± 4.5
Current smoker	46 (7.6)	27 (14.8)
Patient medical history		
Congestive heart failure	38 (6.3)	35 (19.2)
Hypertension	282 (46.6)	96 (52.8)
Diabetes	68 (11.2)	27 (14.8)
Cerebrovascular accident	43 (7.1)	10 (5.5)
End stage renal disease	3 (0.5)	2 (1.1)
CHA <sub>2</sub> DS <sub>2</sub> -VASc Score		
0–1	283 (46.8)	79 (43.4)
≥ 2	306 (50.6)	99 (54.4)
Missing	16 (2.6)	4 (2.2)
Baseline medications		
Antiarrhythmic drugs	499 (82.5)	151 (83.0)
Anticoagulation	272 (45.0)	96 (52.8)
Ejection fraction (%)	58.4 ± 7.3	53.9 ± 9.6
Collected for 2015 Procedures Only	( <i>N</i> = 327)	( <i>N</i> = 101)
Mitral insufficiency		
Grade 1	158 (26.1)	56 (30.8)
Grade 2	30 (5.0)	19 (10.4)
Grade 3	0 (0.0)	2 (1.1)
Grade 4	0 (0.0)	1 (0.6)
Left atrial size (ml)	158.9 ± 31.7	194.4 ± 42.6

**Table 2** Procedural detail

	PAF ( <i>N</i> = 605)	PsAF ( <i>N</i> = 182)
Ablations performed		
PVI only	539 (89.1)	155 (85.2)
PVI plus additional ablation lines	63 (10.5)	27 (14.8)
Missing	3 (0.5)	0 (0.0)
Acute pulmonary vein isolation	605 (100.0)	182 (100.0)
Total procedure time (minutes)		
Mean ± SD	96.1 ± 26.2	109.2 ± 35.6
Interquartile range (Q1, Q3)	(80, 110)	(90, 120)
Total fluoroscopy time (minutes)		
Mean ± SD	6.1 ± 3.8	6.9 ± 4.7
Interquartile range (Q1, Q3)	(3.6, 7.6)	(3.7, 8.5)
Radiation dose (Gy*cm <sup>2</sup> )		
Mean ± SD	5.9 ± 3.4	7.4 ± 4.9
Interquartile range (Q1, Q3)	(4.0, 6.5)	(4.4, 8.4)
Complications (captured in 2014 and 2015)		
Stroke	0 (0.0)	0 (0.0)
Cardiac tamponade	0 (0.0)	0 (0.0)
Death	0 (0.0)	0 (0.0)
Complications (captured in 2015 only) ( <i>N</i> = 333) ( <i>N</i> = 102)		
Pericardial effusion	7 (2.1)	0 (0.0)
Bleeding complication	1 (0.3)	0 (0.0)

**Table 3** Typical times for components of ablation procedure (subset of  $N=20$  PAF ablations)

Component of procedure	Time (minutes)
Groin puncture to 1st transeptal puncture	$4.5 \pm 0.9$
1st transeptal puncture to pigtail insertion	$1.7 \pm 0.7$
Pigtail insertion to end of 3DRA acquisition	$3.3 \pm 0.7$
End of 3DRA acquisition to 2nd transeptal puncture	$3.2 \pm 1.2$
2nd transeptal puncture to 1st RF application (LPV)	$9.9 \pm 1.2$
1st RF application (LPV) to end of LPV ablation	$14.7 \pm 1.6$
End of LPV ablation to end of RPV ablation	$15.0 \pm 2.3$

**Table 4** Multivariable logistic regression models of freedom from atrial arrhythmia recurrence

Variable	<i>P</i> value	Odds ratio (95% Wald confidence interval)
Full population:		
Paroxysmal AF	0.0003	2.02 (1.38, 2.95)
<i>De novo</i> AF ablation	0.0004	1.88 (1.33, 2.67)
Age (per year)	0.0410	0.98 (0.97, 1.00)
<i>De novo</i> ablations only:		
Paroxysmal AF	0.0080	2.11 (1.22, 3.67)

## Chapter 4

ORIGINAL - ELECTROPHYSIOLOGY

WILEY

### Reproducibility of pulmonary vein isolation guided by the ablation index: 1-year outcome of the AIR registry

Giuseppe Stabile MD<sup>1,2,3</sup>  | Antoine Lepillier MD<sup>4</sup> | Ermenegildo De Ruvo MD<sup>5</sup> | Marco Scaglione MD<sup>6</sup> | Matteo Anselmino MD<sup>7</sup> | Frederic Sebag MD<sup>8</sup>  | Domenico Pecora MD<sup>9</sup> | Mark Gallagher MD<sup>10</sup> | Mariano Rillo MD<sup>11</sup> | Graziana Viola MD<sup>12</sup> | Luca Rossi MD<sup>13</sup> | Valerio De Santis MD<sup>14</sup> | Maurizio Landolina MD<sup>15</sup> | Antonello Castro MD<sup>16</sup> | Massimo Grimaldi MD<sup>17</sup> | Nicolas Badenco MD<sup>18</sup> | Maurizio Del Greco MD<sup>19</sup>  | Antonio De Simone MD<sup>2</sup>  | Ennio Pisanò MD<sup>20</sup> | Salim Abbey MD<sup>21</sup> | Filippo Lamberti MD<sup>22</sup> | Antonio Pani MD<sup>23</sup> | Giulio Zucchelli MD<sup>24</sup> | Giuseppe Sgarito MD<sup>25</sup> | Daniela Dugo MD<sup>26</sup> | Emanuele Bertaglia MD<sup>27</sup> | Teresa Strisciuglio MD<sup>1,28</sup> | Francesco Solimene MD<sup>1</sup>

*J Cardiovasc Electrophysiol.* 2020;1-8.

## **Introduction**

The wide outcome variability among several operators still remain the main limitations of AF catheter ablation, and the rates of pulmonary vein (PV) reconnection responsible for arrhythmia recurrence are still high.

Ablation index (AI) is a new lesion quality marker that has been demonstrated to allow a high single-procedure arrhythmia-free survival in single center studies. The aim of this prospective, multi - center study, is to evaluate the reproducibility and outcome of PV isolation guided by the AI. Furthermore, as there is still a debate on the best AI values that allow effective, safe and durable PV isolation, we evaluated the ablation with different AI settings.

## **Methods**

The ablation index registry (ClinicalTrials.gov Identifier: NCT03277976) is a prospective, multi - center, research study designed to evaluate the acute achievement of PV isolation with ThermoCool SmartTouch (ST) or ThermoCool SmartTouch surround flow SF (STSF) (Biosense Webster) catheter using the AI Module. Enrollment started in November 2017 and ended in July 2018 and included patients with paroxysmal and persistent AF, who underwent their first ablation.

Each operator performed AF catheter ablation using its own ablation technique as concerning the ablation catheter (ST or STSF) and the AI setting (380 posterior - 500 anterior and 330 posterior - 450 anterior). No randomization was required nor was there any deviation from the clinical practice of each center and operator. Therefore the enrolled population was



divided in four groups: group ST 330 to 450, group ST 380 to 500, group STSF 330 to 450, and group STSF 380 to 500.

Given that the rate of PV isolation with a standard wide antral circumferential ablation technique (first - pass isolation) is about 70%, we wanted to test if one of two catheters or one of two AI settings could increase the first - pass isolation rate of at least 10% (from 70% - 80%, 95% confidence interval, 75% - 85%). Patients were divided in four groups and enrollment stopped when at least 80 patients were enrolled in each group.

We report the 1 - year follow - up, comparing the outcome in the four study groups, between the two AI settings, between the two ablation catheters, and among different operators.

Patients with paroxysmal AF were discharged without antiarrhythmic drugs. Patients with persistent AF were discharged with or without antiarrhythmic drugs according to clinician's preference. Patients were scheduled for follow - up examinations 1, 3, 6, and 12 months after the initial treatment, and the clinical assessment of AF recurrence during the follow - up visits was performed by ECG and 24 - hour Holter monitoring.

## **Results**

### *Study population and Procedural data*

A total of 490 patients were enrolled: 96 patients in ST 330 to 450 group, 81 in ST 380 to 500 group, 162 in STSF 330 to 450 group, and 151 in STSF 380 to 500 group.

The rate of firstpass PV isolation was similar among the four study groups, whereas procedure (ST330  $129 \pm 44$ minutes, ST380  $144 \pm 44$ minutes, STSF330  $120 \pm 72$  minutes, STSF380  $125 \pm 73$ minutes;  $P < .001$ ) and fluoroscopy time (ST330  $542 \pm 285$  seconds, ST380  $540 \pm 416$  seconds, STSF330  $257 \pm 356$  seconds, STSF380  $379 \pm 454$  seconds;  $P < .001$ )

significantly differed. A complication (four pericardial effusions, two transient phrenic nerve palsy, one cardiac tamponade, one pneumonia) was observed in eight (1,6%) patients without any difference among the four study groups ( $P = .55$ ).

### *One - year outcome*

One - year follow - up was available in 452/490 (92.2%) patients. During the blanking period 43/452 (9.5%) patients had an atrial tachyarrhythmia recurrence. There was no difference in the 1 year AF recurrence rate between patients with and without early relapses (18,6 vs 12.2%;  $P = .23$ ). At 12 months follow - up a higher rate of freedom from AF recurrences was observed in patients with both paroxysmal (91%) versus persistent (83.3%;  $P = .039$ ) AF (Figure 1). Twenty - five/96 (26%) of patients with persistent AF were on antiarrhythmic drugs: 13 patients were on flecainide, eight on amiodarone, one on propafenone, one on sotalol, one on dronedarone, and one not specified. During the 12 months follow - up 22 (4.9%) patients had an atrial tachycardia or atrial flutter recurrence: 15 patients during the blanking period, and 7 patients after. There was no difference in the rate of atrial arrhythmias recurrence among the four study groups (4.5% in group ST330 - 450, 12.2% in group ST380 - 500, 14.9% in group STSF330 - 450, 9.4% in group STSF380 - 500;  $P = .083$ ) (Figure 2). At 12 months follow - up the rate of atrial arrhythmias recurrence was also similar between patients treated with a ST (8%) and STSF catheter (12.1%;  $P = .2$ ) (Figure 3), and between patients targeting an AI setting of 330 to 450 (10.9%) or 380 to 500 (10.3%;  $P = .64$ ) (Figure 4).

### *Reproducibility*

Overall 25 European centers enrolled patients in the study, and the ablation procedures were performed by 40 operators. To avoid bias due to the low number of patients effectively treated and the use of antiarrhythmic drugs, we limited the analysis only to patients with paroxysmal AF. There was no difference ( $P = .12$ ) in the 1 - year freedom from AF recurrence among 14 operators that performed  $\geq 10$  ablation procedure. When we considered all operators, there was no difference in 1 - year freedom from AF recurrence between the 14 operators that performed  $\geq 10$  procedures and the 26 operators that performed  $< 10$  procedures ( $P = .5$ ) (Figure 5).

## **Conclusion**

An ablation protocol respecting strict criteria for contiguity and quality of lesions resulted in high rate of 1 - year freedom from AF recurrence, irrespective of the ablation catheters, and AI settings. The result was reproducible among different operators, both in patients with paroxysmal and persistent AF.

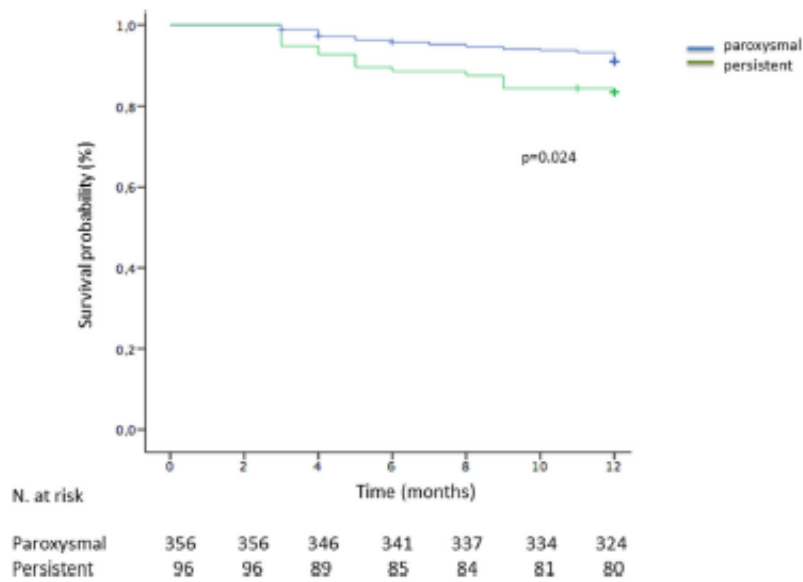


**FIGURE 1** Kaplan-Meier estimation of the time to atrial arrhythmia recurrence after the blanking period in patients with paroxysmal and persistent atrial fibrillation. The Kaplan-Meier curve for persistent atrial fibrillation refers to freedom from atrial arrhythmias with and without drugs, and for paroxysmal atrial fibrillation without drugs

**FIGURE 2** Kaplan-Meier estimation of the time to atrial arrhythmia recurrence after the blanking period in the four study groups

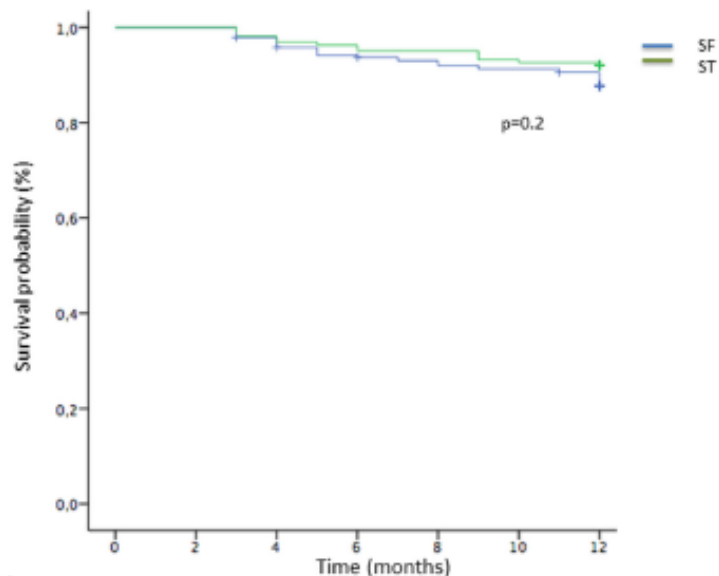
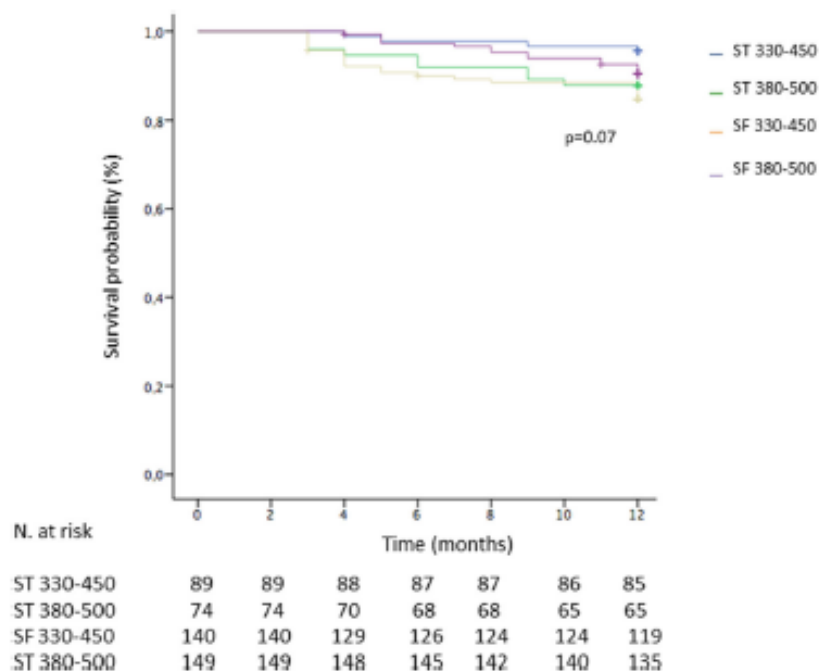


**FIGURE 3** Kaplan-Meier estimation of the time to atrial arrhythmia recurrence after the blanking period in patients ablated with the ThermoCool SmartTouch (ST) or ThermoCool SmartTouch SF (STSF) catheter

N. at risk	0	2	4	6	8	10	12
SF	289	289	277	271	266	264	254
ST	163	163	158	155	155	151	150

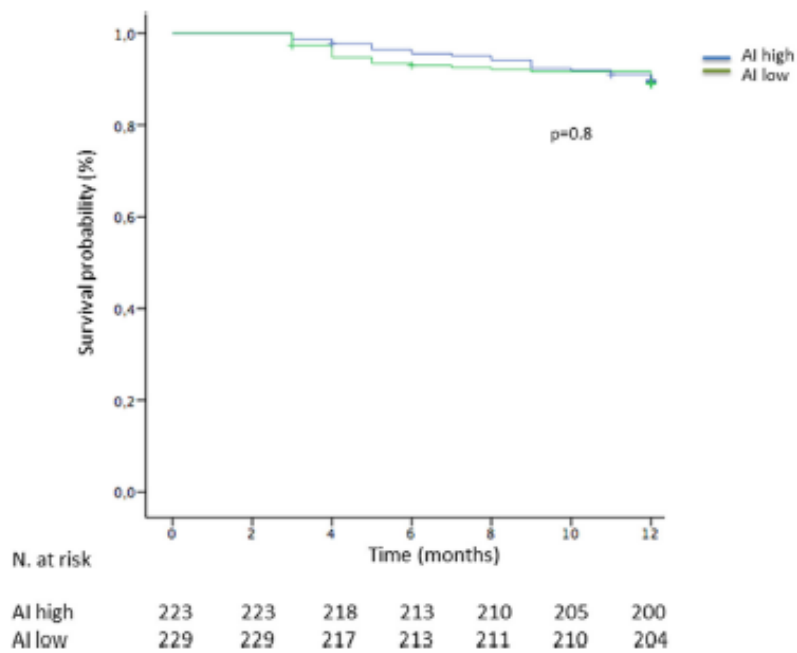


**FIGURE 4** Kaplan-Meier estimation of the time to atrial arrhythmia recurrence after the blanking period in patients ablated using the high (380-500) or low (330-450) AI setting. AI, ablation index

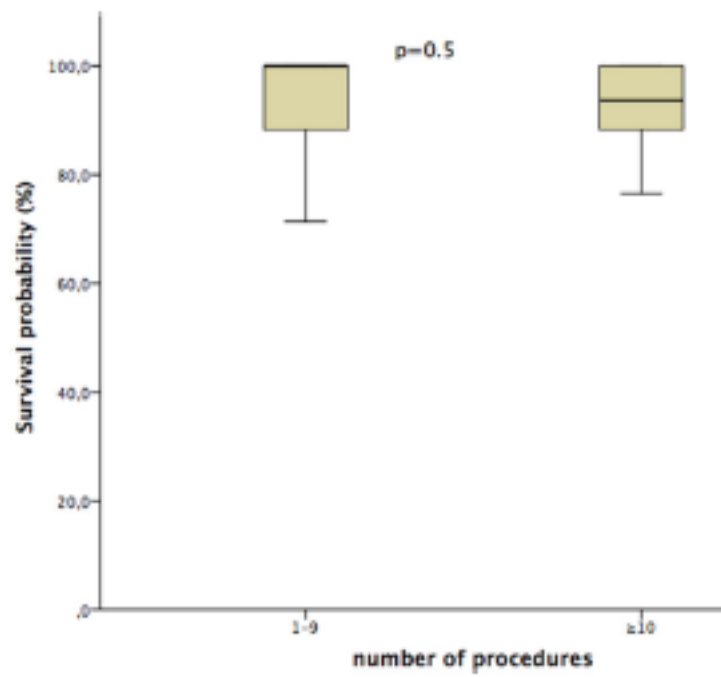


**FIGURE 5** Atrial fibrillation recurrence rate between low-volume (<10 procedures) and high-volume (≥10 procedures) operators

## Chapter 5



**Long-term impact of catheter ablation on arrhythmia burden in low-risk patients with paroxysmal atrial fibrillation: the CLOSE to CURE study**

**Mattias Duytschaever, MD, PhD, Jan De Pooter, MD, PhD, Anthony Demolder, MD, Milad El Haddad, MSc, PhD, Thomas Philips, MD, Teresa Strisciuglio, MD, Philippe Debonnaire, MD, PhD, Michael Wolf, MD, Yves Vandekerckhove, MD, Sebastien Knecht, MD, PhD, Rene Tavernier, MD, PhD**



## **Introduction**

Few studies evaluated the impact of catheter ablation (CA) on atrial tachyarrhythmia (ATA) burden in paroxysmal atrial fibrillation (AF). ATA burden, defined as % of time spent in ATA, is associated with AF-related symptoms, heart failure and stroke.

In the prospective, patient-controlled CLOSE to CURE (C2C) study we determine the longer term impact of PVI on ATA burden in PAF. To reliably quantify ATA burden patients were implanted with an insertable cardiac monitor (ICM) at least 2 months before PVI. Ablation consisted of a point-by-point contact force (CF)-guided RF approach aiming to enclose the PVs with contiguous, stable and optimized RF lesions.

## **Methods**

The C2C study (NCT02925624) is a single-center, patient-controlled, prospective cohort study. Enrollment started July 2016 until July 2017 at the St Jan Hospital Bruges.

Patients were eligible if there was a history of symptomatic ECG-1 proven PAF (either resistant, intolerant or unwilling to take ADT) with at least  $\geq 3$  AF episodes (anamnestic or documented) in the last 3 months. Exclusion criteria were persistent AF, prior AF ablation, left atrial (LA) diameter  $> 50$ mm, ejection fraction  $< 35\%$ , AF secondary to reversible causes, unstable angina or uncontrolled heart failure, myocardial infarction or CABG within the last 3 months. PAF patients were implanted with an ICM 65 [61-78] days before CA. CA consisted of contact force guided pulmonary vein isolation (PVI) targeting an intertag distance  $\leq 6$ mm and a region-specific ablation index (figure 1). Primary endpoint was reduction in ICM detected ATA burden, secondary endpoints were single-procedure freedom from ATA, quality of life (QOL), and adverse events.

For the follow-up clinical visits, 12-lead ECG and ICM data review were performed at enrollment, at 1, 3, 6, 12, 18 and 24 months after CA or in case of symptoms. Three months after CA, ADT was stopped whereas anticoagulation was continued according to stroke risk. Quality of life (QOL) was assessed before and every 6 months after CA via the Short Form 36 Health Survey, AF Symptom Checklist, and EHRA symptom score. Repeat ablation was advised in case of symptomatic ATA recurrence and consisted of re-isolation or an empirical trigger or substrate ablation.

The primary endpoint, ICM-detected ATA burden, was defined as the % of time spent in ATA (hours of ATA/hours of monitoring) (Figure 2).

## **Results**

### *Study population*

The study included 105 patients. The median number of monitoring days was 65 [61-78] days. Overall, 21 patients did not reveal any ATA episode during monitoring. In these patients the time from diagnosis to CA was 9.0 [6.5-20] months and the last ECG documented-AF episode was 17 [9-28] days before enrollment.

### *Primary endpoint: ATA burden before and after ablation*

Results for ATA burden for the entire study population are given in the upper panels of Figure 3. After PVI ( $1.13 \pm 0.39$  procedure per patient throughout 2 year follow-up), ATA burden decreased from 2.68 [0.09-15.02] % at baseline to 0 [0-0] % during the first year (reduction in ATA burden 100 [100-100] %,  $p < 0.001$ , left panel) and 0 [0-0] % during the second 2-year (reduction in ATA burden 100 [100-100] %,  $p < 0.001$ , right panel). Burden reduction was seen both in patients without (black bars) and with any 2-min ATA recurrence

(red and green bars). None of the patients progressed to persistent AF after CA. Results for the subset of 84 patients with documented ATA during the monitoring period were similar (Figure 3, lower panels).

#### *Secondary ATA burden-related endpoints*

ATA burden without adjudication decreased from 6.61 [1.80-19.00] % to 0 [0-0.03] % during the first 12 months after PVI and to 0 [0-0.03] % during the second year ( $p < 0.001$  for both). The proportion of patients with  $>95\%$  reduction in ATA burden was 94% and 96% at 1 and 2-y FU. Finally, throughout the first and second year after ablation, only 5 (6%) and 1 (1%) had a residual ATA burden  $>0.5\%$ .

#### *Single-procedure, off-ADT freedom from ATA*

In Figure 4 we plotted the time to the first day with any 2-min ATA for the entire population (blue curve) and subpopulation (red curve). Single-procedure, off-ADT freedom from any ATA declined from 87% after 1 year to 78% after 2 years ( $p = 0.343$ ).

#### *Quality of Life*

Physical and mental Health SF36 score, symptom

frequency and severity scores, and EHRA score all improved significantly at 1 and 2 year ( $p < 0.001$ ). Improvement in QOL was comparable among patients with and without ATA recurrence.

#### *Safety*

Ablation-related adverse events were observed in 5 patients (4.7%): three patients with groin site hematoma (all treated conservatively by mechanical pressure), one patient with femoral pseudoaneurysm (requiring surgery) and one patient with symptomatic left PV stenosis (treated with percutaneous stenting at 104 days after PVI with resolution of symptoms throughout 2-year FU). In none of the patients undergoing repeat ablation narrowing of PVs was observed.

## **Conclusion**

CA has become an effective procedure in paroxysmal AF with a major impact on ICM-detected ATA burden. Whereas conventional survival analysis suggests progressive decline in efficacy, we observed that burden reduction is maintained at longer follow-up.

These data imply that ATA burden is a more optimal endpoint for assessing ablation efficacy.

Figure 1:

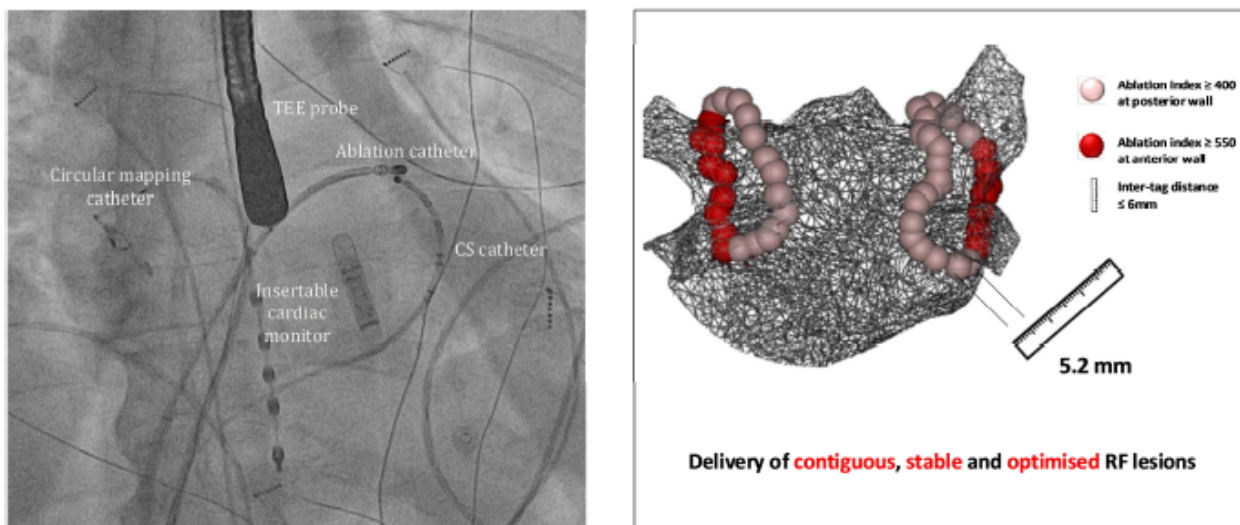


Figure 2:



Figure 3:

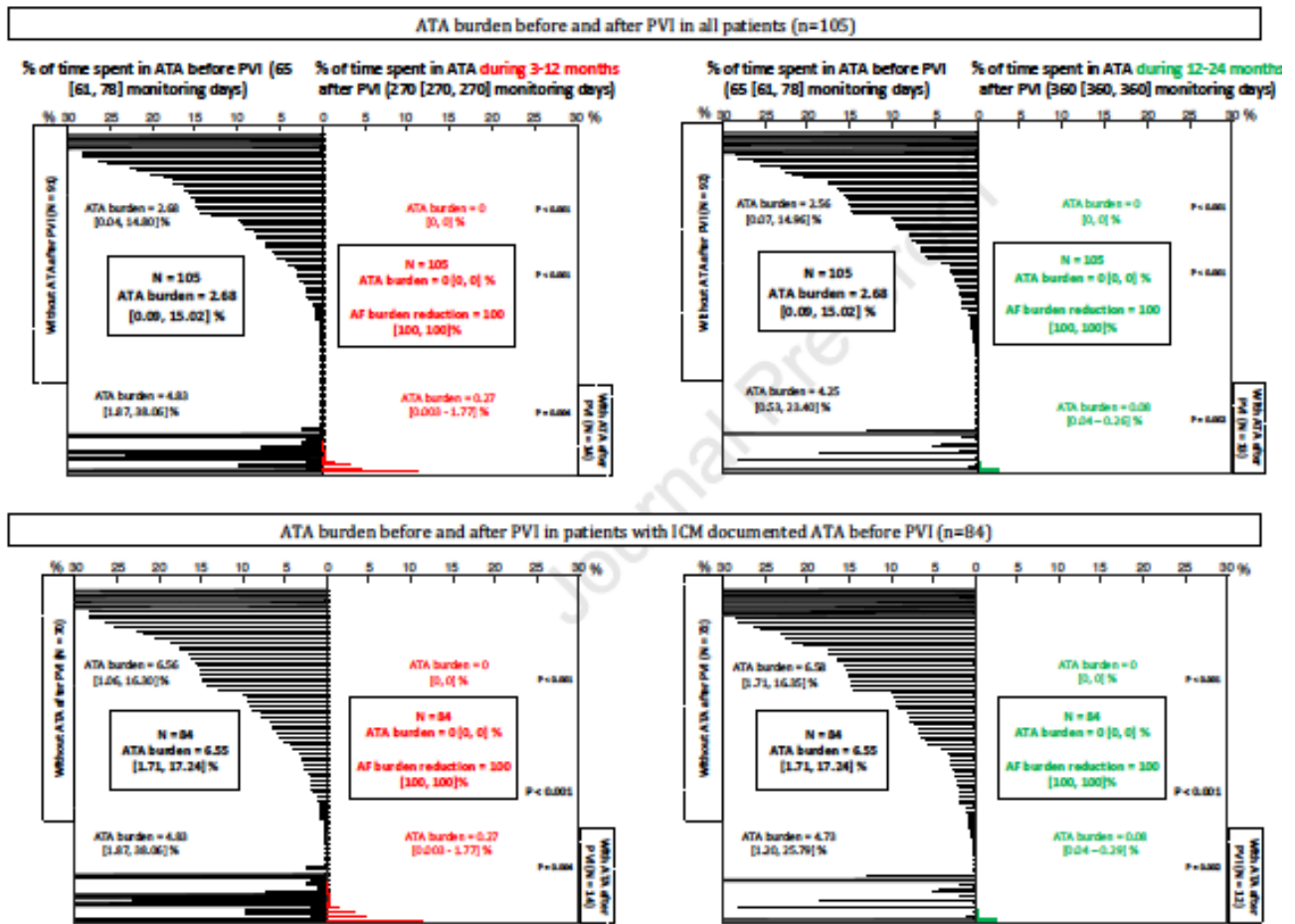
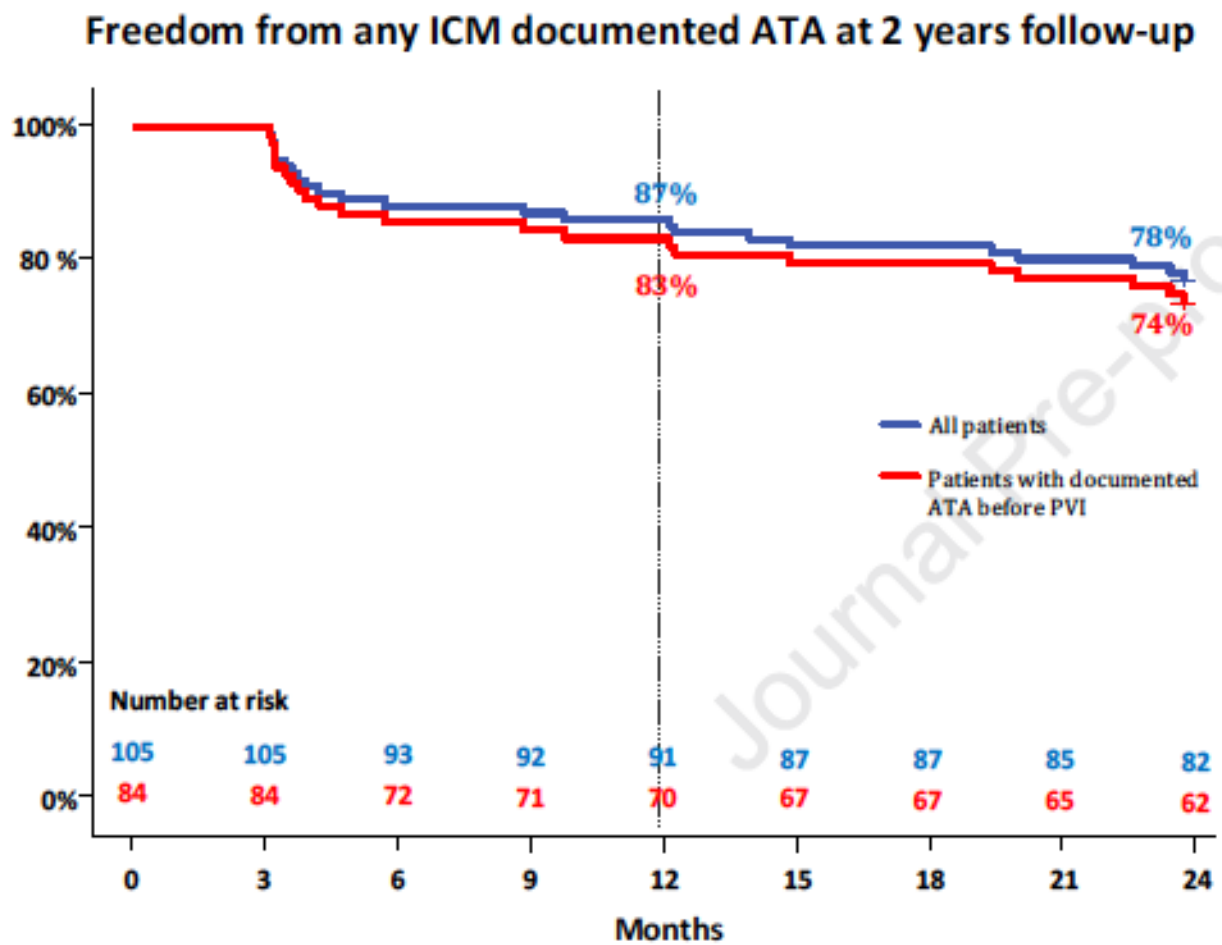


Figure 4:



## Chapter 6



**ESC**

European Society  
of Cardiology

*Europace* (2020) 0, 1–8

doi:10.1093/europace/euaa071

**CLINICAL RESEARCH**

---

# Paroxysmal atrial fibrillation with high vs. low arrhythmia burden: atrial remodelling and ablation outcome

**T. Strisciuglio** <sup>1,2</sup>, **M. El Haddad**<sup>1</sup>, **P. Debonnaire**<sup>1</sup>, **J. De Pooter**<sup>1,3</sup>,  
**Anthony Demolder**<sup>3</sup>, **M. Wolf**<sup>1</sup>, **T. Philips**<sup>1</sup>, **M. Kyriakopoulou**<sup>1</sup>, **A. Almorad**<sup>1</sup>,  
**S. Knecht**<sup>1</sup>, **R. Tavernier**<sup>1</sup>, **Y. Vandekerckhove**<sup>1</sup>, and **Mattias Duytschaever**<sup>1,3\*</sup>

<sup>1</sup>Department of Cardiology, Sint-Jan Hospital, Riddershovestraat 10, 8000 Bruges, Belgium; <sup>2</sup>Department of Advanced Biomedical Sciences, University of Naples Federico II, Italy; and <sup>3</sup>Ghent University Hospital, Heart Center, De Pintelaan 185, 9000 Ghent, Belgium



## **Introduction**

Atrial tachyarrhythmia (ATA) burden in paroxysmal atrial fibrillation (AF)—defined as the percentage of time spent in AF—is associated with impaired quality of life and increased risk of stroke. In patients with heart failure (HF), higher burden is associated with worsening of functional class, while its reduction is associated with improved outcome. These data suggest that burden reduction might improve outcome, especially in AF patients with high ATA burden. Catheter ablation (CA) reduces ATA burden. However, it is unknown whether paroxysmal AF patients with high burden are characterized by distinct clinical characteristics or distinct electromechanical properties of the left atrium (LA) and how this might affect outcome after CA. In this analysis of the CLOSE to CURE study, in which patients with paroxysmal AF were followed by an insertable cardiac monitor (ICM) after pulmonary veins isolation (PVI), we evaluated the relation between baseline ATA burden and electromechanical properties of the LA. Second, we evaluated how baseline ATA burden influences efficacy of CA, especially in terms of burden reduction.

## **Methods**

### *Study population and atrial tachyarrhythmia burden*

The CLOSE to CURE population consisted of 105 patients undergoing CA for symptomatic paroxysmal AF. At least 2 months before ablation, patients underwent implantation of a loop recorder (Reveal Linq™ Insertable Cardiac Monitor, Medtronic). Programming of automated ATA detection was standardized across all patients. Atrial tachyarrhythmia burden at baseline was defined as the percentage of monitoring time spent in ATA (total number of hours spent in AF, AT, or flutter/total number of recording hours).

### *Mechanical and electrical properties of the left atrium*

All patients underwent at baseline a comprehensive transthoracic two-dimensional echocardiography on a VividE9 System (GE-Vingmed, Milwaukee, WI). Echocardiography was performed by a single operator blinded to data on ATA burden (PD). Left atrium antero-posterior linear diameter was measured in the 2D left parasternal long-axis view. Left atrium volume was assessed using Simpson's biplane method. Left atrium longitudinal strain was assessed using 2D speckle-tracking analysis with QRS onset as the reference point, applying a commercially available Left ventricle (LV) strain software package to the LA (EchoPAC version 113.0.x). The values of LA strain were calculated as the average value of the four-chamber and two-chamber views. Left atrium reservoir function was calculated as peak systolic LA strain (LA reservoir strain), while LA contractile function was measured as the LA strain value at P-wave onset on electrocardiography (LA contractile strain). In case of ongoing AF, echocardiography was limited to assessing LA diameter and volume.

Prior to CA, we determined atrial effective refractory period (AERP), AF inducibility, electrogram (EGM) voltage, and intra-atrial conduction velocity (IACV). Atrial effective refractory period and AF inducibility were determined by single premature stimulation during pacing (600ms) at the proximal and distal bipole of the coronary sinus catheter (Figure 1A). Electrogram voltage was determined by averaging amplitude of all bipolar EGMs recorded at >\_300 LA sites [homogenously distributed, contact force (CF) >\_4 g, Figure 1B] during sinus rhythm. A region of >\_1 cm<sup>2</sup> with low-voltage EGMs was defined as a region of 'scar'. In addition, we calculated for each patient the percentage of low-voltage EGMs (i.e. <0.5mV, Figure 1C). The electro-anatomical map (with local activation times for each triangle within the geometry) allowed to calculate and average local IACVs (Coherent module, Carto, Biosense-Webster Inc, Figure 1D).

### *Catheter ablation and follow-up*

Catheter ablation was performed according to the CLOSE protocol under general anaesthesia. Point-by-point radiofrequency (RF) delivery was performed aiming for a contiguous circle enclosing the ipsilateral veins, respecting a maximal interlesion distance of  $<_6$ mm. Clinical visits including 12-lead electrocardiogram (ECG) and ICM data review were performed at the time of enrolment and at 1, 3, 6, and 12 months post-ablation or in case of symptoms. Three months after CA, anti-arrhythmic drug therapy was stopped in all patients whereas anticoagulation was continued according to stroke risk. The primary endpoint in the CLOSE to CURE study was ICM-detected ATA burden, defined as the percentage of time spent in ATA (hours of ATA/hours of monitoring). Atrial tachyarrhythmia burden before PVI was compared with ATA burden during the first 12 months after PVI (excluding a 3-month blanking window).

## **Results**

### *Atrial tachyarrhythmia burden at baseline*

Patients were implanted with an ICM at 64 (61–78) days before PVI.

During this monitoring time ATA burden was 2.7 (0.1–14.9) %. Based upon the highest tertile, patients with  $\geq 9.3\%$  time spent in ATA were classified as the high ATA burden group whereas the lowest tertiles comprised the low ATA burden group (Figure 2). Overall, 21 patients did not reveal any ATA episode during monitoring. These low-burden patients, however, all had an ECG-documented AF episode 17 (9–28) days before enrolment in the study.

### *High vs. low atrial fibrillation burden: clinical characteristics*

Clinical characteristics are given in Table 1. There were no significant between-group differences in age, gender, body mass index, prevalence of comorbidities, or CHA2DS2VASc score. Furthermore, exposure to anti-arrhythmic drug therapy and to oral anticoagulant therapy did not differ between groups. Patients with high burden had a longer, albeit non-significant, time interval from the first apparent AF episode to actual PVI [24 (12–36) vs. 8 (4–24) months;  $P = 0.17$ ].

*High vs. low atrial fibrillation burden: electrical and mechanical properties of the left atrium*

There was no difference in AF inducibility, AERP, or IACV (Table 2 and Figure 3). Likewise the EGM voltage ( $1.9 \pm 0.8$  vs.  $1.9 \pm 0.6$  mV,  $P = 0.74$ ), percentage of EGMs with low voltage [1 (0–5) vs. 2 (0–6);  $P = 0.68$ ] and the proportion of patients with scar (12% vs. 9%;  $P = 0.73$ ) did not differ in between patients with high vs. low ATA burden.

In contrast, there were significant differences in atrial size and function (Table 2 and Figure 4). Patients with high ATA burden had larger LA diameter ( $46.5 \pm 6$  vs.  $42.5 \pm 6$  mm,  $P = 0.008$ ), volume ( $93.8 \pm 22$  vs.  $80.4 \pm 21$  mL,  $P = 0.011$ ), and lower LA reservoir and contractile strain ( $19.7 \pm 6$  vs.  $24.7 \pm 6$ %,  $P = 0.002$ ;  $10.3 \pm 3$  vs.  $12.8 \pm 4$ %,  $P = 0.014$ ). Similarly, when analysing ATA burden as a continuous variable, a significant correlation was found between burden and LA diameter ( $P < 0.01$ ), volume ( $P = 0.04$ ), reservoir strain ( $P = 0.00$ ), and contractile strain ( $P = 0.04$ ). Both reservoir and contractile strain function were independently associated with high burden f[OR 95%CI 0.79 (0.66–0.94)]  $P = 0.01$  and [OR 95%CI 0.71 (0.53–0.96)]  $P = 0.03$ , respectively. Patients with high ATA burden had a higher, albeit non-significant, atrial size indexed to body surface area ( $47 \pm 12$  vs.  $42 \pm 10$  mL/m<sup>2</sup>,  $P = 0.061$ ).

### *High vs. low atrial fibrillation burden: efficacy of catheter ablation*

Results are given in Figure 5. No patient was lost to follow-up. In lowburden patients, CA reduced ATA burden from 0.7 (0–2.7) at baseline to 0 (0–0) during the 1st year [100 (100–100) % reduction,  $P < 0.001$ ]. Also in high-burden patients, CA reduced ATA burden from 20.3 (14.8–33.3) at baseline to 0 (0–0) during the 1st year [100 (100–100) % reduction,  $P < 0.001$ ]. Atrial tachyarrhythmia burden throughout the 1st year after CA was equally low in between groups [0 (0–0) % vs. 0 (0–0) %,  $P = 1$ ]. Single procedure 1-year freedom from any ATA was equally high in both groups (83% high burden vs. 89% low burden) (Figure 6).

### **Conclusion**

Paroxysmal AF patients with high vs. low ATA burden have no distinct clinical profile, but altered LA mechanical properties, reflected by larger size and more impaired function (strain). Despite such structural and functional remodelling, high-burden patients are excellent responders to CA at 1 year. Most likely the lack of fibrosis and/or advanced electrical remodelling explains why pulmonary veins remain the dominant trigger for AF in this patient cohort.

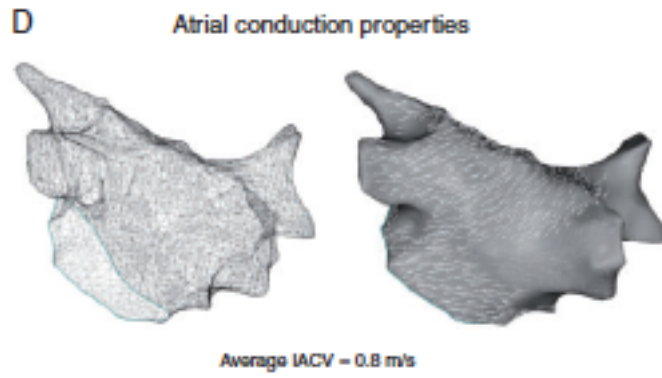
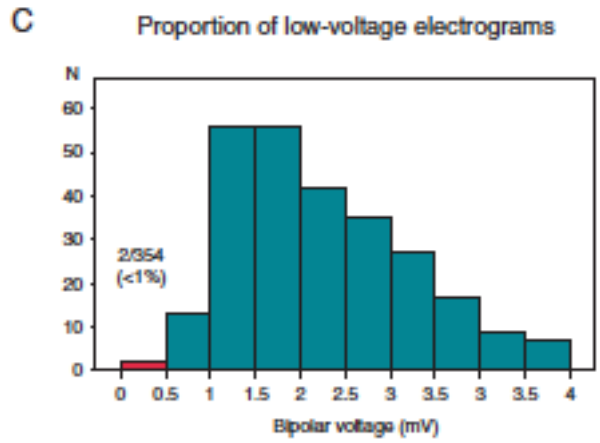
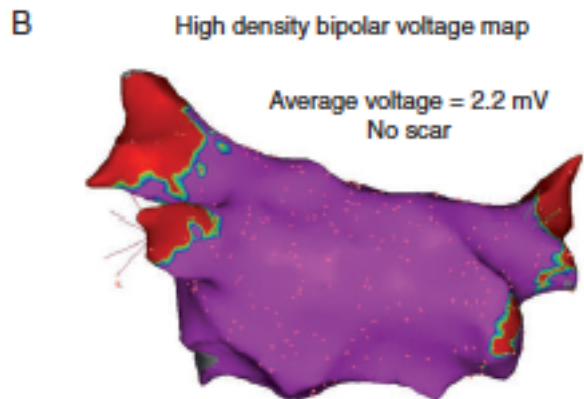
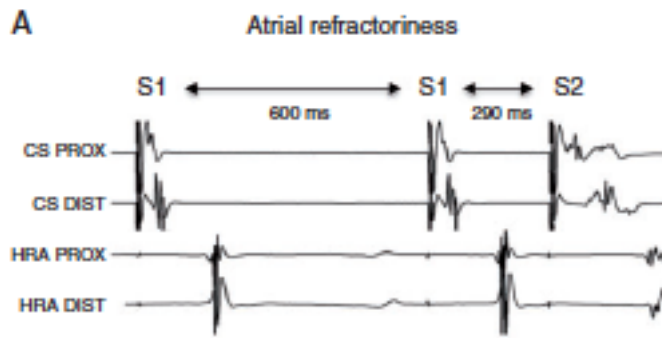


**Figure 1** Assessment of electrical properties of the left atrium (see text for explanation).

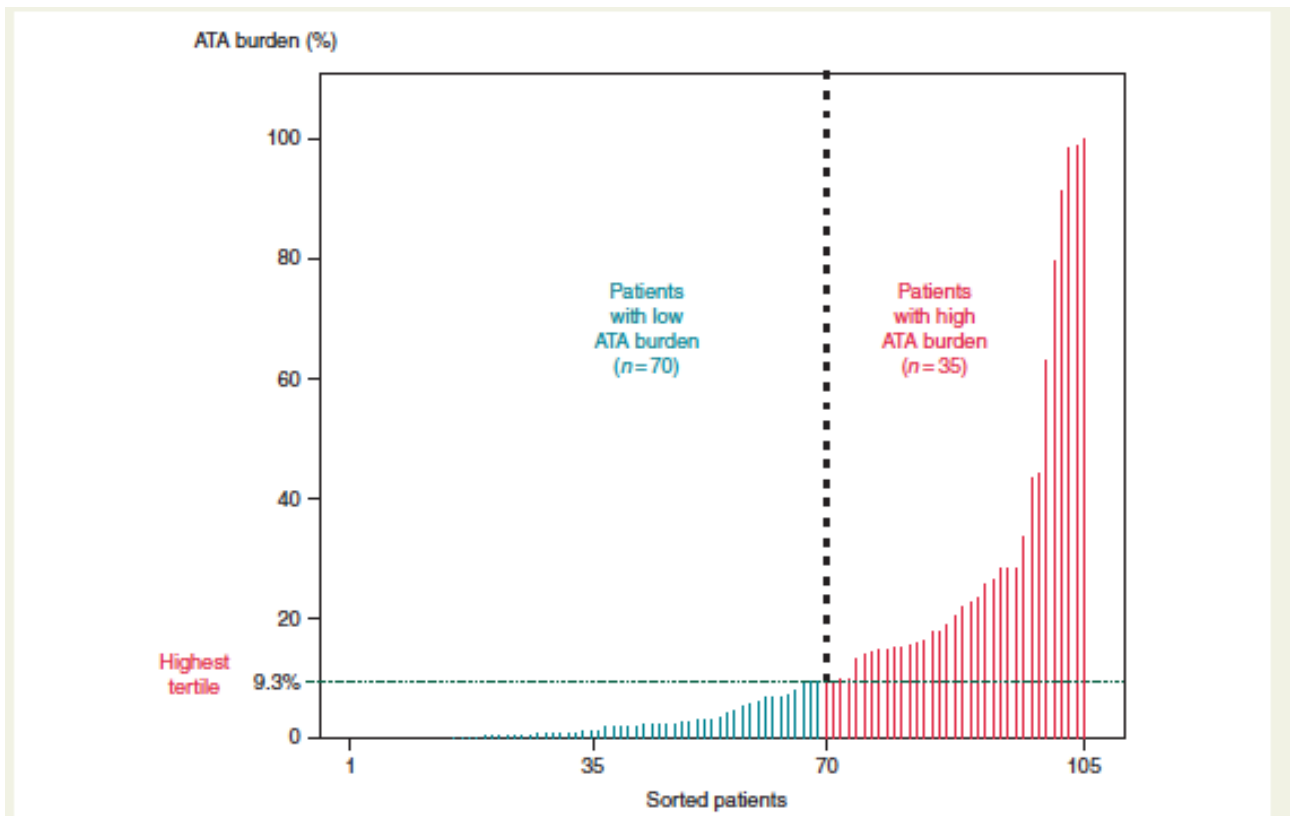


**Figure 2** Distribution of ATA burden, patients are sorted based on ATA burden. One-third of patients had a burden  $\geq 9.3\%$  (high ATA burden patients). ATA, atrial tachyarrhythmia.

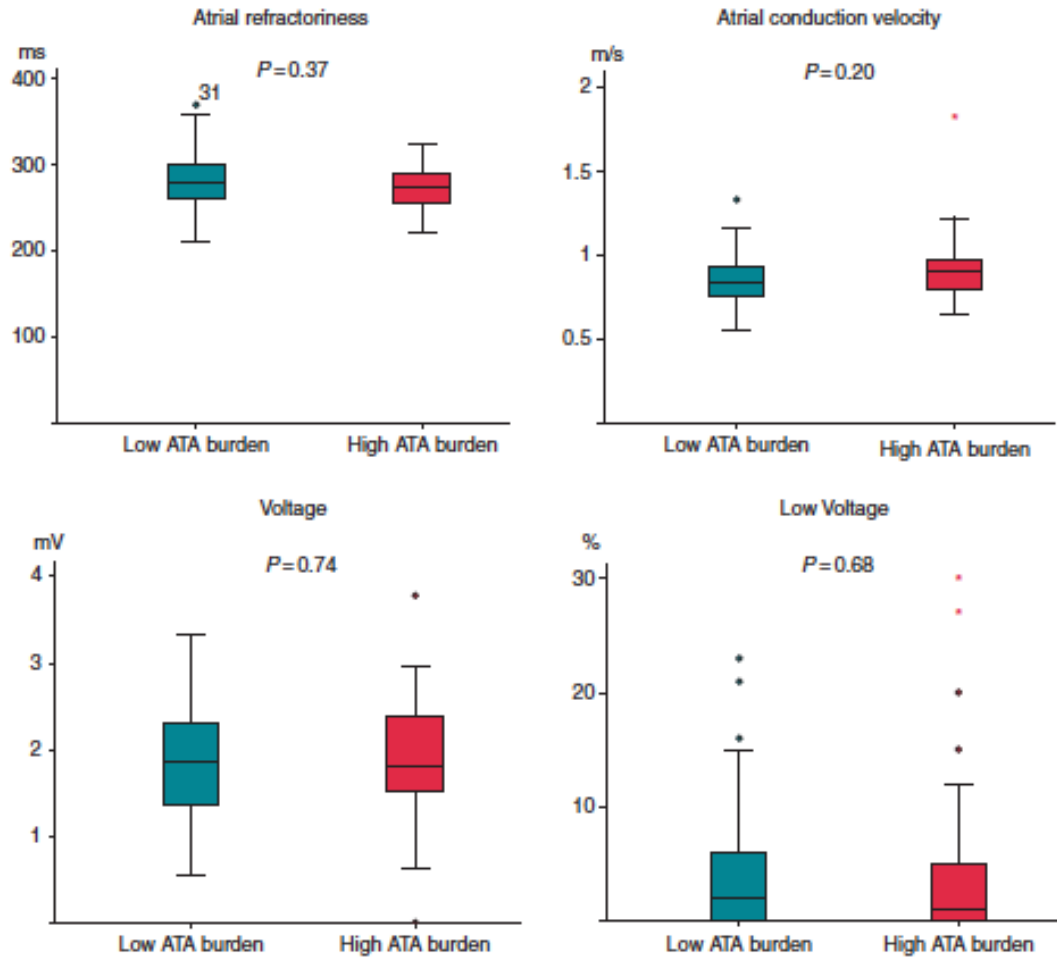


**Figure 3** Electrical properties of the left atrium in patients with high vs. low ATA burden. There are no differences in atrial effective refractory period (AERP), intra-atrial conduction velocity (IACV), voltage and percentage of low-voltage EGMs. ATA, atrial tachyarrhythmia; EGM, electrogram.



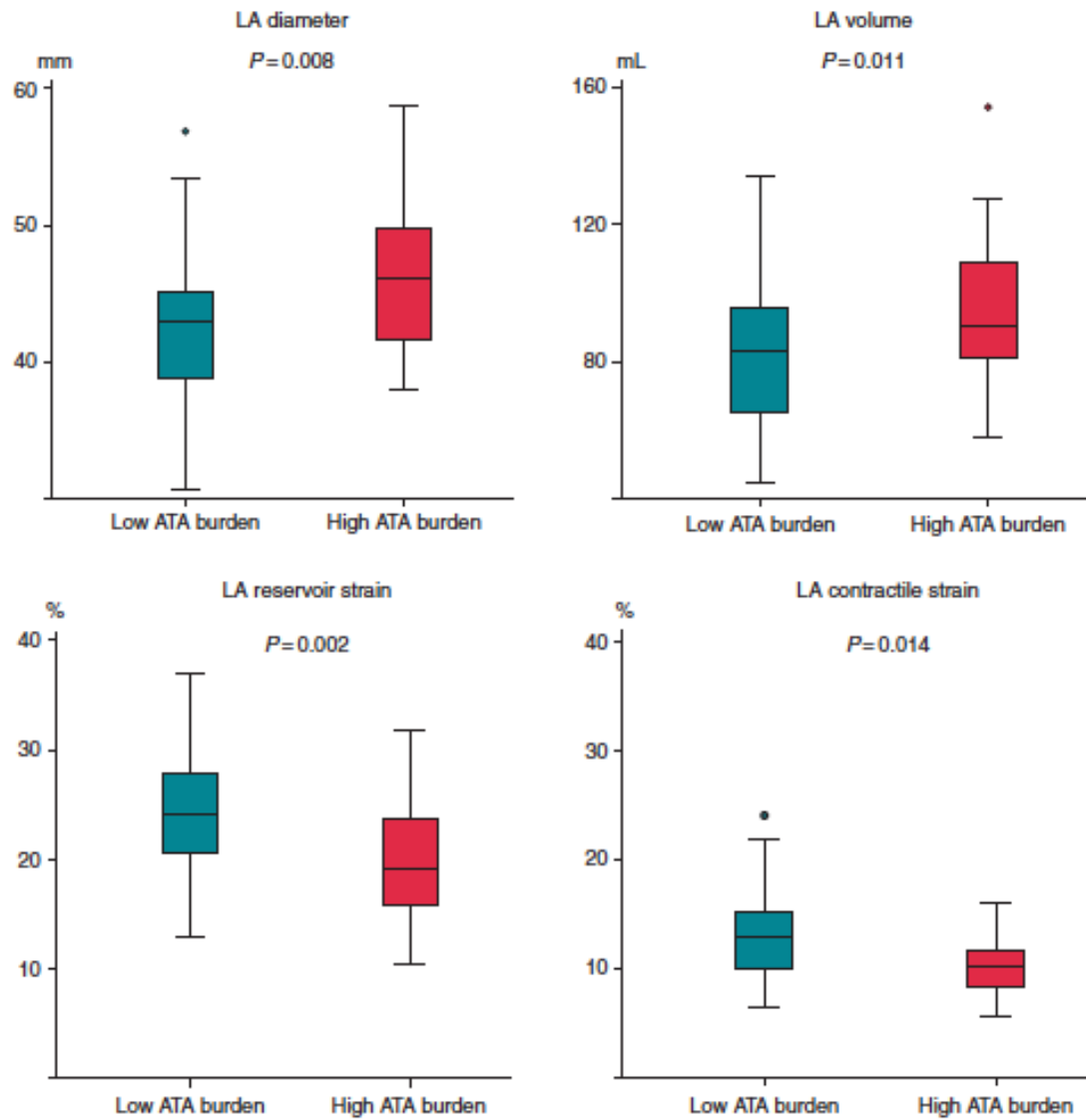


**Figure 4** Mechanical properties of the left atrium in patients with high vs. low ATA burden. Patients with high burden are characterized by larger LA dimensions (diameter and volume) and impaired LA function (reservoir and contractile strain). Strain measurement was performed during sinus rhythm (71 patients overall, 52 in the low-burden group, 19 in the high burden group). ATA, atrial tachyarrhythmia; LA, left atrium.

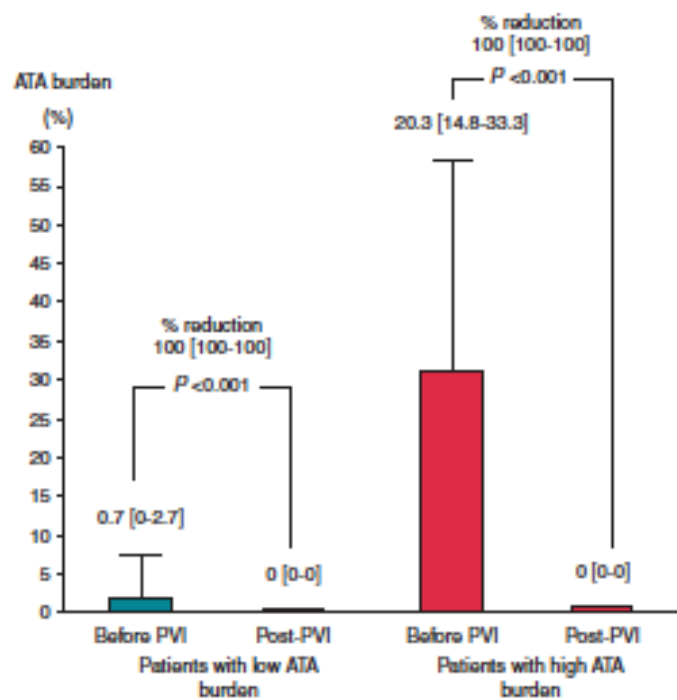


**Figure 5** Impact of CA on ATA burden in high vs. low ATA burden patients. Catheter ablation significantly reduced ATA burden in both groups. ATA, atrial tachyarrhythmia.

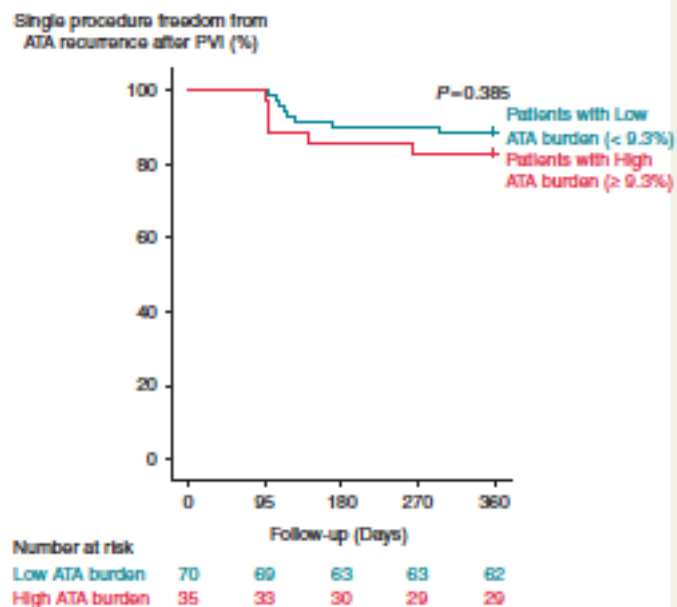


**Figure 6** Single-procedure freedom from any ATA in high vs. low ATA burden patients. ATA, atrial tachyarrhythmia.

**Table 1** Clinical characteristics

	Overall	Patients with low burden	Patients with high burden	P-value
Number	105	70	35	
Age, years	64 (56–70)	66 (56–70)	63 (56–66)	0.11
Male gender, n (%)	65(62)	40 (57)	25 (71)	0.20
CHA2DS2VASc	2 (1–2)	2 (1–3)	1 (0–2)	0.45
BMI, kg/m <sup>2</sup>	26 (24–29)	26 (23–29)	27 (24–28)	0.68
BMI>30, n (%)	20 (20)	15 (22)	5 (14)	0.43
Hypertension, n (%)	35 (33)	26 (37)	9 (26)	0.28
Diabetes, n (%)	8 (8)	6 (9)	2 (6)	0.72
ADT, n (%)	81 (77)	54 (77)	27 (77)	1
OAC, n (%)	71 (68)	51 (73)	20 (57)	0.12
Months from 1st AF to PVI	12 (6–25)	8 (4–24)	24 (12–36)	0.17

BMI, body mass index; ADT, anti-arrhythmic drug therapy; OAC, oral anticoagulant; PVI, pulmonary vein isolation.

**Table 2** Electrical and mechanical properties of the left atrium

	Overall	Patients with low burden	Patients with high burden	P-value
Number	105	70	35	
AF inducibility, n (%)	8 (8)	5 (7)	3(9)	0.63
AERP, ms	279 ± 32	281.6 ± 31	275.9 ± 26	0.37
IACV, m/s	0.8 (0.8–0.9)	0.8 (0.8–0.9)	0.9 (0.8–1)	0.20
EGM voltage, mV	1.9 ± 0.7	1.9 ± 0.6	1.9 ± 0.8	0.74
Percentage of EGMs with low voltage	2 (0–6)	2 (0–6)	1 (0–5)	0.68
Area of low voltage, n (%)	10 (10)	6 (9)	4 (12)	0.73
LA diameter, mm	43.8 ± 6	42.5 ± 6	46.5 ± 6	0.008
LA volume, mL	84.8 ± 22	80.4 ± 21	93.8 ± 22	0.011
LA volume/BSA, mL/m <sup>2</sup>	45 (35–50)	42 (35–49)	48 (38–51)	0.42
Reservoir strain, %	23.5 ± 6	24.7 ± 6	19.7 ± 6	0.002
Contractile strain, %	12.1 ± 4	12.8 ± 4	10.3 ± 3	0.014

AERP, atrial effective refractory period; AF, atrial fibrillation; IACV, intra-atrial conduction velocity; EGM, electrogram; LA, left atrium; BSA, body surface area.

## Chapter 7

JACC: CLINICAL ELECTROPHYSIOLOGY  
© 2019 BY THE AMERICAN COLLEGE OF CARDIOLOGY FOUNDATION  
PUBLISHED BY ELSEVIER

VOL. ■, NO. ■, 2019

# Pulmonary Vein Reconnection No Longer Occurs in the Majority of Patients After a Single Pulmonary Vein Isolation Procedure

Jan De Pooter, MD, PhD,<sup>a,b</sup> Teresa Strisciuglio, MD,<sup>a</sup> Milad El Haddad, PhD,<sup>a</sup> Michael Wolf, MD,<sup>a</sup> Thomas Philips, MD,<sup>a</sup> Yves Vandekerckhove, MD,<sup>a</sup> René Tavemier, MD, PhD,<sup>a</sup> Sebastien Knecht, MD, PhD,<sup>a</sup> Mattias Duytschaever, MD, PhD<sup>a,b</sup>

## **Introduction**

Pulmonary vein isolation (PVI) is considered the cornerstone for successful ablation in atrial fibrillation (AF). AF recurrence after PVI is assumed to be mediated by pulmonary vein reconnection (PVR). This assumption is based 1) on the observation that the likelihood of finding 4 isolated veins at repeat ablation is extremely low (varying from 41% to as low as 0%) and 2) on the good outcome after re-isolation of reconnected veins.

The "CLOSE" -protocol is a contact force (CF)- guided ablation protocol aiming to enclose the veins with stable, contiguous, and optimized (ablation index- guided) radiofrequency (RF) applications. This new approach of PVI is associated with a high rate of first-pass and adenosine-proof isolation and a high single-procedure arrhythmia-free survival at 1 year. In the present study, we determined the prevalence of patients presenting with 4 isolated veins at repeat ablation for AF recurrence after CLOSE-guided PVI. This endpoint is a relevant and objective parameter to evaluate effectiveness of any PVI strategy. We further investigated whether those patients (with non-PV-mediated AF recurrence) are characterized by specific clinical, first procedural, or post-procedural characteristics and whether outcome of repeat ablation in those patients is different from patients with reconnected veins.

## **Methods**

Patients undergoing repeat ablation for AF recurrence after first CLOSE-guided PVI were included. At repeat, 1) the status of the PV was evaluated and 2) high-density voltage mapping was performed. PVR was defined as residual PV potentials at the LA-PV junction detected by the decapolar lasso catheter or by the Thermocool Smart Touch catheter.

Patients with PVR underwent re-isolation of the reconnected vein(s). Patients revealing 4 isolated veins were treated by ablation of the empirical trigger or substrate. Empirical trigger

ablation consisted of superior vena cava isolation and/or widening of the circle around the veins. Adenosine or isoproterenol to elicit triggers was not systematically used. Substrate ablation was preferred in patients with ongoing AF at the time of procedure or in case of AF episodes lasting longer than 24 h. Empirical substrate ablation consisted of deployment of linear lesions (i.e., CLOSE-guided linear ablation at the roof, mitral isthmus, and anterior wall) during sinus rhythm or AF. Ablation was continued until there was a proven block over the roof and mitral isthmus line.

All patients had standard follow-up with clinical evaluation and 12-lead electrocardiograms at 1, 6, and 12 months and Holter at 6 months after repeat procedure. In case of symptoms, additional Holter analyses were performed. Recurrence of AF was registered after a 3-month blanking window. Of interest, 12 patients (27%) had continuous rhythm evaluation by implantable loop recorders (ILR).

## **RESULTS**

### *Status of the PV at repeat ablation for af recurrence after first close-guided PVI.*

Of 326 patients undergoing first CLOSE-guided PVI for paroxysmal AF, 45 patients underwent repeat ablation for AF recurrence (Figure 1). Of those 45 patients, 28 patients (62%) revealed 4 isolated veins. In patients with PVR (n =17) the mean number of reconnected veins was  $2 \pm 1$  with no predilection sites of PV reconnection (Figure 2, left).

### *Patients with 4 isolated veins: clinical characteristics, first procedural characteristics, and time to recurrence after first PVI*

Baseline clinical characteristics of all patients undergoing repeat ablation are listed in Table 1. Patients revealing 4 isolated veins at repeat had similar clinical characteristics as patients

with PVR. Also, the arrhythmic profile of the initial paroxysmal AF was not different, with similar AF burden, both in terms of frequency and duration of AF episodes. Compared with patients with PVR, patients revealing 4 isolated veins had also similar first procedural and RF characteristics (Table 2). We did not observe any difference in the RF characteristics (RF timeMed, AIMed, FTIMed, ILDMed, CFMed, or D-impedanceMed) of the RF circle deployed during the first procedure. Comparing circles with PVR to circles without reconnection could also not identify any differences in RF timeMed, AIMed, FTIMed, ILDMed, CFMed, or D-impedanceMed (Figure 2, right).

Finally, also the mean time to recurrence after prior PVI did not differ between groups ( $8 \pm 7$  vs.  $6 \pm 6$  months,  $p=0.453$ ) (Figure 3). Of interest, patients revealing 4 isolated veins at repeat (i.e., non-PV mediated AF recurrence) presented with a wide variation in time to AF recurrence after initial PVI.

#### *High-density bipolar voltage mapping of the LA*

Compared with patients with PVR, patients with 4 isolated veins were characterized by a higher incidence of low atrial voltage in the residual LA surface.

Representative examples are given in Figure 4 (left). Whereas the patient with AF recurrence and PVR showed no low voltage area in the posterior LA, the patient with AF recurrence and complete PV isolation presented with a distinct area of low voltage at the posterior LA (8.3 cm<sup>2</sup>). Overall results are summarized in the right panels of Figure 4. In patients with AF recurrence and 4 isolated veins, the incidence of low voltage was significantly higher (57% vs. 17% in PVR patients,  $p = 0.033$ ) and the area of low voltage was significantly larger (median: 4.6 [IQR: 2.3 to 7.9] cm<sup>2</sup> vs. 0.0 [IQR: 0.0 to 0.0] cm<sup>2</sup> in PVR patients,  $p = 0.049$ ). As can be

seen in Figure 3 (in which we color-coded in red those patients with low voltage), patients with low voltage present with both early and late recurrence after first PVI.

In 10 of 45 patients, we could compare the presence or absence of low voltage at repeat to a baseline high-density voltage map created during the first PVI procedure. None of these patients revealed any change in low voltage characteristics between baseline and repeat at  $7 \pm 6$  months. Representative maps are plotted in Figure 5 (left). Overall, in 3 patients presenting with low voltage at baseline, the surface of low voltage remained identical over time. Likewise, none of the 7 patients presenting with normal voltage at baseline developed low voltage (Figure 5, right).

#### *Outcome after repeat ablation*

In patients with PVR, all reconnected veins were reisolated. Of 28 patients with 4 isolated veins, 15 patients (54%) underwent empirical ablation of the trigger and 13 patients (46%) underwent ablation of the empirical substrate. Median follow-up after repeat ablation was  $13 \pm 11$  months. Patients with AF recurrence and complete vein isolation, tended to have a lower freedom of AF than did patients with PVR (61% vs. 88%,  $p=0.045$ ) (Figure 6). Time to AF recurrence after repeat procedure was  $6.5 \pm 4.8$  months in the PVR group versus  $5.7 \pm 2.1$  months in patients with a status of 4 isolated veins ( $p=1.00$ ).

#### *Repeat ablation in patients with ILR*

Of interest, from the 12 patients who were implanted with an ILR, AF recurrence was paroxysmal in 10 patients (83%) and persistent in 2 (17%). Of these ILR patients, 5 (42%) presented with PVR, whereas 7 (58%) presented with a status of all veins being isolated. In patients with ILR undergoing reisolation of all reconnected PV, 80% remained free

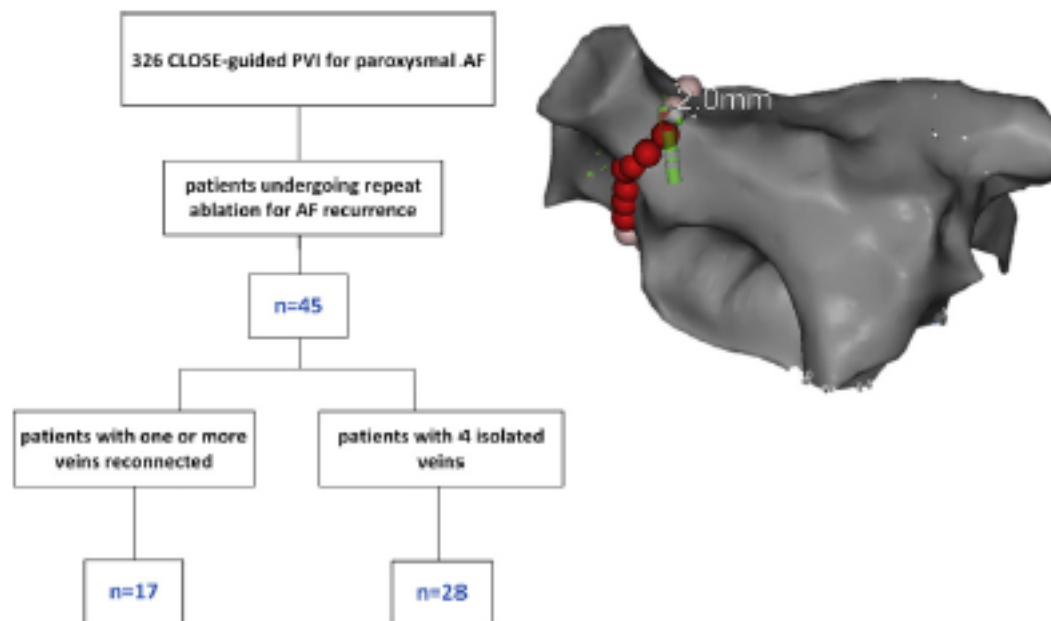


of AF, whereas 1 patients with ILR who underwent substrate or trigger ablation, 57% remained free of AF (p = 0.636).

## **Conclusion**

After PVI with stable, contiguous, and optimized (AI-guided) RF lesions (CLOSE-protocol), PVR is no longer the rule in patients experiencing AF recurrence. Patients with AF recurrence and 4 isolated veins present with a clinical profile and time to recurrence that is not different from patients with reconnected veins. The presence of low voltage regions and moderate outcome after repeat suggest that a patient-tailored strategy is required to treat patients with non-PV-mediated AF.

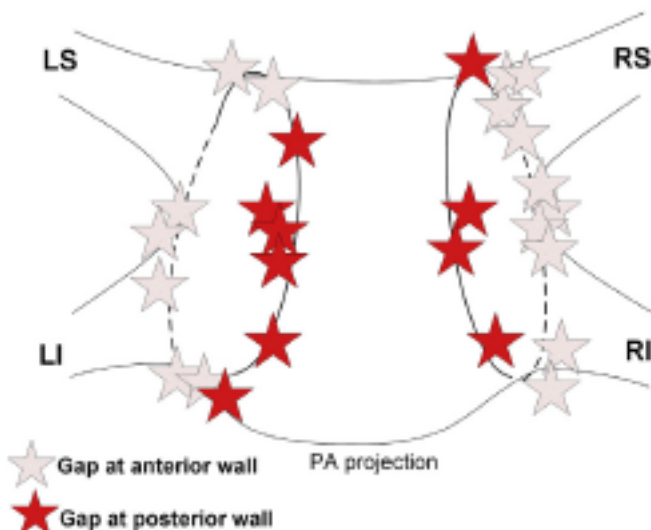
**FIGURE 1** Incidence of Four Isolated Veins After First CLOSE-Guided PVI



High incidence (28 of 45, 62%) of 4 isolated veins in patients with atrial fibrillation (AF) recurrence after first CLOSE-guided pulmonary vein isolation (PVI).

**FIGURE 2** Location of Gaps and Quality Analysis of Radiofrequency Circles

Localisation of gaps in patients with PV reconnection (27 gaps, 17 patients)

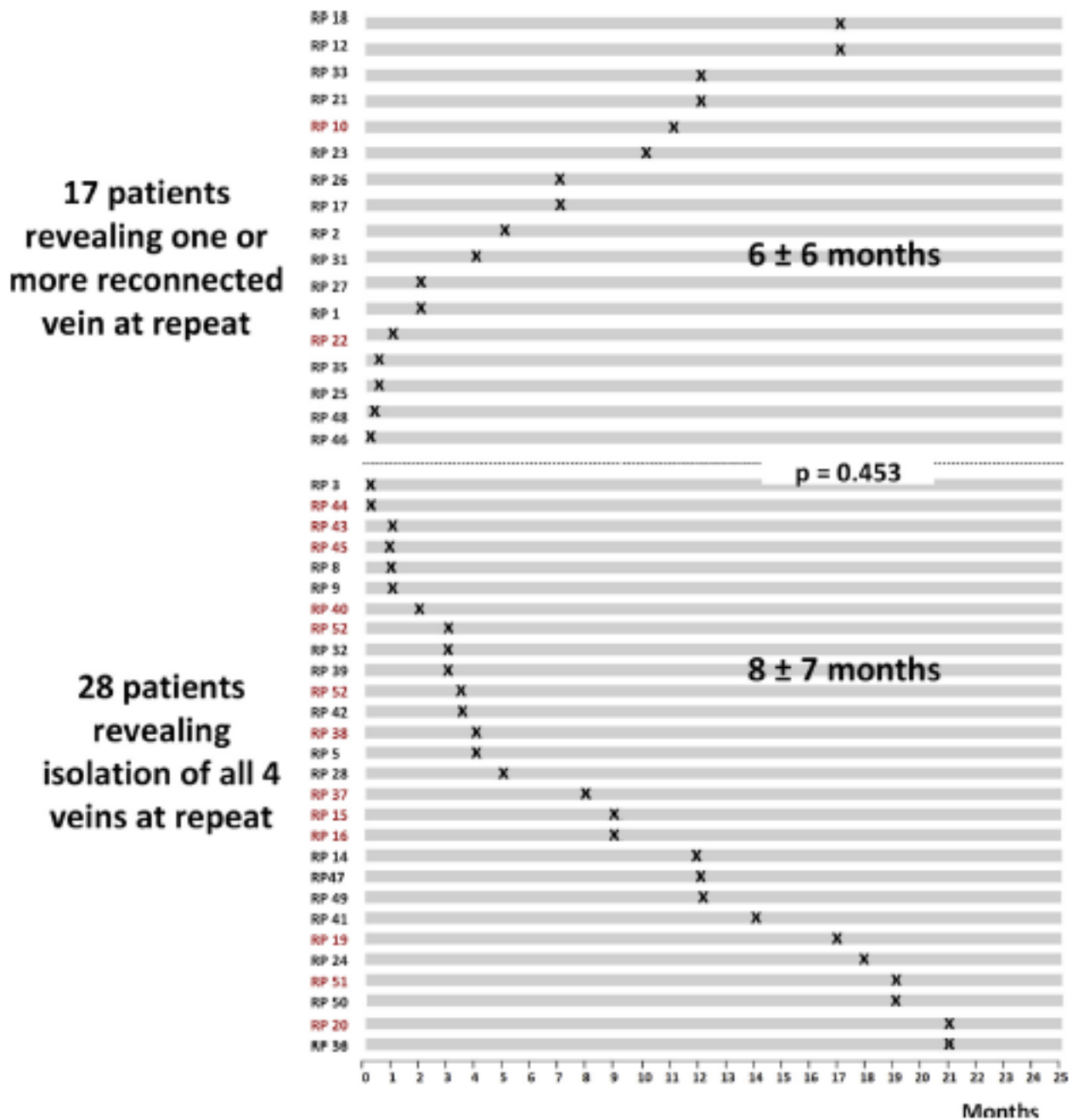


Quality analysis of the radiofrequency circle (circles with versus without reconnection)

Radiofrequency characteristics	Circles with PV reconnection	Circles with isolated veins	p value
Time <sub>total</sub> (min)	29 [27-31]	29 [26-32]	0.262
Ablation index <sub>total</sub> (au)	483 [477-487]	488 [478-496]	0.540
Force Time Integral <sub>total</sub> (gr)	412 [370-448]	428 [380-499]	0.244
Inter lesion distance <sub>total</sub> (mm)	4.1 [3.7-4.6]	3.9 [3.7-4.3]	0.112
Contact force <sub>total</sub> (g)	15 [13-18]	15 [13-18]	0.172
Δ Impedance <sub>total</sub> (ohm)	11 [10-16]	12 [11-13]	0.740

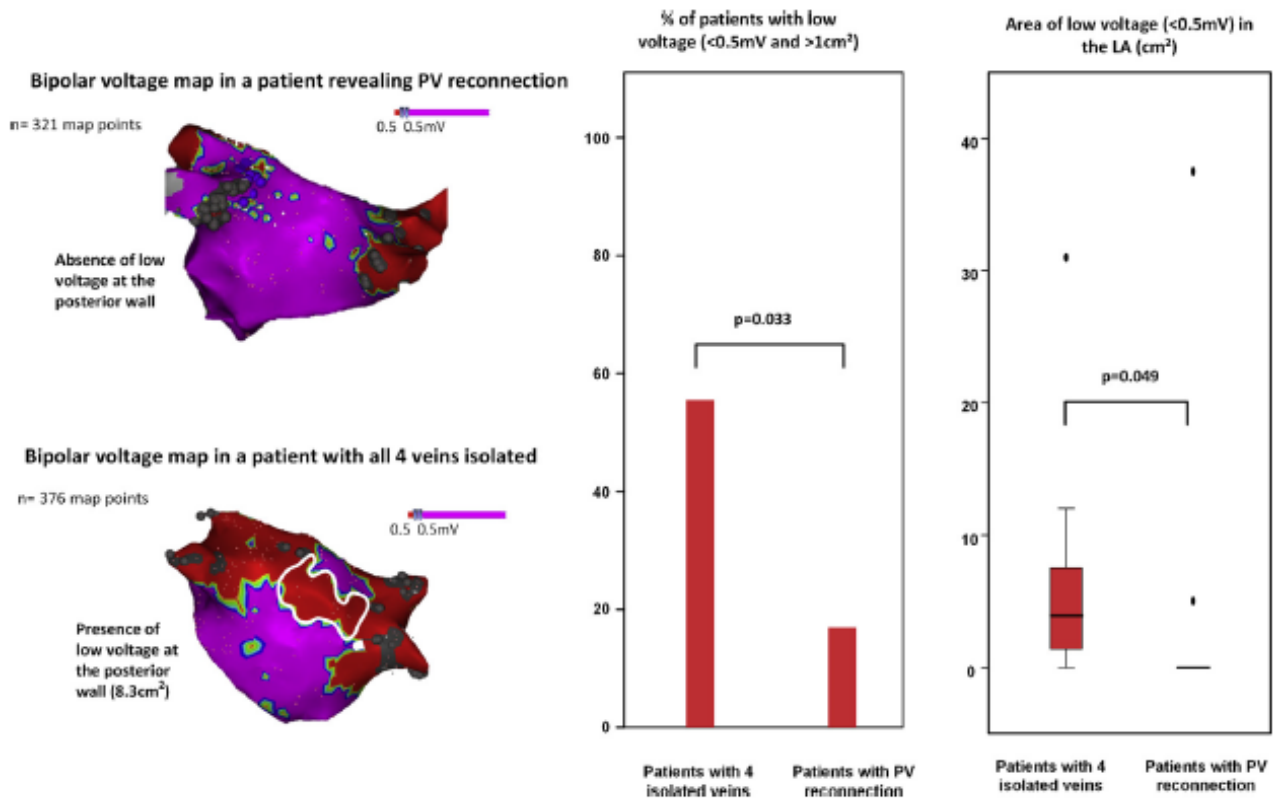
(Left) Localization of gaps in the ablation circles among patients (n = 17, 27 gaps) with atrial fibrillation recurrence and pulmonary vein (PV) reconnection. No predilection sites of PV reconnection could be identified. (Right) Circles with gaps showed similar lesion quality compared with circles with durable PV isolation. LI = left inferior; LS = left superior; PA = postero-anterior; RI = right inferior; RS = right superior.

**FIGURE 3** Timing of the First AF Recurrence After Initial PVI



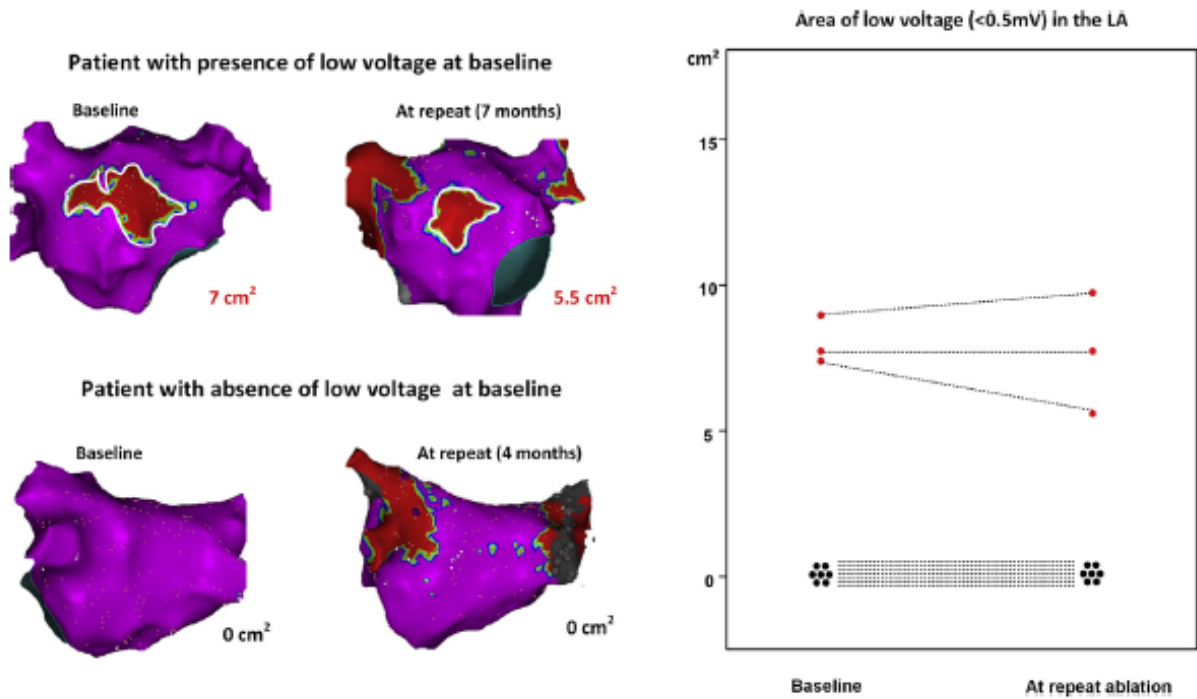
Time course to atrial fibrillation (AF) recurrence after first CLOSE-guided pulmonary vein isolation (PVI). Patients with a status of 4 veins being isolated, showed similar time course to first AF recurrence as patients with pulmonary vein reconnection. Of interest, patients with low voltage (red) present with both early and late recurrence after first PVI. RP – repeat patient (patient identification number).

**FIGURE 4 Low Voltage Assessment**



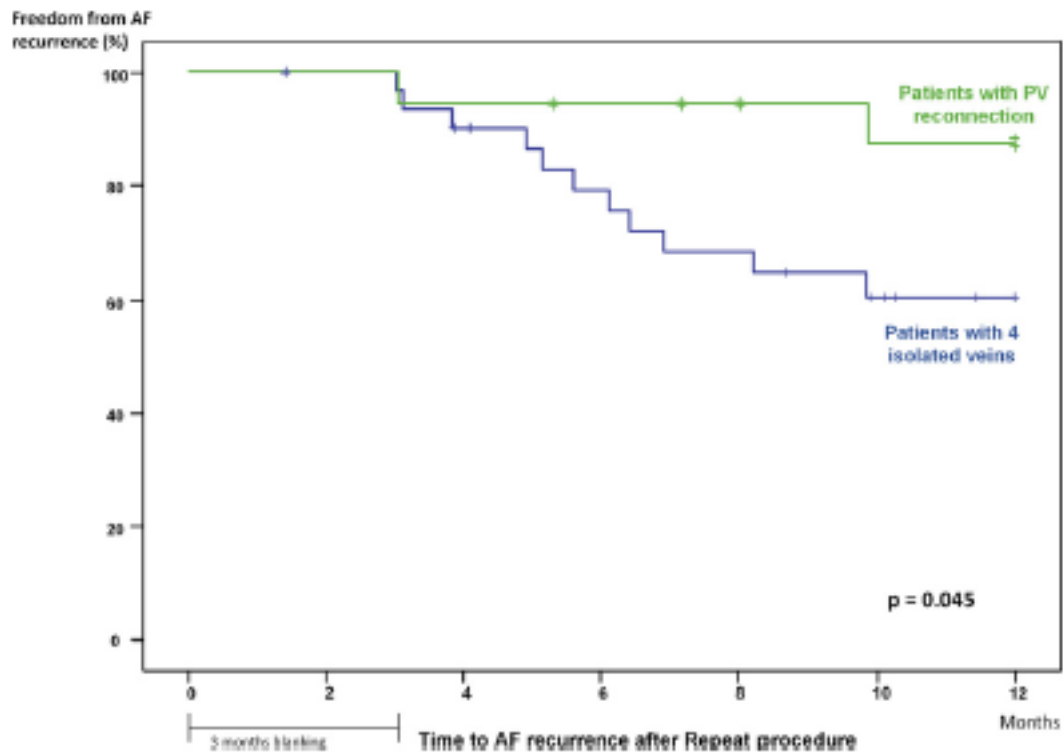
**(Left)** Representative examples of left atrial (LA) voltage mapping (bipolar voltage cut off 0.5 mV) in 2 patients with atrial fibrillation (AF) recurrence after first CLOSE-guided pulmonary vein (PV) isolation. **(Upper left)** The panel represents a patient with reconnection of the left inferior PV. The LA shows a normal bipolar voltage with absence of low voltage zones. **(Lower left)** The panel shows the voltage map of a patient with AF recurrence despite all 4 veins being isolated. A large area of low voltage at the posterior wall is documented. **(Right)** Overall, patients with AF recurrence despite isolated veins more often have areas (>1 cm<sup>2</sup>) of bipolar voltage <0.5 mV and have larger areas of low voltage compared with patients with PV reconnection.

**FIGURE 5 Evolution of Low Voltage Maps Between First Procedure and Repeat Ablation**



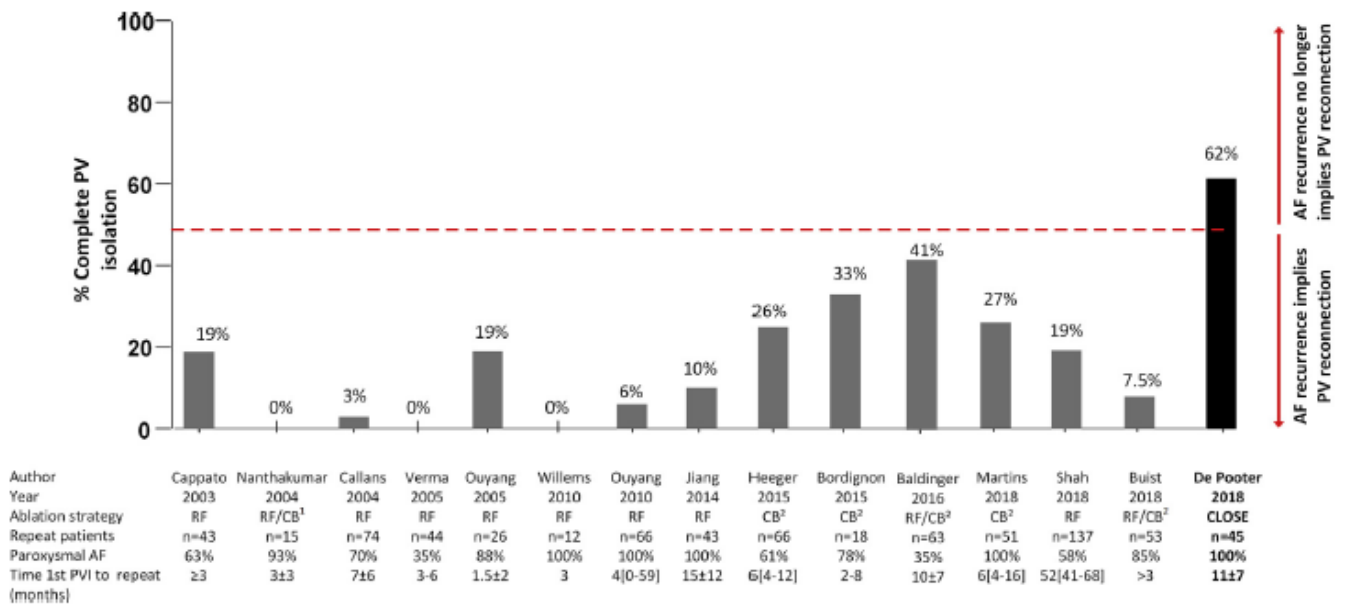
Comparison of the presence or absence of low voltage at repeat ablation to a baseline high-density voltage map created during the first pulmonary vein isolation procedure. **(Upper left)** The patient presented with an area of 7 cm<sup>2</sup> on the posterior wall, but showed no progression of this low voltage area 7 months later at repeat procedure. **(Lower left)** The patient without left atrial (LA) low voltage at baseline did not develop low voltage over a period of 4 months. **(Right)** Overall, in 3 patients presenting with low voltage at baseline, the surface of low voltage remained identical over time. Likewise, none of the 7 patients presenting with normal voltage at baseline developed low voltage.

**FIGURE 6** Time to AF Recurrence After Repeat Ablation



Kaplan-Meier curves depicting time to AF recurrence after repeat ablation for patients with and without PV reconnection at repeat ablation. Patients with all 4 veins being isolated (treated with either ablation of the empirical trigger or substrate) showed worse outcome. Abbreviations as in Figures 1 and 2.

**FIGURE 7** Incidence of Four Isolated Veins at Repeat Procedures for AF Recurrence



Overview of studies assessing the likelihood of finding 4 isolated veins after single PVI. After CLOSE-guided PVI, AF recurrence no longer implies PV reconnection. CB = cryoballoon; other abbreviations as in [Figures 1 and 2](#).

**TABLE 1** Clinical Characteristics of Patients Undergoing Repeat Procedure

	All Repeat Patients (n = 45)	Patients With 4 Isolated Veins (n = 28)	Patients With Reconnected Veins (n = 17)	p Value
<b>Patient characteristics</b>				
Age, yrs	61 ± 10	63 ± 10	59 ± 10	0.153
Male	23 (51)	12 (43)	11 (65)	0.221
BMI, kg/m <sup>2</sup>	27 ± 5	26 ± 5	28 ± 4	0.271
Obesity (BMI >25 kg/m <sup>2</sup> )	26 (58)	15 (54)	11 (65)	0.543
CHA <sub>2</sub> DS <sub>2</sub> -VASc-score	1 ± 1	1 ± 1	1 ± 1	0.617
Arterial hypertension	13 (29)	9 (32)	4 (24)	0.737
Diabetes	2 (4)	1 (4)	1 (6)	1.00
Obstructive sleep apnea	2 (4)	0 (0)	2 (12)	0.137
Left atrial diameter, mm	41 ± 4	41 ± 5	41 ± 4	0.811
<b>Characteristics of paroxysmal AF before PVI</b>				
Paroxysmal AF	45 (100)	27 (100)	17 (100)	1.00
AF duration, months	67 ± 86	75 ± 100	55 ± 61	0.916
ADT resistant	39 (87)	25 (89)	14 (82)	1.00
<b>Frequency of AF episodes</b>				
<1 episode/month	20 (45)	14 (50)	6 (35)	0.336
>1 episode/month	16 (36)	8 (29)	8 (47)	0.209
>1 episode/week	3 (7)	2 (7)	1 (6)	0.869
>1 episode/day	6 (13)	4 (14)	2 (12)	0.809
<b>Duration of AF episodes</b>				
>24 h	8 (18)	4 (14)	4 (24)	0.431
12-24 h	7 (15)	2 (7)	4 (24)	0.116
1-12 h	16 (36)	13 (47)	4 (24)	0.124
<1 h	14 (31)	9 (32)	5 (29)	0.848
<b>Characteristics of recurrence of AF after first PVI</b>				
Time to recurrence, months	7 ± 7	8 ± 7	6 ± 6	0.453
Initial responder (>1 month free of AF)	28 (62)	18 (64)	10 (59)	0.759

Values are mean ± SD or n (%).

ADT = antiarrhythmic drug therapy; AF = atrial fibrillation; BMI = body mass index; CHA<sub>2</sub>DS<sub>2</sub>-VASc = Congestive Heart Failure, Hypertension, Age ≥75 Years, Diabetes Mellitus, Prior Stroke or Transient Ischemic Attack or Thromboembolism, Vascular Disease, Age 65 to 74 Years, Sex; PVI = pulmonary vein isolation.



**TABLE 2** Characteristics of the First PVI Procedure in Patients Revealing 4 Isolated Veins at Repeat

	All Repeat Patients (n = 45)	Patients With 4 Isolated Veins (n = 28)	Patients With Reconnected Veins (n = 17)	p Value
<b>Procedure characteristics</b>				
General anesthesia	30 (67)	20 (74)	9 (53)	0.193
Common pulmonary vein	4 (9)	2 (7)	2 (12)	0.626
Procedure duration, min	162 ± 37	158 ± 41	168 ± 29	0.378
RF applications, points	71 ± 13	68 ± 13	75 ± 13	0.114
Total time of RF energy, min	33 ± 7	32 ± 6	35 ± 7	0.076
Fluoroscopy time, min	15 ± 8	13 ± 6	16 ± 9	0.211
DAP, mGy/cm <sup>2</sup>	7,569 ± 7,249	7,157 ± 7,366	8,252 ± 7,244	0.398
AK, mGy	36 ± 35	35 ± 37	38 ± 31	0.353
<b>RF circle characteristics</b>				
Time <sub>Med</sub> , min	29 (26-32)	29 (26-33)	28 (27-31)	0.365
Ablation index <sub>Med</sub> , AU	486 (478-494)	484 (478-496)	487 (479-494)	0.689
Force time integral <sub>Med</sub> , g · s	426 (379-484)	426 (370-501)	426 (386-451)	0.567
Interlesion distance <sub>Med</sub> , mm	3.9 (3.7-4.4)	4.1 (3.7-4.4)	3.9 (3.7-4.3)	0.907
Contact force <sub>Med</sub> , g	15 (13-18)	15 (13-18)	16 (14-18)	0.716
Δ-Impedance <sub>Med</sub> , Ω	12 (11-13)	12 (11-14)	12 (11-13)	0.772

Values are n (%), mean ± SD, or median (interquartile range).

AK – air kerma; AU – arbitrary unit; DAP – dose area product; PVI – pulmonary vein isolation; RF – radiofrequency.

Part III: What can we do better? Can we further improve the stability and/or increase the RF power?

## Chapter 8



**ESC**

European Society  
of Cardiology

Europace (2019) **21**, 1185–1192  
doi:10.1093/europace/euz115

**CLINICAL RESEARCH**

*Ablation for atrial fibrillation*

---

# Evaluation of a simple technique aiming at optimizing point-by-point isolation of the left pulmonary veins: a randomized study

**Maria Kyriakopoulou<sup>1,2</sup>, Teresa Strisciuglio<sup>1</sup>, Milad El Haddad<sup>1</sup>, Jan De Pooter<sup>1,3</sup>, Alexandre Almorad<sup>1</sup>, Katarina Van Beeumen<sup>1</sup>, Philippe Unger<sup>4</sup>, Yves Vandekerckhove<sup>1</sup>, René Tavernier<sup>1</sup>, Mattias Duytschaever<sup>1,3</sup>, and Sébastien Knecht<sup>1\*</sup>**

## **Introduction**

The standard endpoint during ablation of paroxysmal atrial fibrillation (AF) is pulmonary vein isolation (PVI), which can be reached in almost 100% of patients and which is associated with up to 92% success rates. Recent publications about radiofrequency (RF) point-by-point PVI have shown that criteria combining contiguity, stability, and lesion depth were associated with the best acute and long-term success rates. However, it remains sometimes challenging or time consuming to apply these criteria in all patients at the anterior part of the left pulmonary veins (PVs), where anatomy is complex and the catheter is therefore unstable. This can result in prolonged manoeuvring time of the catheter and/or catheter dislocations. In less experienced hands, it might even lead to inability to ensure contiguous or effective ablation lesions.

During the last years, we have developed a new technique with the goal of overcoming these potential problems. This consists of bending the ablation catheter in the left atrium, creating a loop that is then cautiously advanced together with the long sheath towards the ostium and then within the left superior PV (LSPV). The curve is then progressively released to reach a stable contact with the anterior part of the left PVs and the catheter can be gradually moved with stability from the inferior to the superior part of the left atrial ridge between the left atrial appendage (LAA) and the left PVs (Figures 1 and 2). This so-called 'Loop' technique has already been used in different circumstances during AF ablation<sup>11</sup> but has never been evaluated in the context of left PV encirclement with strict criteria concerning ablation index (AI) and contiguity.

The aim of the study was to prospectively evaluate the efficiency and the safety of this new technique (the so-called 'Loop' technique) for encircling the left PVs in patients ablated for the first time for paroxysmal AF.

## Methods

Eighty consecutive patients (age  $64 \pm 11$  years, left atrial diameter  $43 \pm 8$  mm) undergoing 'CLOSE'-guided PV isolation were prospectively randomized into two groups depending on whether the loop technique was used or not.

The 'loop' technique consisted of bending the ablation catheter in the left atrium, creating a loop that was then cautiously advanced together with the long sheath at the ostium and then within the LSPV. The curve was then progressively released to reach a stable contact with the anterior part of the left PVs and the catheter could be gradually moved from the inferior to the superior part of the LAA-left PVs ridge (Figures 1 and 2). To move on from one ablation point to the following one (at a more superior portion of the ridge), the sheath was somewhat rotated counterclockwise. The catheter was slightly curved in during its rotation to avoid high contact during manipulation and then carefully released to reach adequate contact again. The 'conventional' technique consisted of a more 'direct' approach of the catheter. Basically, for this technique, any manoeuvre could be used to reach the desired contact and stability at the anterior part of the left PVs, with the exception of what has been described for the loop technique. During ablation at the anterior part of the left PVs, if three consecutive dislocations (VisitagVR counting stop VisitagVR before reaching the desired AI) occurred for the same point in one of both groups, an attempt using the other technique could be used to reach the local contiguity and AI endpoint.

The ablation technique was the same for both groups concerning the encirclement of the right PVs and the other portions of the left PVs. All procedural parameters were recorded. Each procedure in both groups was exported and analysed offline. For each RF tag at the left PVs, we determined time of application (s), median delivered power (W), impedance drop ( $^{\circ}$ -Imp, X), average CF (CF, g), force-time integral (FTI, gs), and AI (arbitrary unit, au).

## Results

### *Population and procedural characteristics*

There were 80 patients (47 males) aged  $64 \pm 11$  years with a CHA2DS2-VASc score of 2 (range 0–6), an European Heart Rhythm Association (EHRA) symptoms score of 2 (range 1–3), and a left atrial diameter of  $43 \pm 8$  mm.

The global procedural time was 93 min [interquartile range (IQR) 73–117] [93 min (IQR 81–110) vs. 96 min (IQR 70–120) in the loop (Group A) and conventional (Group B) groups, respectively,  $P=0.7$ ], including a CTI line 20/80 patients (25%, 12 vs. 8 in loop vs. conventional groups,  $P=0.4$ ). There were no procedural complications and no steam pops in either group. All four PVs were isolated at the end of the procedure and after adenosine challenge in all patients.

### *Encirclement of the left pulmonary veins*

The 'loop' technique was associated with more efficient results for the entire left PV encirclement time [20 min (IQR 17–24) vs. 26 min (IQR 18–33),  $P < 0.01$ ] (see Figure 3).

The 'loop' technique resulted in a high rate of first pass isolation [40/40 (100%) (Group A) vs. 39/40 (97%) (Group B),  $P=0.9$ ] and adenosine proof isolation [37/40 (93%) Group A and 38/40 (95%) Group B,  $P=0.67$ ]. In total, three patients needed anterior touch ups at the anterior portion of the left PVs: one in the loop group and two in the conventional group.

The RF duration was shorter with the 'loop' technique [523 s (IQR 417–608) vs. 629 s (IQR 502–747),  $P=0.004$ ], however there was no significant difference concerning fluoroscopy time ( $37 \pm 23$  s vs.  $35 \pm 28$  s in Groups A and B, respectively,  $P=0.68$ ), radiation [DAP 183 mGy.cm<sup>2</sup> (IQR 90–346) vs. 140 mGy.cm<sup>2</sup> (IQR 72–210),  $P=0.332$ ; AK 1 mGy (IQR 0–1) vs.  $\pm 1$  mGy (IQR 0–2),  $P=0.69$ , in Groups A and B, respectively] and the dimensions of the left PV

encirclement [ $31 \pm 5$  mm (long diameter) X  $16 \pm 3$  mm (short diameter) in both groups]. See Table 1 for details.

#### *Anterior left pulmonary vein ablation*

The loop technique was possible in all 40 patients, from the anterior portion of the left inferior PV (LIPV) (middle part) to the anterior portion of the LSPV (middle or superior part,  $7 \pm 2$  ablation points per patient, see Figure 4). Using the loop technique significantly reduced ablation time [ $433$  s (IQR 344–576) vs.  $629$  s (IQR 460–914),  $P = 0.039$ ], RF duration ( $272 \pm 85$  s vs.  $378 \pm 122$  s,  $P < 0.001$ ), the amount of ablation points ( $9 \pm 2$  vs.  $12 \pm 4$ , in Groups A and B, respectively,  $P < 0.001$ ), and the amount of dislocation points [ $0$  (IQR 0–0) vs.  $1$  (IQR 0–4),  $P < 0.001$ ]. Using the loop technique was associated with higher average CF during RF applications [ $20$  g (IQR 13–27) vs.  $11$  g (IQR 9–16),  $P < 0.001$ ], higher FTI [ $524$  gs (IQR 427–687) vs.  $398$  gs (IQR 354–451),  $P < 0.001$ ], and higher impedance drop for the entire anterior portion of the left PVs [ $12$  X (IQR 9–19) vs.  $10$  X (IQR 7–14),  $P < 0.001$ ] and for the antero-superior part of them [ $14$  X (IQR 10–19) vs.  $10$  X (IQR 7–13),  $P < 0.001$ ]. The AI was similar in both groups [ $560$  (IQR 557–563) vs.  $561$  (IQR 557–564)]. In the conventional group, three consecutive dislocations for the same ablation points occurred in eight out of 40 patients. For these dislocation points, the loop technique was then allowed and was always successful at the first attempt. Not a single dislocation occurred when using the loop technique.

#### **Conclusion**

This study describes a simple way to position the ablation catheter at the anterior part of the left PVs. This easy and straightforward technique enables better catheter stability in a complex anatomical region, resulting in faster and more efficient left PV encirclement, without compromising safety.

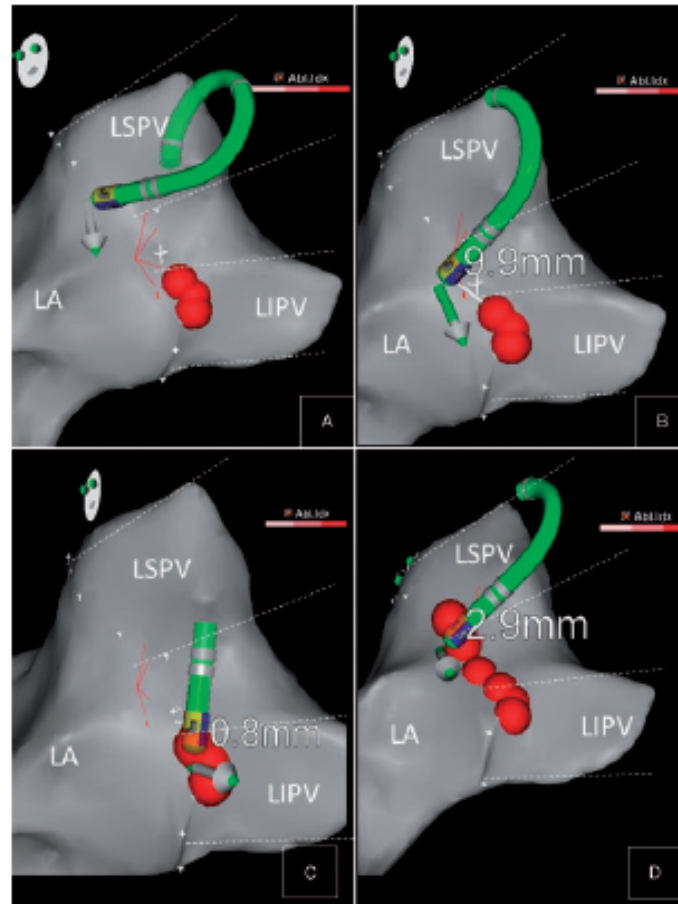


**Figure 1** The loop technique: CARTO modified LAO views of the LAA-left PVs ridge. The tagged white points correspond to the most proximal portion of the left PV ostium. The LAA has intentionally been cut-off for the clarity of the image. A loop of the ablation catheter is performed in the LA. The bended ablation catheter is then inserted in the LSPV (white dotted lines) (A). The curve is then progressively released to reach a stable contact with the anterior part of the left PVs (B). The catheter is then gradually moved from the LIPV (white dotted lines) to the superior part of the LAA-left PVs ridge to allow for RF ablation points (C and D). LA, left atrium; LAA, left atrial appendage; LAO, left anterior oblique; LIPV, left inferior PV; LSPV, left superior PV; PV, pulmonary vein; RF, radiofrequency.

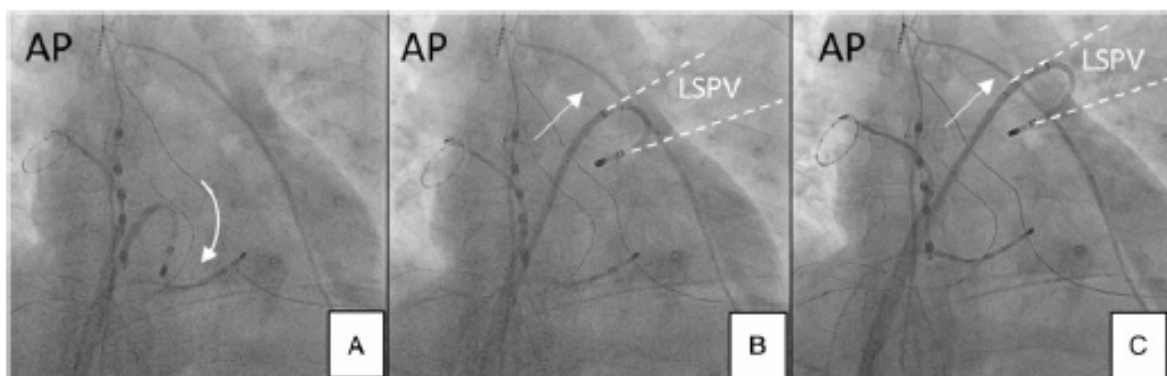


**Figure 2** The LOOP technique: AP fluoroscopic views showing the heart contour, a catheter inserted in the coronary sinus, a lasso catheter inserted in the right superior PV and oesophageal temperature monitoring. Ablation catheter curved into the LA (loop) (A) and then cautiously advanced together with the long sheath towards the ostium (B) and then within (C) the LSPV (white dotted lines). AP, antero-posterior; LA, left atrium; LSPV, left superior PV; PV, pulmonary vein.

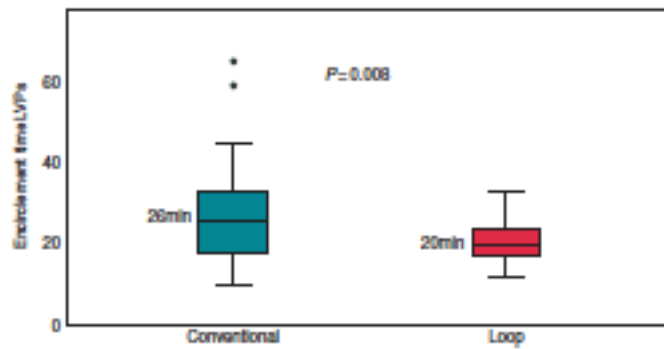


**Figure 3** Duration of left PV encirclement using either the loop or a conventional technique.

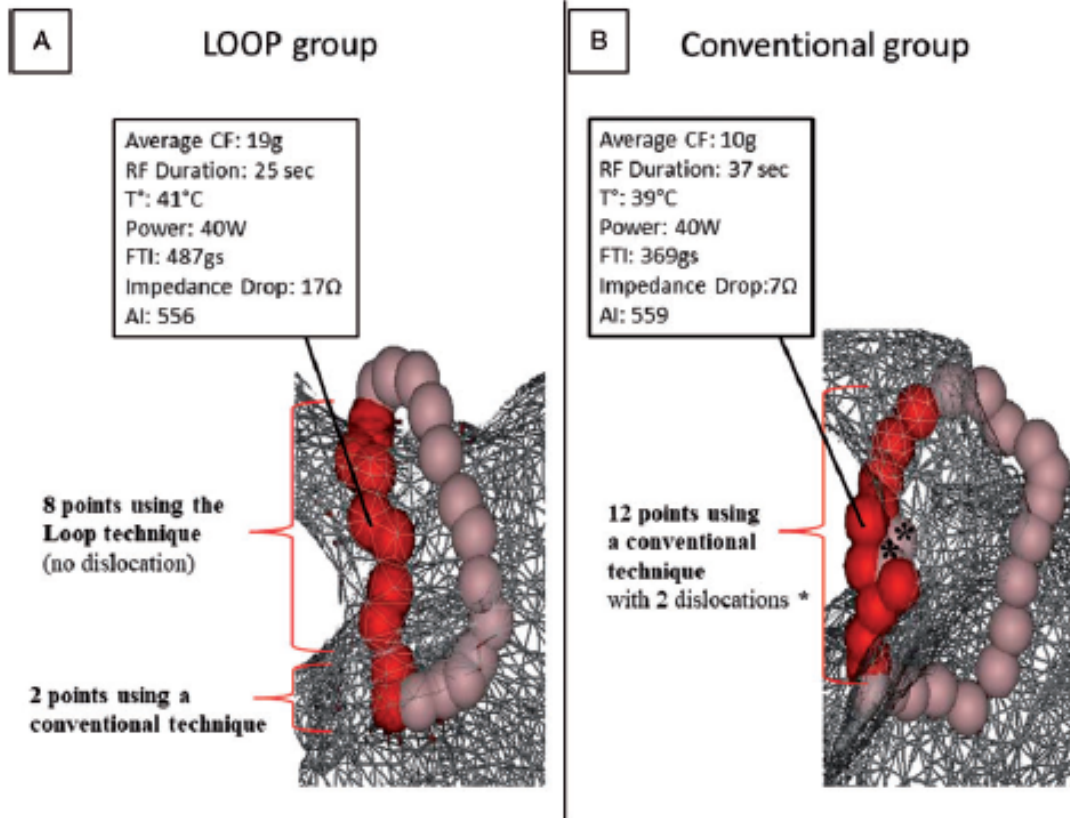


**Figure 4** Two illustrative examples of left PV encirclement (and the parameters of one ablation point on the anterior part of it) using the loop technique (A) or a conventional technique (B). AI, ablation index; FTI, force-time integral; PV, pulmonary vein; RF, radiofrequency.



**Table 1**

	Loop (n = 40)	Conventional (n = 40)	P-value
Encirclement time (min), median (IQR)	20 (17–24)	26 (18–33)	0.008
First pass encirclement isolation rate	40/40 (100%)	39/40 (97.5%) <sup>a</sup>	0.9
Acute reconnection (after adenosine)	3/40 (7%) <sup>b</sup>	2/40 (5%) <sup>b</sup>	0.671
Amount of ablation points, median (IQR)	22 (20–25)	28 (22–31)	0.001
RF duration (s), median (IQR)	523 (417–608)	629 (502–747)	0.004
Long diameter (mm), mean ± SD	31 ± 5	31 ± 5	0.879
Short diameter (mm), mean ± SD	16 ± 3	16 ± 3	0.935
DAP (mGy·cm <sup>2</sup> ), median (IQR)	183 (90–346)	140 (72–210)	0.332
AK (mGy), median (IQR)	1 (0–1)	1 (0–2)	0.690
Fluoroscopy time (s), mean ± SD	37 ± 23	35 ± 28	0.680

AK, air kerma; DAP, dose area product; IQR, interquartile range; RF, radiofrequency; SD, standard deviation.

<sup>a</sup>Patient 28 (conventional group): gap at the mid portion of the anterior wall.

<sup>b</sup>Patient 17 (conventional) two touch ups at the anterior wall (anteroinferior portion), patient 28 (conventional) two touch ups at the anterior wall (anterosuperior portion), patient 78 (conventional) three touch ups at the posterior wall, patient 30 ('loop' group) two touch ups at the anterior wall (anteromedian portion), patient 66 ('loop') four touch ups at the posterior wall, patient 73 ('loop') three touch ups at the posterior wall.

## Chapter 9

ORIGINAL - ELECTROPHYSIOLOGY

WILEY

### Evaluation of higher power delivery during RF pulmonary vein isolation using optimized and contiguous lesions

Maria Kyriakopoulou MD<sup>1,2</sup> | Jean-Yves Wielandts MD, MSc, PhD<sup>1</sup> |  
Teresa Strisciuglio MD<sup>1</sup>  | Milad El Haddad MSc, PhD<sup>1</sup> | Jan De Pooter MD, PhD<sup>3</sup> |  
Alexandre Almorad MD<sup>1</sup> | Gabriela Hilfiker MD<sup>1</sup> | Thomas Philips MD<sup>1</sup> |  
Philippe Unger MD, PhD<sup>4</sup> | Michelle Lycke MSc, PhD<sup>1</sup> | Yves Vandekerckhove MD<sup>1</sup> |  
Rene Tavernier MD, PhD<sup>1</sup> | Mattias Duytschaever MD, PhD<sup>1</sup> |  
Sebastien Knecht MD, PhD<sup>1</sup> 

*J Cardiovasc Electrophysiol.* 2020;31:1091–1098.

## **Introduction**

The “CLOSE” protocol consists of contact force (CF) - guided delivery of closely spaced (interlesion distance  $\leq 6$  mm) and optimized lesions (ablation index (AI)  $\geq 400$  posteriorly and  $\geq 550$  anteriorly) close to the pulmonary vein (PV) ostia. It has been associated with a high rate of the first - pass PVI, a lower rate of acute PV reconnection and a high rate of singleprocedure freedom of atrial fibrillation (AF). The AI formula has shown its correlation with lesion depth and combines RF power, CF between the catheter and the atrial wall and the duration of each RF application. Nonetheless, the optimal RF power to reach the desired AI target according to the “CLOSE” protocol for PVI remains unknown. Increased power theoretically results in reduced RF application duration when there is a similar CF. - However, the use of higher power could also potentially increase the complication rate, the risk of steam pop or esophageal injury. While historically the power was set below 35W (mostly  $\leq 25$ W at the posterior wall), recent studies using AI as targeted endpoint have shown promising results with a power  $\geq 35$  W. In all three of these studies, STSF catheters were used (SmartTouch Surround Flow; Biosense Webster Inc, Irvine, CA). The aim of the present study was to evaluate the efficiency and safety of an ablation strategy using higher power (40 W) as compared with the patients enrolled in the “CLOSE to Cure” study who were treated with a more conventional approach (35 W) during a first time “CLOSE” - guided PVI for paroxysmal AF, using an ST open - tip irrigation catheter (ThermocoolSmartTouch; Biosense Webster Inc).

## **Methods**

Eighty consecutive patients undergoing “CLOSE” - guided PVI for symptomatic paroxysmal atrial fibrillation were ablated with 40W(group A). Results were compared

with 105 consecutive patients enrolled in the “CLOSE to CURE” - study and were ablated using the same protocol with 35W (group B). A 1 - month follow - up was conducted in all of the patients to exclude any short - term procedural complications.

One - year clinical follow - up data for both groups were also analyzed. This data consisted of procedure - related complications, arrhythmia recurrence, and antiarrhythmic drug treatment continued up to 1 year after the ablation procedure.

Arrhythmia recurrence in group A was defined as any atrial tachyarrhythmia (ATA) > 30 seconds on Holter at 1 year or earlier on the anamnestic indication. This was put in comparison to the data from the “CLOSE to CURE” population - based on internal loop recorder (ILR) data for the duration of 1 year. Both groups respected a postprocedural arrhythmia recurrence blanking period of 3 months. Antiarrhythmic drug therapy (ADT; class I or class III) continuation was left at the discretion of the treating physician in group A. In group B, ADT was stopped after the 3 - month blanking period and only reinstated at the discretion of the treating physician at ATA recurrence.

## **Results**

### *Global procedural results*

When using an RF power of 40W (group A), there was a shorter ablation procedure time (91 minutes [IQR: 80 - 103] vs 111 minutes [IQR: 94 - 162];  $P < .001$ ), a shorter fluoroscopy time (5 minutes [IQR: 3 - 9] vs 11 minutes [IQR: 8 - 14];  $P < .001$ ), less radiation (air Kerma: [9 mGy (IQR: 4 - 13) vs 18 mGy (IQR: 12 - 29);  $P < .001$ ]); lower dose area product ([1638 mGy/cm<sup>2</sup> (IQR: 905 - 2666) vs 4040 mGy/cm<sup>2</sup> (IQR: 2552 - 6393);  $P < .001$ ]) in groups A

and B, respectively, despite the fact that there were more CTI ablations in group A (20/80 [25%] vs 6/105 [6%];  $P < .001$ ) (Table 2 and Figure 1).

#### *PVI characteristics*

In group A, the total RF time was shorter (20 minutes [IQR: 16 - 22] vs 28 minutes [IQR: 24 - 32];  $P < .001$ ), the time to isolate the PVs was shorter (48 minutes [IQR: 37 - 57] vs 64 minutes [IQR: 55 - 77];  $P < .001$ ), the number of RF applications was lower (52 [IQR: 46 - 58] vs 58 [IQR: 52 - 64];  $P < .001$ ), the RF time per application was shorter (22 seconds [IQR: 21 - 24] vs 29 seconds [IQR: 27 - 30];  $P < .001$ ) and the number of dislocations was lower (1 [IQR: 0 - 3] vs 2 [IQR: 1 - 4];  $P = .002$ ) (Table 2 and Figure 2). In group A, the median CF (13 g [IQR: 12 - 15] vs 14 g [IQR: 12 - 15];  $P = .035$ ) and force - time integral (FTI) were lower (283 gs [IQR: 258 - 314] vs 365 gs [IQR: 339 - 402];  $P < .001$ ) when compared with group B. The impedance drop was similar in both groups (12  $\Omega$  [IQR: 11 - 13] vs 13  $\Omega$  [IQR: 11 - 14];  $P = .192$ ), in group A and group B, respectively (Table 2 and Figure 2).

#### *Anterior wall and posterior walls*

In group A, the RF time per RF application was shorter (anterior wall: 34 seconds [IQR: 28 - 40] vs 42 seconds [IQR: 35 - 51];  $P < .001$  and posterior wall: 16 seconds [IQR: 14 - 19] vs 20 seconds [IQR: 16 - 25];  $P < .001$ ), as well as the FTI (anterior wall: 426 gs [IQR: 383 - 501] vs 540 gs [IQR: 479 - 629];  $P < .001$  and posterior wall: 177 gs [IQR: 149 - 225] vs 240 gs [IQR: 197 - 304];  $P < .001$ ). The average CF was lower at the posterior wall in group A (11 g [IQR: 8 - 14] vs 12 g [IQR: 9 - 17];  $P < .001$ ), but it was similar at the anterior wall in both groups

(13 g [IQR: 10 - 18] vs 13 g [IQR: 10 - 18]; P = .196, group A and Group B, respectively).

Finally, the impedance drop was lower at the posterior wall in group A (11  $\Omega$  [IQR: 7 - 15] vs 11  $\Omega$  [IQR: 8 - 16]; P < .001), but it was similar at the anterior wall in both groups (12  $\Omega$  [IQR: 9 - 16] vs 12  $\Omega$  [IQR: 9 - 17]; P = .778), group A and group B, respectively (Tables 3 and 4).

#### *Procedural outcome and complications*

The first - pass isolation rate was similar (79/80 patients [99%] vs 98/ 105 patients [93%]; P = .1414), as well as the reconnection rate after adenosine test (5/80 patients [6%] vs 4/97 patients [4%]; P = .733), in group A and group B, respectively (Table 2). No procedural complication, especially no steam pop, no cardiac perforation, no stroke, and no death occurred in both groups. In group A, a gastroscopy was performed in five patients with esophageal temperature rise more than 42°C during PVI after a median of 10 days (range 7 - 13) after ablation and did not reveal any esophageal injury. None of the patients developed esophageal fistula at a 1 - month clinical follow - up.

#### *One - year follow - up*

ATA recurrence within the first year was not significantly different between both groups (8/80 patients [10%] vs 14/105 patients [13.3%]; P = .647).

Use of ADT after 3 months blanking period was 19 of 80 in group A and 5 of 105 in group B (this was left at the discretion of the treating physician in group A and only reinstated in case of ATA recurrence after 3 months blanking period in group B). ADT used were Flecainide (8 vs 2), Sotalol (8 vs 3), and Amiodarone (3 vs 0) in groups A and B, respectively. By considering

both ATA recurrence or continued use of antiarrhythmic drugs at 1 year postprocedure as a failure, 1 - year failure was not significantly different in both groups either (20/80 patients [25%] vs 14/105 patients [13.3%]; P = .06).

Moreover, no esophageal injury or atrioesophageal fistula was noted during the follow - up.

## **Conclusion**

High power during “CLOSE” - guided AF ablation increases the efficiency of PVI, mostly by reducing RF duration, the time to isolate the PVs, the amount of dislocations and the ablation procedure time, without compromising patient's safety. These results still have to be confirmed by a randomized prospective study.

Table 2 Procedural characteristics of the study population

	Group A (40 W) (n = 80)	Group B (35 W) (n = 105)	P value
Total RF time, min	20 (IQR: 16-22)	28 (IQR: 24-32)	<.001
Amount of RF applications, (n)	52 (IQR: 46-58)	58 (IQR: 52-64)	<.001
Median RF time per application, s	22 (IQR: 21-24)	29 (IQR: 27-30)	<.001
Median CF, g	13 (IQR: 12-15)	14 (IQR: 12-15)	.035
Median T, °C	39 (IQR: 37-40)	39 (IQR: 39-40)	.039
Median power, W	39 (IQR: 38-40)	34 (IQR: 34-35)	<.001
Median FTI, gs	283 (IQR: 258-314)	365 (IQR: 339-402)	<.001
Median impedance drop, Ω	12 (IQR: 11-13)	13 (IQR: 11-14)	.192
Ablation index	466 (IQR: 459-474)	470 (IQR: 459-481)	.085
First-pass isolation, (n)	79/80 (99%)	98/105 (93%)	.141
Reconnection rate after adenosine, (n)	5/80 (6%)	4/97 (4%) <sup>a</sup>	.733
Dislocation points, (n)	1 (IQR: 0-3)	2 (IQR: 1-4)	.002
PVI time, min	48 (IQR: 37-57)	64 (IQR: 55-77)	<.001
Ablation procedure time, min	91 (IQR: 80-103)	111 (IQR: 94-162)	<.001
Fluoroscopy time, min	5 (IQR: 3-9)	11 (IQR: 8-14)	<.001
Air kerma (AK), mGy	9 (IQR: 4-13)	18 (IQR: 12-29)	<.001
Dose area product (DAP), mGy/cm <sup>2</sup>	1638 (IQR: 905-2666)	4040 (IQR: 2552-6393)	<.001

Note: Results are presented as median (interquartile range) or n(%). Bold values indicate a significance level of  $P < .05$ .

Abbreviations: CF, contact force; FTI, force-time integral; IQR, interquartile range; PVI, pulmonary vein isolation; RF, radiofrequency.

<sup>a</sup>Adenosine test performed in 97 out of 105 patients.



Table 3 RF applications characteristics at the anterior wall of pulmonary veins

<b>Anterior wall median (IQR)</b>	<b>Group A (40 W) (n = 1326 RF applications)</b>	<b>Group B (35 W) (n = 2182 RF application)</b>	<b>P value</b>
RF time per application, s	34 (IQR: 28-40)	42 (IQR: 35-51)	<b>&lt;.001</b>
Average CF, g	13 (IQR: 10-18)	13 (IQR: 10-18)	.196
Maximum T, °C	39 (IQR: 37-41)	40 (IQR: 39-41)	<b>&lt;.001</b>
Maximum power, W	40 (IQR: 40-40)	35 (IQR: 35-35)	<b>&lt;.001</b>
Force-time integral, gs	426 (IQR: 383-501)	540 (IQR: 479-629)	<b>&lt;.001</b>
Impedance drop, Ω	12 (IQR: 9-16)	12 (IQR: 9-17)	.778
Ablation index	560 (IQR: 558-564)	566 (IQR: 560-574)	<b>&lt;.001</b>

Abbreviations: CF, contact force; IQR, interquartile range; RF, radiofrequency. Bold values indicate a significance level of  $P < .05$ .

Table 4 RF applications characteristics at the posterior wall of pulmonary veins

<b>Posterior wall median (IQR)</b>	<b>Group A (40 W) (n = 2697 RF applications)</b>	<b>Group B (35 W) (n = 3940 RF application)</b>	<b>P value</b>
RF time per application, s	16 (IQR: 14-19)	20 (IQR: 16-25)	<b>&lt;.001</b>
Average CF, g	11 (IQR: 8-14)	12 (IQR: 9-17)	<b>&lt;.001</b>
Maximum T, °C	38 (IQR: 36-40)	39 (IQR: 38-40)	<b>&lt;.001</b>
Maximum power, W	40 (IQR: 38-40)	35 (IQR: 35-35)	<b>&lt;.001</b>
Force-time integral, gs	177 (IQR: 149-225)	240 (IQR: 197-304)	<b>&lt;.001</b>
Impedance drop, Ω	11 (IQR: 7-15)	11 (IQR: 8-16)	<b>&lt;.001</b>
Ablation index	420 (IQR: 413-431)	424 (IQR: 412-440)	<b>&lt;.001</b>

Abbreviations: CF, contact force; IQR, interquartile range; RF, radiofrequency. Bold values indicate a significance level of  $P < .05$ .

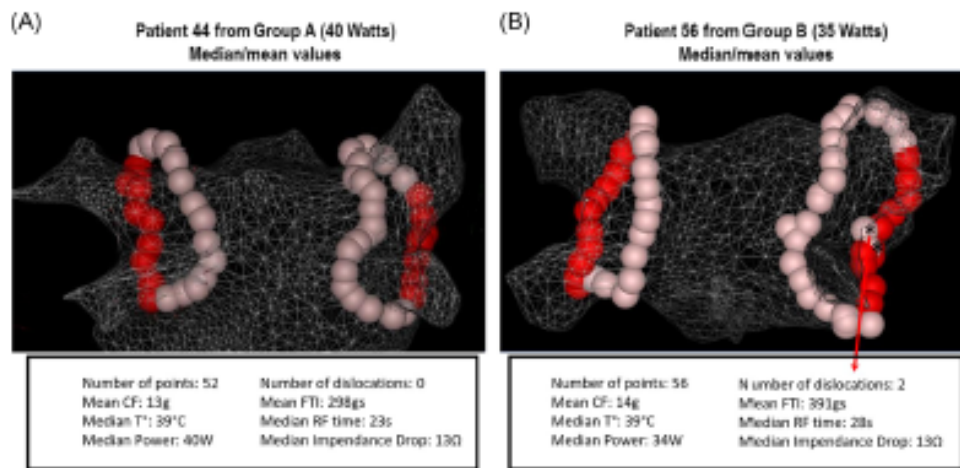
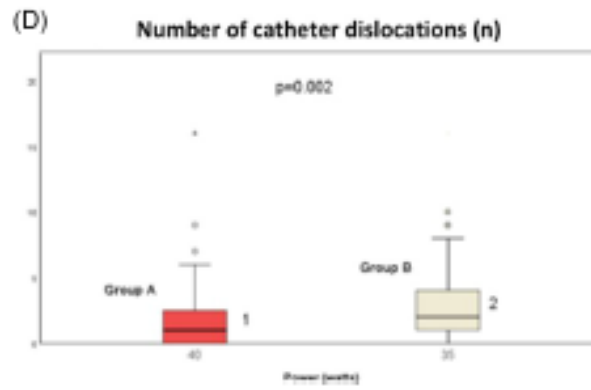
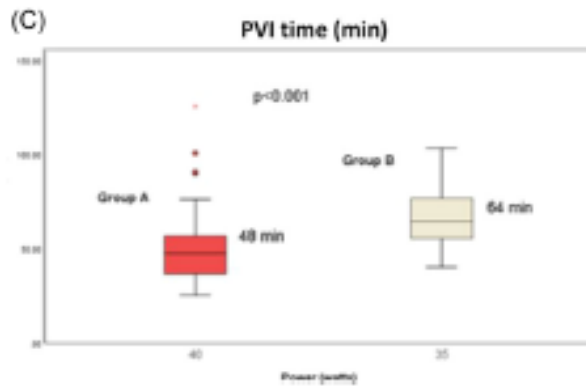
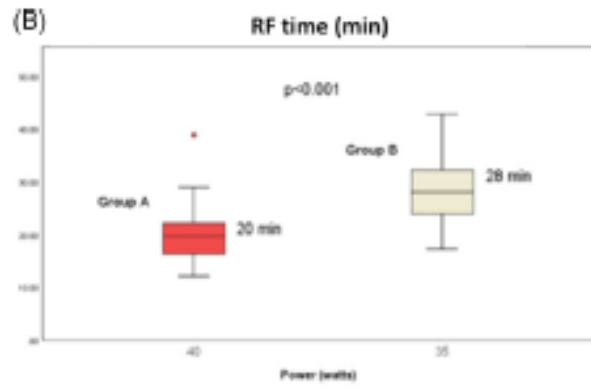
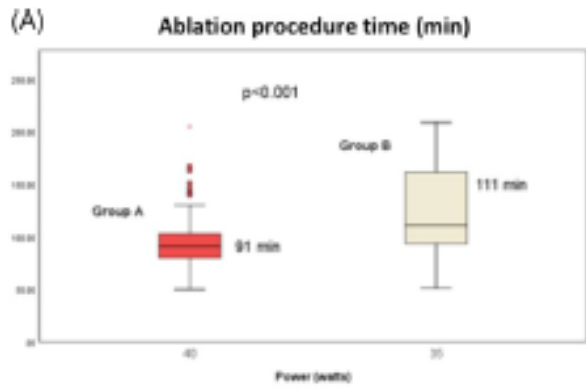


**FIGURE 1** Two representative examples of "CLOSE"-guided encirclement of the pulmonary veins (PV) and the radiofrequency parameters (median/median value) of all VISITAG points in one patient from group A (40 W; A) and one patient from group B (35W; B). Poster anterior view. Red VISITAG points with ablation index (AI) > 550 and pink VISITAG points with AI > 400. Asterisk (\*) on two dislocation points in group B (35W)



## Chapter 10

### **Prospective Randomized Evaluation of High Power during CLOSE-guided Pulmonary Vein Isolation: The POWER-AF study**

Jean-Yves Wielandts, MD, MSc, PhD<sup>1</sup>; Maria Kyriakopoulou, MD<sup>1</sup>; Alexandre Almorad, MD<sup>1</sup>; Gabriela Hilfiker, MD<sup>1</sup>; Teresa Strisciuglio, MD<sup>1</sup>; Thomas Phlips, MD<sup>1</sup>; Milad El Haddad, MSc, PhD<sup>1</sup>; Michelle Lycke, MSc, PhD<sup>1</sup>; Philippe Unger, MD, PhD<sup>2</sup>; Jean-Benoît Le Polain de Waroux, MD, PhD<sup>1,3</sup>; Yves Vandekerckhove, MD<sup>1</sup>; Rene Tavernier, MD, PhD<sup>1</sup>; Mattias Duytschaever, MD, PhD<sup>1,4</sup>; Sebastien Knecht, MD, PhD<sup>1</sup>.

*Under peer review*

## **Abstract**

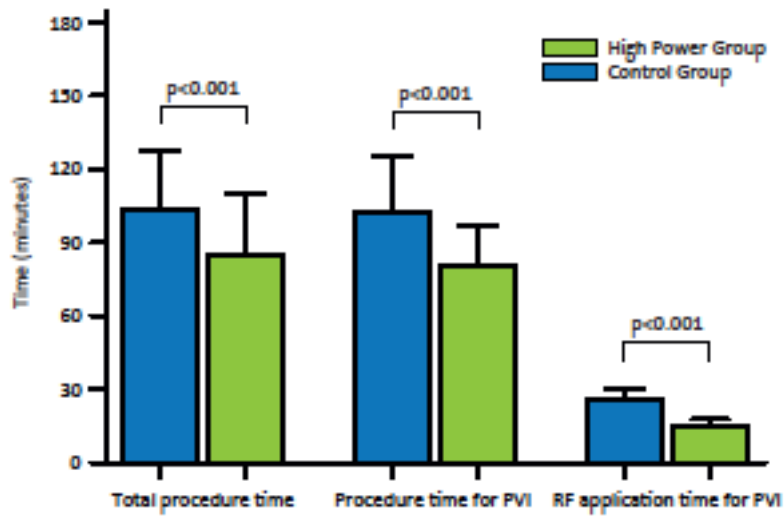
**Background:** CLOSE-guided atrial fibrillation (AF) ablation is based on contiguous (inter-tag distance  $\leq 6$ mm), optimized (Ablation Index (AI)  $>550$  anteriorly and  $>400$  posteriorly) point-by-point radiofrequency (RF) lesions. The optimal RF power remains unknown.

**Methods:** The POWER-AF study is a prospective, randomized controlled monocentric study including patients with paroxysmal AF, planned for first CLOSE-guided PVI using a contact force RF catheter (Thermocool SmartTouch®, Biosense Webster Inc., Irvine, CA, USA). A total of 100 patients were randomized into two groups (1:1). The control group received AF ablation using the standard CLOSE protocol (35W), while in the experimental group PVI was performed using high power (45W). Endoscopic evaluation was performed in patients with intraesophageal temperature rise  $>38.5$ {degree sign}C.

**Results:** The resulting sample size was 96 (48+48) patients. In the high power group, shorter procedure time (80min vs. 102min,  $p<0.001$ ), shorter total RF application time [16min vs. 26min ( $p<0.001$ )] and RF time per application [26 vs. 37s anteriorly,  $p<0.001$  and 13 vs. 17s posteriorly,  $p<0.001$ ] were observed. Endoscopic evaluation (performed in 19/48 vs. 25/48 patients respectively,  $p=0.31$ ) showed an ulcerative perforation in a high power group patient (treated by endoscopic stenting and normalization after ~4months) and a superficial ulcerative lesion in a control group patient (conservative treatment). Both occurred following excessive AI applications (up to 460 and 480 resp.) with excessive CF (30g on average, with peaks up to 50g). Six-months AF recurrence was not significantly different (10% in High Power vs. 8% in Control,  $p=0.74$ ).

**Conclusions:** This randomized controlled study shows that a 45W RF-power CLOSE-protocol in paroxysmal AF patients significantly increases the global procedural efficiency with similar mid-term efficacy. However, our study showed a narrower safety margin and a limited

increased efficiency at the posterior wall using high power. This advocates against the use of high power in the region neighboring the esophagus.



## Chapter 11

# Endoscopic evaluation of the esophagus after catheter ablation of atrial fibrillation using contiguous and optimized radiofrequency applications

Michael Wolf, MD,<sup>\*†‡</sup> Milad El Haddad, MSc, PhD,<sup>\*</sup> Vincent De Wilde, MD,<sup>§</sup>  
Thomas Phlips, MD,<sup>\*</sup> Jan De Pooter, MD, PhD,<sup>\*</sup> Alexandre Almorad, MD,<sup>\*</sup>  
Teresa Strisciuglio, MD,<sup>\*</sup> Yves Vandekerckhove, MD,<sup>\*</sup> René Tavernier, MD, PhD,<sup>\*</sup>  
Harry J. Crijns, MD, PhD,<sup>‡</sup> Sébastien Knecht, MD, PhD,<sup>\*</sup>  
Mattias Duytschaever, MD, PhD<sup>\*</sup>

(Heart Rhythm 2019;16:1013–1020) © 2019

## Introduction

Atrioesophageal fistula (AEF) is a life-threatening complication of pulmonary vein isolation (PVI) for treatment of atrial fibrillation (AF). Whereas the incidence of AEF is low (0.02%–0.11%), there is a high (2%–30%) incidence of subclinical esophageal or periesophageal injury on endoscopy performed within 7 days after radiofrequency or cryoenergy ablation. Halbfass et al showed that the only risk factor associated with the occurrence of esophageal injury or ulcer is intraesophageal temperature rise (ITR). Furthermore, they found that an esophageal ulcer is a necessary precursor for AEF.

We recently introduced a new strategy to enclose the veins using contiguous and optimized radiofrequency (RF) applications. This strategy, referred to as CLOSE-PVI, is characterized by relatively high-power (35 W), short duration applications to target a prespecified ablation index (AI). It is associated with a high rate of adenosine-proof, first-pass isolation, favorable 1-year freedom of AF, and a high rate of durable isolation at repeat procedure. To assess the incidence of esophageal injury (and potential risk of AEF) using this ablation strategy, we performed echoendoscopy in patients revealing ITR during CLOSE-PVI.

## Methods

### *PVI according to the CLOSE protocol*

Patients with paroxysmal or persistent AF underwent a first CLOSE-guided PVI were monitored with a luminal esophageal temperature probe. According to institutional protocol all patients revealing ITR  $>38.5^{\circ}\text{C}$  were advised to undergo endoscopic evaluation of the esophagus within the first 2 weeks after PVI. PVI consisted of contact force (CF)-guided encircling of the veins using 35-W applications, respecting strict criteria of intertag distance ( $\leq 6$  mm) and ablation index (AI; 550 arbitrary unit [au] anterior wall, 400 au posterior wall). During encirclement of PVs, the position of the temperature probe was manually adjusted in order to place the 3 sensors as closely as possible to the respective ablation site (Figure 1). If ITR  $>38.5^{\circ}\text{C}$  occurred early, RF was continued until target AI  $\geq 300$  au (Figure 2). If ITR  $>38.5^{\circ}\text{C}$  was observed between AI 300 and 400 au, RF was stopped. If ITR was  $>38.5^{\circ}\text{C}$  after 400 au was reached, the site was noted. Before RF energy was applied to the next adjacent position, we waited for the temperature to drop  $>38.5^{\circ}\text{C}$ . During this waiting period, the operator could either stay on site and wait for temperature drop (preferred strategy if minor ITR and quick decline of temperature after RF cessation) or choose to ablate at a remote locus before going



to the adjacent position (preferred strategy if high ITR and/or slowdecline). RF power, as previously described, was only reduced in case of catheter tip temperature rise  $>43^{\circ}\text{C}$  or high CF ( $\geq 20\text{g}$ ), which might lead to overshoot of the AI target. In the absence of first-pass isolation, touchup ablation was performed, guided by the earliest PV potential on the Lasso catheter until PVI was achieved.

#### *Postprocedural care and follow-up*

Complications were reported and the data collected during follow-up. According to institutional protocol, all PVI patients were prescribed omeprazole 40 mg daily for 1 month. Follow-up consisted of clinical visits at 1, 3, 6, and 12 months.

#### *Endoscopic evaluation of the esophagus*

Endoscopic examinations were scheduled 14 days after PVI and performed by 4 experienced operators. All patients were kept fasting overnight before examination. As standard of care, all patients underwent clinical evaluation for symptoms (chest pain, dysphagia, fever, or neurological symptoms) before endoscopy. They were examined while in left lateral position under conscious sedation with midazolam 2.5 mg and/or alfentanil 0.5 mg IV. Oxygen saturation, pulse rate, and blood pressure were monitored. Evaluation of the esophagus, stomach, and duodenum was performed using a standard video endoscope (Pentax EG 29-i10, Pentax Medical Redwood City, CA) and Olympus GIF-H180, Olympus America, Center Valley, PA). Endoscopic lesions were attributed to AF ablation if they were located on the anterior wall of the mid esophagus. Esophageal lesions were classified into erythema/erosion, ulcer, or perforation. Endoscopic ultrasound (EUS) was performed using a radial scanning ultrasound endoscope (Pentax EG 3670URK) and the Hi Vision AVIUS ultrasound system (Hitachi Ltd, Tokyo, Japan). Careful examination of the mediastinum and esophageal wall was performed to assess mucosal and periesophageal/mediastinal lesions.

#### *Offline analysis of the deployed RF circle*

PVI procedures of all patients with ITR were analyzed offline. For each RF tag on the posterior wall, we determined application time (seconds), power (watts), CF (g), force time integral (FTI; gs), AI (arbitrary units), and maximum intraesophageal temperature ( $^{\circ}\text{C}$ ) (Figure 2). To anatomically allocate sites with ITR, the posterior hemisphere of each circle was divided into

5 segments. To assess the lesion length associated with ITR, we calculated the distance between the most cranial and caudal RF tags causing ITR.

## **Results**

### *Patients population*

Eighty-five patients with ITR during CLOSE-PVI underwent endoscopy of the esophagus (with ultrasound in 38 patients). Mean number of applications per patient was  $57 \pm 15$ , mean number of dislocations was  $2 \pm 1$ , and mean number of dislocations on the posterior wall was  $0 \pm 1$ . First-pass isolation was obtained in 162 of 170 circles (95%). During median follow-up of 8.9 months [interquartile range (IQR) 7.1–11.1], no complications of esophageal fistula, stroke, or death were noted.

### *Characteristics of RF applications*

A representative example is given in Figure 2. At the posterior wall, median power was 35 W [IQR 35–35], application time 18.5 seconds, CF  $13 \pm 6$ g, and AI  $403 \pm 38$  au. Because of high baseline CF, power was reduced to  $<35$  W (median 25 W, [IQR 25–30]) with a median of 1 [IQR 0–3] RF application per patient. For the left PV circle, a median of 10 [IQR 9–12] RF applications and for the right PV circle a median of 12 [IQR 10–14] RF applications were located on the posterior wall. A median of 5 [IQR 4–7] RF applications per patient resulted in ITR  $38.5^\circ\text{C}$ , covering a mean length of  $21.8 \pm 8$  mm along the posterior wall. The spatial distribution of sites with ITR is shown in Figure 3. In 53 patients, ITR was observed deploying the left PV circle and in 36 patients deploying the right (in 4 patients in both circles). Baseline esophageal temperature at those sites was  $36.2^\circ\text{C} \pm 0.3^\circ\text{C}$ . Maximal temperature observed was  $39.9^\circ\text{C}$  ([IQR  $39.2^\circ\text{C}$ – $41.2^\circ\text{C}$ ], range  $38.6^\circ\text{C}$ – $50.0^\circ\text{C}$ ) (Figure 4). Of interest, of the 405 RF applications resulting in ITR, only 36 (8.9%) were characterized by delayed ITR (ie, occurring only after stopping RF at AI target of 400 au). For applications resulting in ITR, median power was 35W [IQR 30–35], application time  $14 \pm 3$  seconds, CF  $12 \pm 5$ g, and AI  $351 \pm 38$  au. In cases of ITR, the median time between neighboring applications was 22 seconds [IQR 14–34]. In 14 patients with ITR, the operator chose to ablate at a remote locus (median 3, [IQR 2–4] applications) before resuming RF at the neighboring spot.

### *Ultrasound evaluation*

In none of the 38 patients undergoing additional sonographic evaluation were direct signs of injury to the esophageal wall observed. Periesophageal lymph nodes at the atrial level were observed in 13 patients, minimal pleural effusion in 17, physiological pericardial effusion in 7, and focal pleural thickening in 2.

#### *Patients not undergoing endoscopy*

In the present study, 48 ITR patients declined endoscopy (large distance from home to hospital, undesired absence from work, aversion to endoscopy). Of interest, the clinical, RF, and ITR characteristics of these 48 patients were not different from those of the 85 patients undergoing endoscopy. More specifically, at the posterior wall, median power was 35W[IQR 35–35], application time  $18 \pm 6$  seconds, CF  $12 \pm 6$ g, and AI  $404 \pm 44$  au, with a median of 4 [IQR 4–6] RF applications per patient resulting in ITR. Finally, in none of the patients was an adverse event noted at follow-up.

#### **CONCLUSION**

The occurrence of esophageal or periesophageal injury after CLOSE-PVI is markedly low (1.2%). Absence of esophageal ulceration in patients with ITR suggests that this strategy of delivering contiguous, relatively high-power, and short-duration radiofrequency applications at the posterior wall is safe.

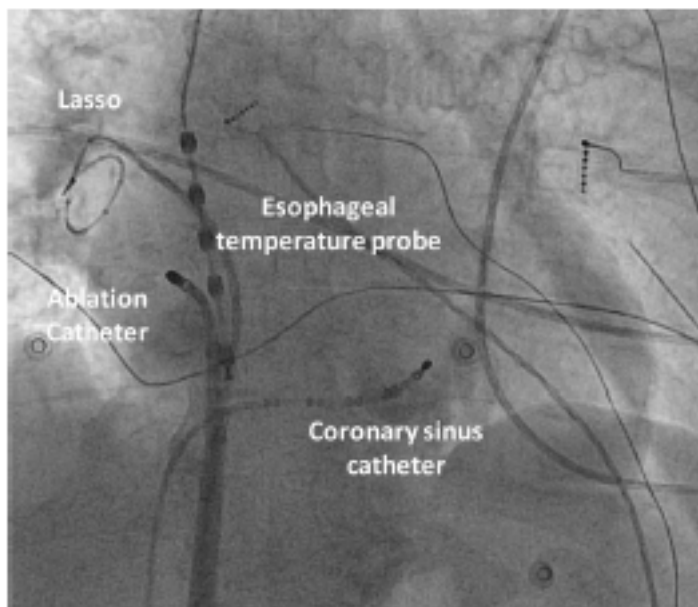


**Figure 1** Luminal esophageal temperature probe. During encirclement of the right veins, a circular mapping catheter is positioned in the right superior pulmonary vein. The position of a luminal esophageal temperature probe (SensiTherm, St Jude Medical) is adjusted so that the 3 thermosensors are as close as possible to the respective ablation site.

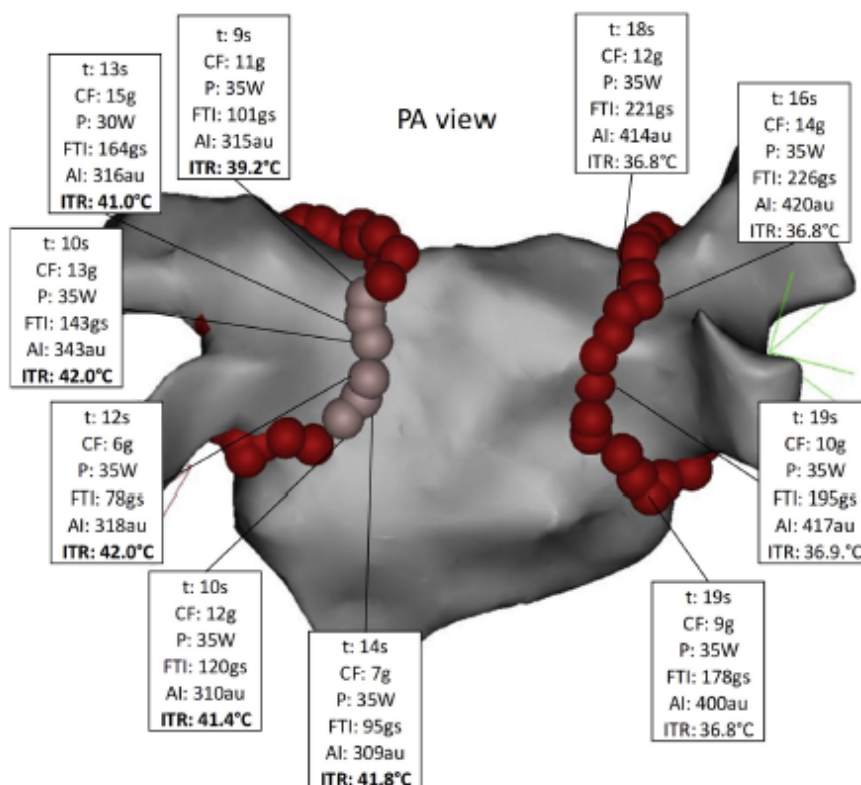


**Figure 2** CLOSE-guided PVI. Representative example of CLOSE-PVI and offline analysis. In this patient, applications on the posterior wall of the right circle did not result in temperature rise, whereas 6 applications on the posterior wall of the left circle resulted in intraesophageal temperature rise  $>38.5^{\circ}\text{C}$ . The ablation index target was reduced to  $\geq 300$  au (pink VisiTags). AI = ablation index; CF = contact force; FTI = force-time integral; ITR = intraesophageal temperature rise; P = power; PA = posteranterior; t = radiofrequency time.

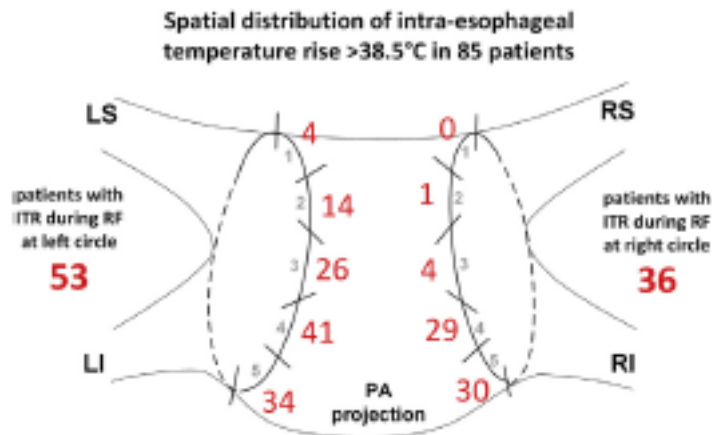


**Figure 3** Spatial distribution of intraesophageal temperature rise (ITR) in 85 patients. Number of patients showing ITR >38.5°C: frequency per circle and per segment. LI – left inferior; LS – left superior; PA – posteroanterior; RF – radiofrequency; RI – right inferior; RS – right superior.

#### 405 RF applications with ITR >38.5° C

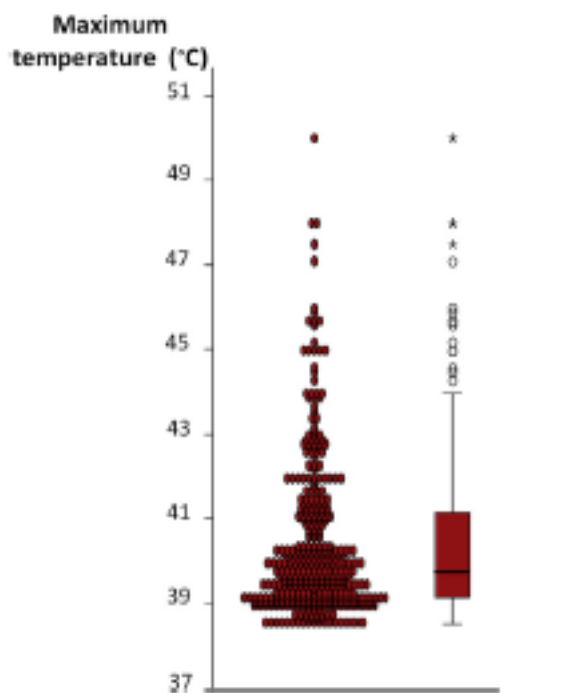


**Figure 4** Maximum intraesophageal temperature rise (ITR). All radiofrequency (RF) applications resulting in ITR >38.5°C and their respective maximum intraesophageal temperature are shown.

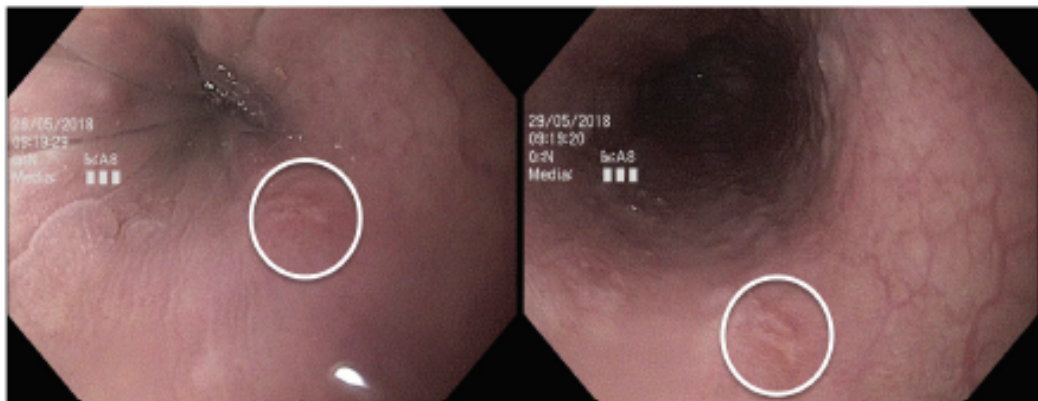
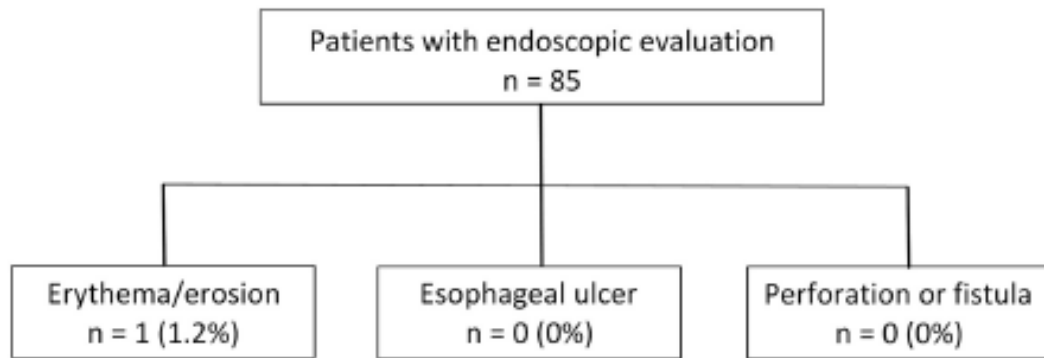


**Figure 5** Results of endoscopic evaluation. Endoscopy revealed 2 erythematous lesions at day 4 after ablation in only 1 of 85 patients.

## Chapter 12

ORIGINAL ARTICLE

WILEY

### Identification of repetitive atrial activation patterns in persistent atrial fibrillation by direct contact high-density electrogram mapping

Michael Wolf MD<sup>1,2,3</sup>  | René Tavernier MD, PhD<sup>1</sup> | Ziad Zeidan MD<sup>4</sup> |  
Milad El Haddad MSc, PhD<sup>1</sup> | Yves Vandekerckhove MD<sup>1</sup> | Jan De Pooter MD, PhD<sup>1</sup> |  
Thomas Philips MD<sup>1</sup> | Teresa Strisciuglio MD<sup>1</sup>  | Alexandre Almorad MD<sup>1</sup> |  
Maria Kyriakopoulou MD<sup>1</sup> | Michelle Lycke MSc, PhD<sup>1</sup> | Mattias Duytschaever MD, PhD<sup>1</sup> |  
Sébastien Knecht MD, PhD<sup>1</sup>

*J Cardiovasc Electrophysiol.* 2019;1–9.

## **Introduction**

During persistent atrial fibrillation (AF), multiple atrial wavelets and localized (focal or reentrant) sources have been reported to contribute to the maintenance of AF. In the last few years, there has been progress in mapping AF sources and mechanisms, mostly using phase - based analysis of epicardial or endocardial potentials. However, phase mapping has limitations as it is known to generate false rotational activities, particularly in cases of low voltage, variable contact, and when far - field signals are present. Recently, AF propagation maps based on direct contact mapping (without phase transformation) with a dedicated software (CARTOFINDER; Biosense Webster Inc, Diamond Bar, CA) have also been tested. Using a multielectrode basket catheter, the authors were able to reliably and reproducibly identify repetitive activation patterns in the majority of patients. Nevertheless, the basket catheter had long interelectrode distance and could not reach stable contact with the atrial wall in some regions and therefore, some repetitive activation patterns were probably missed. This study sought to evaluate a new mapping method for the Cartofinder software, using a regional high - density contact mapping catheter (PentaRay; Biosense Webster Inc). For the present work, we characterized repetitive atrial activation patterns (RAAPs) during ongoing AF based upon the automated annotation of unipolar electrograms (EGMs) directly obtained by these sequential recordings of the entire biatrial endocardial surface.

## **Methods**

### *Patient population*

During a two - fold period of availability of the Cartofinder software in our center (from May to October 2017 and from May to June 2019) consecutive patients who were referred to our institution for a first ablation of ongoing persistent AF and who consented to participate in the protocol, were enrolled in the study. Persistent AF was defined as continuous AF from 7 days to 12 months. Exclusion criteria were (a) sinus rhythm or atrial tachycardia at the onset of the procedure, (b) prior pulmonary vein isolation or atrial substrate ablation (linear lesions or ablation of fragmented signals).

### *Procedure and contact mapping*



After reconstruction of 3D - geometry of the left atrium with the PentaRay catheter, high - resolution EGMs during ongoing AF were recorded for 30 seconds at sequential PentaRay positions covering the entire left atrial surface, with each position overlapping the previous recording position with the radius of the PentaRay (Figure 1). Recordings were only obtained after optimal positioning of the PentaRay catheter, aiming maximal and even spread of the five splines with optimal electrode - tissue contact (also guided by the Tissue Proximity Indicator [Biosense Webster Inc], which determines the electrode proximity to cardiac tissue based on impedance measurements). After sequential mapping of the left atrium, one transseptal sheath was pulled back and sequential mapping of the entire right atrium was then performed. After EGM acquisition, RF ablation was performed with a lesion set consisting of pulmonary vein isolation with entrance block and linear lesions (roof, mitral, and cavotricuspid isthmus). Ablation was not guided by the Cartofinder analysis.

#### *EGM analysis and translation to activation mapping*

All recordings were reviewed off - line with dedicated software allowing automated annotation of the local activation time of the fibrillatory EGMs (CARTOFINDER; Biosense Webster Inc). Off - line analysis consisted of the following two parts: (a) identification and characterization of RAAPs, (b) Assessment of manual RAAP identification on Cartofinder activation maps and agreement between reviewers.

#### *Identification of RAAPs*

Cartofinder is based on the assessment of the local activation time of atrial signals during ongoing AF. To accurately determine the activation time, the automated Cartofinder software entails the following: (a) first the algorithm filters out the far - field ventricular signals. (b) Then for each electrode, two bipolar atrial signals are created by using the nearest two electrodes, which are determined by the Carto matrix (impedance based). For each electrode, the bipolar EGM window is then established based on measurement of the earliest onset to latest offset of its two bipolar EGMs. This bipolar EGM window establishes the window to record the unipolar atrial signal from each electrode. (c) Next, a wavelet analysis of unipolar signals recorded from the bipolar EGM window is performed. This analysis uses a proprietary algorithm to annotate only high - quality unipolar signals.<sup>13,17</sup> For each electrode the local

activation time is established as the maximal negative slope of the unipolar EGM within its predefined bipolar window, with the purpose of blanking out negative slopes due to far - field potentials. The accuracy of automated annotation of atrial local activation time and V far - field subtraction has been previously validated by experienced electrophysiologists (EPs) as part of the development process and used for the food and drug administration (FDA) submission, and were not routinely manually verified in our study. After automated EGM analysis, RAAPs were identified on a 3D propagation map, which was automatically generated for each recording (Figures 2 and 3 and Video Recordings SA and SB). RAAPs were defined as a consistent activation pattern (for  $\geq 3$  consecutive beats) of either focal activity with centrifugal spread along the PentaRay splines (RAAPfocal; Figure 2) or rotational activity across the PentaRay splines spanning the AF cycle length (RAAProtational; Figure 3). To classify the spatial distribution of RAAPs, the biatrial surface was divided in seven regions (Figure 4). Four regions were defined in the left atrium, two in the right atrium, and one in the anterior interatrial septum. Because of their proximity, left PVs were grouped with the left appendage into one region en bloc. Similarly, the right atrial appendage was grouped with the upper right atrium. Type, number, and location of RAAPs were cataloged per patient.

#### *Validation of RAAP identification from the Cartofinder software*

This part of the study sought to validate the propagation map as generated by the Cartofinder system with the EGM analysis obtained from automated EGM annotation and reviewed by four experienced EPs who were blinded to the Cartofinder results. A total of 46 out of 498 recordings (annotated EGMs and propagation maps) were randomly selected (21 with identified RAAPfocal, 18 with identified RAAProtational, and 7 recordings without RAAP identification). Agreement among the individual classification by four reviewers was documented and compared to the propagation map generated by the Cartofinder software.

## **Results**

### *Identification of RAAPs*

In total 498 PentaRay recordings were achieved and analyzed ( $35.6 \pm 7.6$  recordings per patient,  $13.3 \pm 3.5$  in the right atrium (RA), and  $22.1 \pm 3.2$  in the LA). The duration to perform all recordings was  $44 \pm 6$  minutes. Radiation exposure during mapping was  $6 \pm 3$  minutes. The mean AF cycle per recording was  $172 \pm 25$  ms. The mean number of PentaRay recordings

displaying RAAP was  $9.8 \pm 3.1$  per patient (range = 3 - 15) ( $6.4 \pm 2.5$  in the LA and  $3.4 \pm 2.1$  in the RA). Per RAAP, the median number of consecutive cycle repetitions during the 30 seconds recording was 11 (range = 3 - 225).

#### *Focal firing vs rotational activity*

Per patient, a mean of  $7.4 \pm 4.4$  RAAP<sub>focal</sub> (range = 1 - 13) and  $2.4 \pm 2.4$  RAAP<sub>rotational</sub> (range = 0 - 7) were observed. In total 77% of RAAPs showed focal spread and in 7 out of 14 patients only RAAP<sub>focal</sub> could be observed.

#### *Distribution in left and right atrium*

The distribution of RAAPs is displayed in Figure 4. RAAPs were identified in a mean of  $4.5 \pm 1.1$  regions per patient, in both the right (35%) and the left atrium (65%). RAAPs were most frequently located near the left pulmonary vein (PV)/left atrial appendage region (n = 47 or 35% of all RAAPs) and in the superior RA/right atrial appendage region (n = 31 or 23% of all RAAPs). The distribution of RAAP<sub>rotational</sub> and RAAP<sub>focal</sub> were similar. In the RA, per patient a mean of  $0.9 \pm 1.2$  RAAP<sub>rotational</sub> (range = 0 - 3) and  $2.4 \pm 2.3$  RAAP<sub>focal</sub> (range = 0 - 8) were observed. In the LA, per patient a mean of  $1.5 \pm 1.8$  RAAP<sub>rotational</sub> (range = 0 - 5) and  $4.9 \pm 3.1$  RAAP focal (range = 1 - 11) were identified.

#### *Validation of RAAP identification from the Cartofinder software*

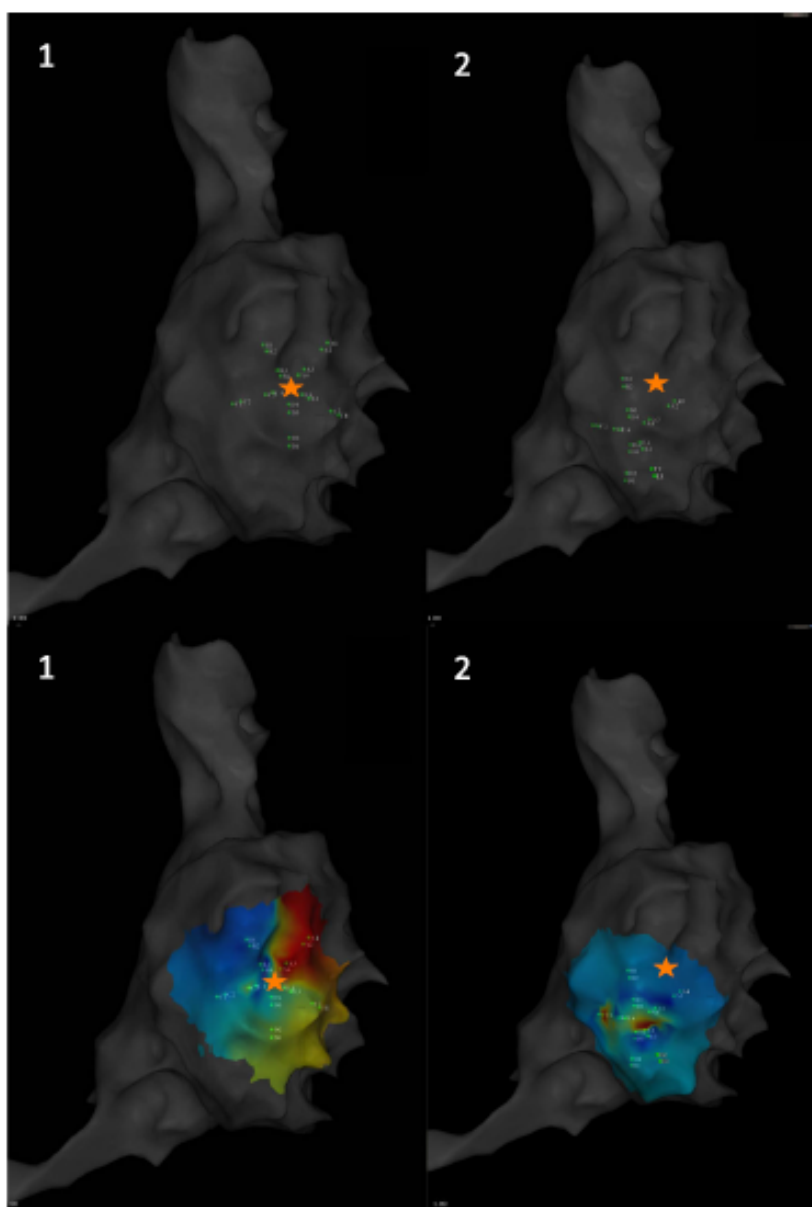
There was good statistical agreement amongst the four operators in identifying RAAP (intraclass correlation = 0.725 [95% confidence interval = 0.571, 0.835],  $P < .001$ ).

In the majority of the selected recordings (37 of 46 or 80%), an agreement between reviewers was obtained. This includes a full agreement amongst the four reviewers in 19 (41%) recordings and an agreement amongst three reviewers in 18 (39%) recordings. In nine recordings (20%), agreement was achieved amongst only two of the four reviewers. More precisely, for rotational activity, agreement amongst four and three reviewers was present in 44% and 50% respectively. For focal activity, agreement amongst four and three reviewers was present in 53% and 75% respectively. In the seven recordings without RAAP, agreement amongst four and three reviewers was present in 43% and 43% respectively.

## **Conclusion**

High - resolution and sequential endocardial EGM - based mapping shows the presence of repetitive activation patterns during persistent AF in all patients. In our series, focal firing was the most frequently observed pattern. The PentaRay high - density mapping catheter has the ability to reach all atrial regions and could potentially enhance RAAP detection

**FIGURE 1** Sequential PentaRay recording positions covering the entire biatrial surface. Recordings were only obtained after optimal positioning of the PentaRay catheter, aiming maximal and even spread of the five splines with optimal electrode-tissue contact. Sequential positions overlap the previous recording position with the radius of the PentaRay: the center of position 1 (star) becomes the radius of position 2 (top panels). Overlapping recordings enhance detection of repetitive atrial activation patterns (rotational in position 1 and focal in position 2, bottom panels)



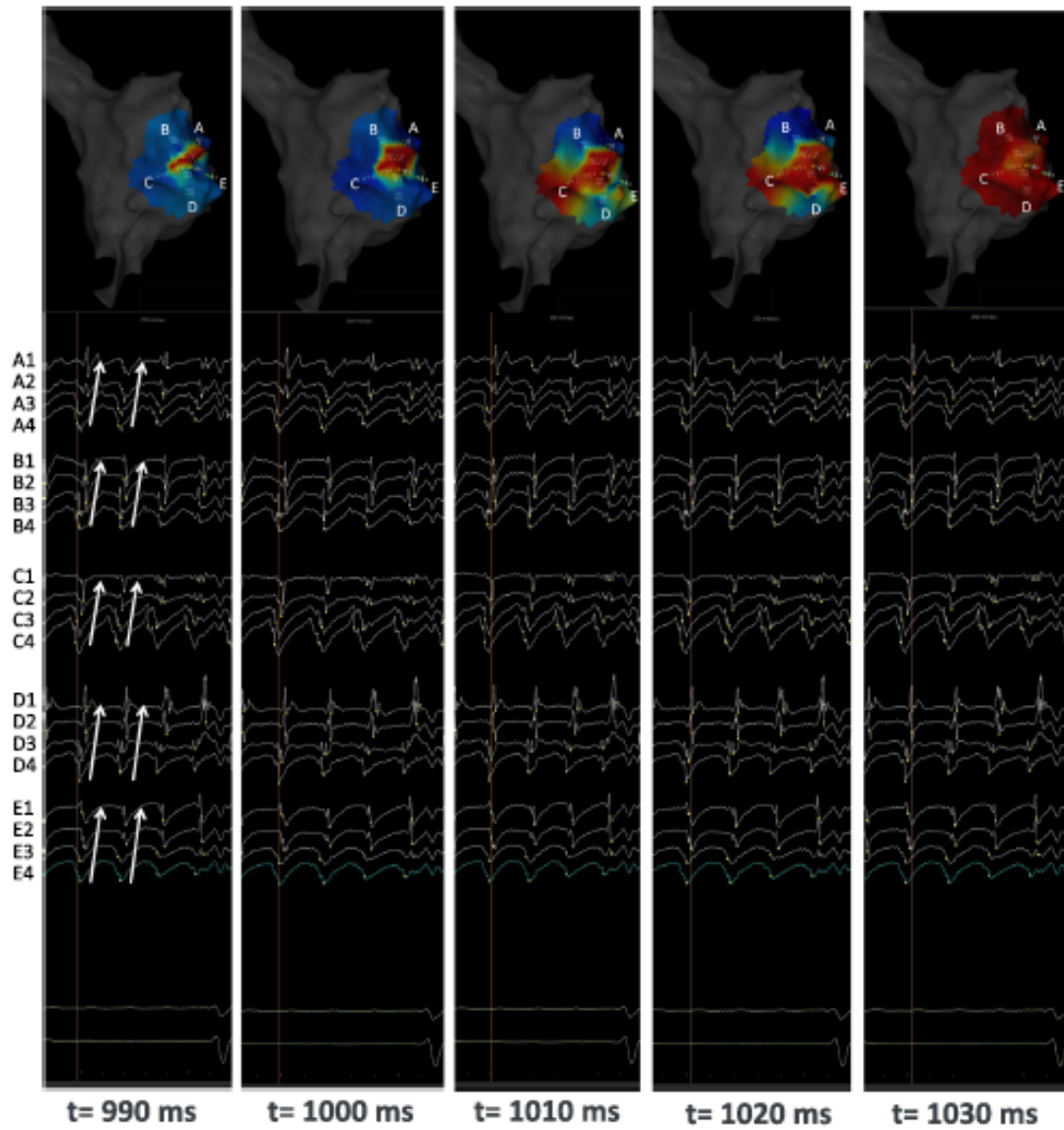


**FIGURE 2** Example of a RAAP<sub>focal</sub>: PentaRay positioned at the lateral wall of the right atrium. Subsequent panels show the propagation during a time window of 990 to 1030 ms of a 30 seconds registration during ongoing atrial fibrillation. The color-coding, as well as the unipolar fibrillatory EGMs recorded at each electrode (here organized per PentaRay spline (A to E) with electrode 4 as the most proximal and electrode 1 as the most distal per spline) show a centrifugal propagation consistent with focal firing (RAAP<sub>focal</sub>). EGM, electrogram; RAAP, repetitive atrial activation pattern

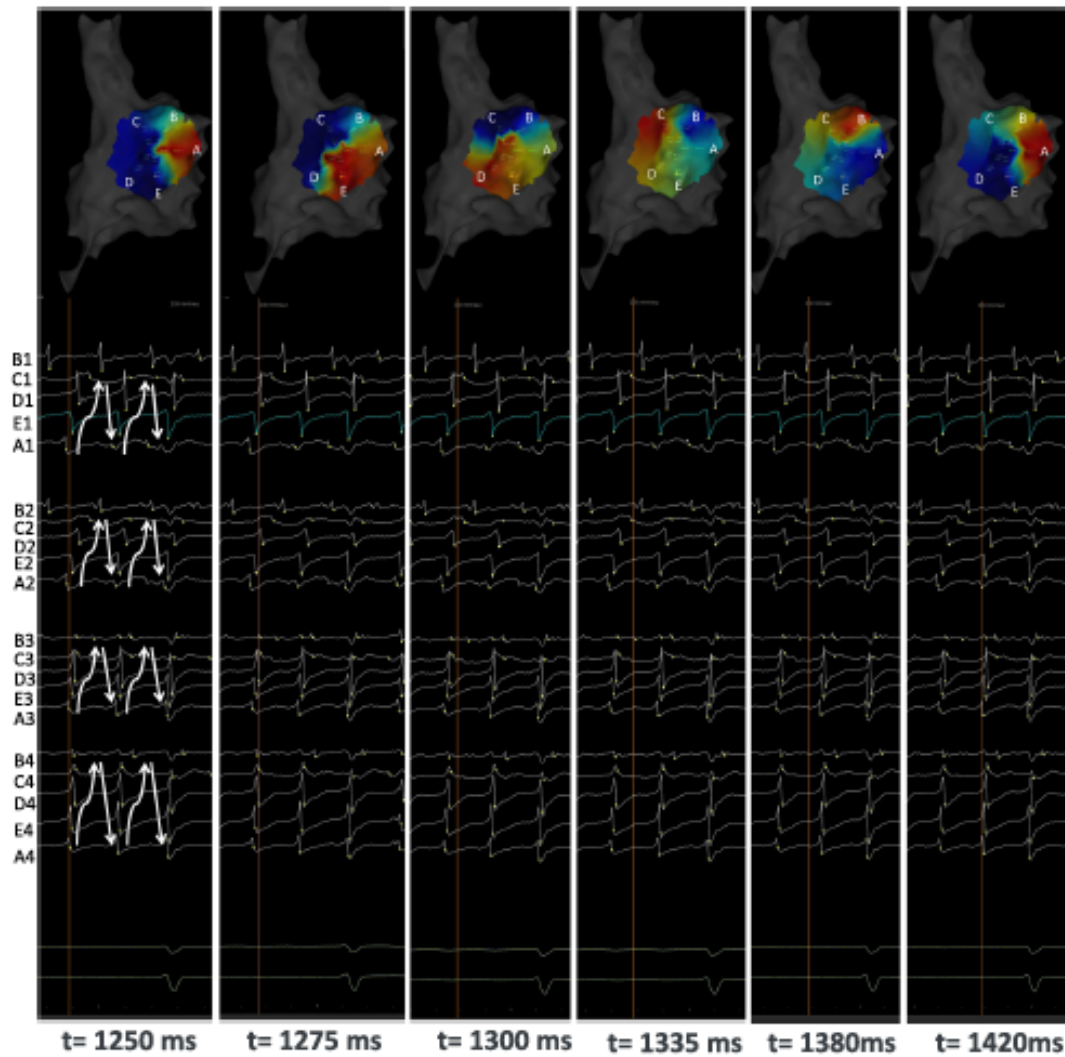


**FIGURE 3** Example of a RAAP<sub>rotational</sub> PentaRay positioned at the lateral wall of the right atrium. Subsequent panels show the propagation during a time window of 1250 to 1420ms of a 30 seconds registration during ongoing atrial fibrillation. The color-coding, as well as the unipolar fibrillatory EGMs recorded at each electrode (here organized per radius with electrode 4 as the most proximal and electrode 1 as the most distal per spline A to E), show a repetitive rotational propagation consistent with a RAAP<sub>rotational</sub>. EGM, electrogram; RAAP, repetitive atrial activation pattern

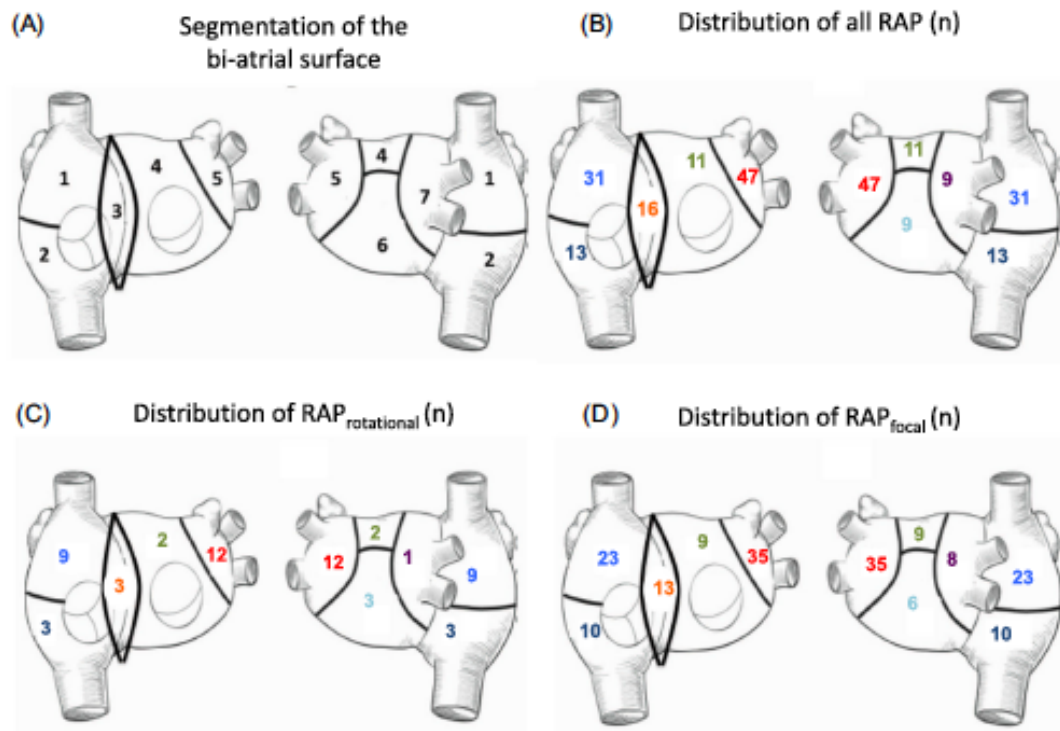


**FIGURE 4** Panel A: To classify the spatial distribution of RAAPs, the biatrial surface was divided in 7 regions. Four regions were defined in the left atrium, 2 in the right atrium, and 1 in the anterior interatrial septum. Because of their proximity, left PVs were grouped with the left appendage into 1 region en bloc. Similarly, the right atrial appendage was grouped with the upper right atrium. Panel B: total number of identified RAAPs per region for all 14 patients. Panel C: number of RAAP<sub>rotational</sub> per region for all 14 patients. Panel D: number of RAAP<sub>focal</sub> per region for all 14 patients. RAAP, repetitive atrial activation pattern



## Chapter 13

Circulation: Arrhythmia and Electrophysiology

### ORIGINAL ARTICLE

---

# Activation Mapping With Integration of Vector and Velocity Information Improves the Ability to Identify the Mechanism and Location of Complex Scar-Related Atrial Tachycardias

Elad Anter, MD  
Mattias Duytschaever, MD,  
PhD  
Changyu Shen, PhD  
Teresa Strisciuglio, MD  
Eran Leshem, MD, MHA  
Fernando M.  
Contreras-Valdes, MD  
Jonathan W. Waks, MD  
Peter J. Zimetbaum, MD  
Kapil Kumar, MD  
Peter S. Spector, MD  
Adam Lee, MD  
Edward P. Gerstenfeld, MD  
Elad Nakar, MSc  
Meir Bar-Tal, MSc  
Alfred E. Buxton, MD

*Circ Arrhythm Electrophysiol.* 2018;11:e006536. DOI: 10.1161/CIRCEP.118.006536

## **Introduction**

Pulmonary vein isolation (PVI) is an effective therapeutic option for patients with paroxysmal atrial fibrillation. However, in patients with persistent atrial fibrillation, PVI is less effective, and additional substrate ablation is frequently performed. This approach often results in development of complex atrial tachycardias (ATs).

Activation mapping of postablation ATs is often difficult to interpret because of (1) inaccurate local activation time (LAT) annotation of multicomponent electrograms, (2) difficulty differentiating active diastolic activity that is part of a reentrant circuit from passive diastolic activity recorded in scar unrelated to the tachycardia (ie, dead-end pathways), and (3) presence of a mapping window of interest with an arbitrarily defined early and late activation. The latter assumes a macroreentrant mechanism and may fail to detect a focal mechanism. Furthermore, the area of early meets late is often incorrectly interpreted as the zone of slow conduction isthmus that should be targeted for ablation. These constraints of current activation mapping limit the overall understanding of complex scar-related ATs. We propose a potential solution to overcome these limitations of activation mapping in complex substrates.

This proposed solution is based on the following electrophysiological principles:

1. Integrative approach for annotation of complex multicomponent electrograms: the mechanism of complex multicomponent electrograms is simultaneous recording of local and remote potentials or recording of multiple local potentials in a complex 3-dimensional structure with anisotropic conduction properties represented in 2 dimensions. Local and remote potentials can be differentiated by the unipolar slope ( $-dV/dt$  value). However, in the presence of multiple local activities with similar  $-dV/dt$  values, annotation of a single potential is arbitrary and can potentially result in LAT inconsistencies.

This can be solved with an algorithmic solution that examines the global pattern of activation in the chamber and forces the physiological constraints of propagation in atrial tissue to reconcile the most coherent activation pattern as further described in the Methods section.

2. Vector map: a vector map allows to follow the propagation path of an excitatory wave front. In macroreentry, it allows one to identify the circular path of the wave front throughout the tachycardia cycle and differentiation of it from passive activation of dead-end pathways. In addition, it allows identification of those areas with slow conduction in the reentrant circuit. In focal tachycardias, it can differentiate a true focal source from a localized reentry: although both tachycardias are localized to a small area, in a true focal source, vectors spread away centrifugally from a point source, whereas in a localized reentry, highly curved vectors surround a small central core. The additional information provided by a vector map can, therefore, be important for understanding the arrhythmia mechanism and for planning the ablation strategy.

3. Activation map independent of a preset mapping window: activation map that displays a color spectrum (or isochrones) based on the relative propagation between areas without predefined early and late activation. This provides an objective presentation of the excitatory path.

We have developed an activation mapping algorithm that incorporates the abovementioned elements. The purpose of this study was to examine its utility for mapping complex scar-related ATs. Specifically, we examined whether it has an additive value for determining the mechanism and location of the arrhythmia

## **Methods**

### *Study Design*

Phase I included 40 ATs from patients who underwent activation mapping using the standard algorithm in Carto 3 and in whom ablation resulted in arrhythmia termination.

These cases were used to retrospectively evaluate the investigational mapping algorithm for identifying the arrhythmia mechanism and site of termination. In phase II, the investigational mapping algorithm was applied to Carto 3 and evaluated prospectively for mapping and guiding ablation in 20 patients with post-PVI ATs.

### *Investigational Mapping Algorithm*

This investigational mapping algorithm (coherent mapping, Biosense Webster) takes into account the inaccuracies related to electrogram timing and presentation of complex activation patterns, as well as inaccuracies related to data projection into a rigid chamber reconstruction:

### *LAT Determination and Its Representation on the 3-Dimensional Chamber Reconstruction*

Electrogram time annotation is determined by the standard Carto 3 mapping algorithm. According to this algorithm, LAT is determined by analysis of each bipolar electrogram with its corresponding unipolar electrograms, such that local time annotation is marked at the component with the maximal unipolar  $-dV/dt$ . However, in complex substrates with multiple potentials of relatively similar  $-dV/dt$  values, annotation of a single potential can be misleading and result in LAT inconsistencies. To solve this problem, the algorithm is designed to identify all possible potentials of each individual electrogram and for the entire chamber data. Once all the chamber data are obtained, the algorithm determines the most coherent global propagation under physiological conductions utilizing all of the possibilities for each individual electrogram.

The reconstructed chamber is a static and rigid representation of a dynamic anatomy. Activation maps are created by sampling LATs from various places in the chamber. However, these measurements rarely fall on the rigid reconstruction because of respiratory changes, catheter mechanical effects on the chamber wall (stretching), or changes in chamber dynamics during arrhythmia. Current mapping algorithms project those points onto the nearest surface, yet the nearest location on the reconstruction is often different from the sampled location. Furthermore, using the nearest location associates samples from different locations and different LATs with a similar location of the reconstruction (Figure 1A). To solve this problem, we divided the surface into a mesh with small triangles reducing the magnitude of interpolation related to errors in projection (Figure 1B). In addition, the effect of each individual data point on the activation map has been designed to be proportional to its distance from the nearest triangle, such that data points obtained farther away from the surface receive lower weight compared with data points obtained closer to the surface (Figure 1C). This solution may reduce activation mapping inaccuracies that are related to projection of data points collected during different beats.

### *Vector Map*

The algorithm assigns each triangle on the reconstructed mesh with 3 descriptors: LAT value, conduction vector, and the probability of nonconductivity. Conduction velocities are calculated using the LAT values and the known distance and direction between triangles. The mathematical representation of this is shown in Figure IA in the Data Supplement. These descriptor values are initially known only for triangles with a direct measurement but unknown for all other triangles on the reconstructed mesh. To solve this problem, the following physiologically based assumptions are applied: (1) velocity continuity: in areas of

conduction continuity, conduction velocity is kept as similar as possible to the neighboring triangles, and only gradual changes are allowed. This relationship between triangles is performed through mathematical equations looking for the minimum mean square difference of the relations set above.

The optimal solution results in minimal differences at most locations, allowing large differences only in areas with enough measurements contradicting continuity; and (2) nonconduction areas are identified by multiple measurements at the same location, indicating that the electrode resides in an area with at least 2 distinct waves. In these areas, the probability of conduction slowing, or complete block, is determined by the vectors of propagation and the calculated conduction velocity. In regions with a structural obstacle for conduction, the vectors of propagation must go around the obstruction or conduct through the obstruction at a slow velocity. Conduction block was defined as a value lower than the lowest physiological conduction velocity in human atria (10 cm/s) as determined by Allesie et al. The above criteria are used to set the probability of a triangle to be in a nonconductive area. The equations are solved until the resulting LAT, conduction velocity, and probability of nonconductivity are stabilized without further changes, representing the optimal solution.

### *Integrative Solution*

The LAT, vector data, and identification of nonconductive or slowly conductive areas are used to generate an integrative activation map. This activation map is displayed as a vector map

### *Phase I: Retrospective Evaluation*

Forty ATs were mapped using the standard activation algorithm (Carto 3; Biosense Webster). The mapping catheters included multielectrode mapping catheters (Pentaray 2-6-2 mm or Lasso 10-pole; Biosense Webster) or a standard 3.5- mm ablation catheter (Thermocool SmartTouch; Biosense Webster). The inclusion criteria for retrospective case analysis were (1) mapping density with  $\geq 300$  activation points per chamber and a filling threshold setting  $\leq 15$  mm without leaving unmapped areas and (2) termination with limited ablation (first of few ablation lesions applied in the same or adjacent location) without a significant change in the tachycardia.

Radiofrequency (RF) ablation data were obtained from electroanatomical mapping system data log, and ablation time is reported in seconds from the initial application until arrhythmia termination (end of application).

For each case, the investigational mapping algorithm was applied retrospectively, and the original operator was asked to answer whether the algorithm was able to determine the (1) mechanism of the tachycardia as identified during the case using the standard activation map alone or in combination with the response to pacing and adenosine and the (2) successful ablation site, defined as the termination site of focal ATs or the strategy of ablation in macroreentrant ATs (ie, mitral line and roof line). The operator was asked to evaluate the standard and investigational mapping algorithms for their ability to identify the mechanism of the tachycardia and its site of termination.

Macroreentry was defined as a circular excitatory pathway  $\geq 30$  mm with electrical activity occurring throughout the tachycardia cycle; localized reentry was defined as a circular excitatory pathway  $< 30$  mm with electrical activity occurring throughout the tachycardia cycle, and a focal source had centrifugal spread from a single-point source. To reduce operator bias, each AT was reviewed by 2 additional independent investigators who were not familiar

with the case and were blinded to the mechanism of the AT, the ablation strategy, and the successful ablation site. The investigators analyzed separately the standard and investigational activation maps to determine its mechanism and the successful ablation site or strategy as determined by the original operator. The reviewers were able to review electrograms at each activation point.

### *Phase II: Prospective Evaluation*

The investigational algorithm was prospectively evaluated in 20 patients with post-PVI ATs. The investigational mapping algorithm was incorporated into a research version of Carto 3, which was able to display activation mapping using the standard and the investigational mapping algorithms.

Activation mapping was performed using multielectrode or linear catheters as described above. After completion of data acquisition at a similar prerequisite density as described above, the operator reviewed the investigational mapping algorithm to determine the mechanism and to plan the ablation strategy. Ablation was performed using an irrigated ablation catheter with energy of 20 to 45 W. RF time is reported in seconds from the initial application targeting the AT/flutter until its termination (end of application).

Pacing maneuvers and administration of adenosine were encouraged for validation of the arrhythmia mechanism and performed according to the operator's preference.

After completion of the case, the AT was analyzed by the operator to compare the standard and investigational mapping algorithms for their ability to determine the arrhythmia mechanism and location. Each case was additionally reviewed by 2 independent investigators who were blinded to the tachycardia mechanism and site of termination as described above.



## Results

The retrospective study group included a total of 40 ATs mapped in 35 patients who presented for first-time atrial ablation (n=5) or redo ablation (n=30;  $1.5 \pm 1.0$  [range, 1–3]) because of organized AT. The prospective study group included 20 patients with history of ablation procedures ( $1.7 \pm 1.1$  [range, 1–3]; median, 1) who presented for AT ablation.

### *Retrospective Evaluation of the Investigational Mapping Algorithm*

The standard activation algorithm identified 28 of 40 ATs (70%): 25 macroreentry and 3 focal tachycardias. The most common tachycardia was mitral annular flutter (n=15) followed by tricuspid annular flutter (n=6) and double-loop mitral annular and roof-dependent flutter (n=3). One patient had left atrial roof-dependent flutter, and 3 patients had right or left focal ATs. In the remaining 12 ATs, the mechanism and location could not be well identified by activation alone and required pacing or empirical ablation for termination. The RF time required for AT termination in the retrospective group was  $17.3 \pm 6.6$  minutes.

In comparison, the investigational mapping algorithm identified 37 of 40 (92.5%) ATs including all of the ATs identified by the standard mapping algorithm and additional 5 macroreentrant, 3 localized reentrant, and 1 focal AT. It also predicted the successful (actual) site of termination for all 37 cases. In focal and localized reentrant tachycardias, it identified the site of termination ( $1.1 \pm 0.8$  cm<sup>2</sup>). In macroreentrant ATs, it identified the strategy required for termination. In 3 of 40 ATs, the investigational algorithm did not identify the mechanism or the successful site of termination. In these cases, the arrhythmia terminated during ablation at the left or right atrial septum and may have included an unmapped chamber involved in a large macroreentrant circuit.

The basic differences between the standard and the investigational mapping algorithms can first be illustrated in a patient with a normal heart and a typical counterclockwise RA flutter. In this simple macroreentrant circuit, both activation maps displayed a similar pattern of propagation around the tricuspid annulus as shown in Figure 2.

However, careful review of these maps highlights important differences: (1) elimination of the mapping window concept: the investigational mapping algorithm does not use a rigid mapping window, such that the arbitrary zone of early meets late is eliminated, and the objective propagation data is displayed as a vector map; (2) velocity information: the investigational mapping algorithm includes velocity information that may be useful for identifying areas of slow conduction (ie, isthmus). In this case, it shows that conduction velocities around the tricuspid annulus including at the cavotricuspid isthmus are relatively uniform; (3) precise description of propagation. In this example, note that the primary excitatory wave front propagates around the tricuspid annulus in counterclockwise direction, whereas a secondary excitatory wave front propagates around the inferior vena cava in clockwise direction. This patient underwent ablation that resulted in bidirectional block across the cavotricuspid isthmus as determined by differential pacing and presence of double potentials separated by 176 ms across the entire ablation line. Figure 3 shows the postablation activation map during proximal coronary sinus pacing. The standard activation map shows significant time difference across the line, which can be consistent with block or slow conduction. The investigational mapping algorithm additionally shows a vector map with the excitatory wave traveling from the pacing site toward the septal aspect of the line, but it does not cross it. The lateral aspect of the line is activated via 2 wave fronts: one that travels around the tricuspid annulus in a counterclockwise direction and a second that travels around the inferior vena cava in a clockwise direction. Note that the vector of propagation

lateral to the ablation line is in perpendicular orientation to the vector of propagation septal to the line, confirming conduction block.

The differences between the standard and the investigational mapping algorithms were more evident in patients with scar-related ATs and complex propagation patterns. In the following case of a patient with persistent atrial fibrillation and history of previous PVI with additional LA ablation lines, including ablation in the coronary sinus, the standard activation map identified a typical counterclockwise RA flutter, whereas the investigational mapping algorithm identified a localized reentry at the coronary sinus ostium (Figure 4).

The diagnosis of a localized reentrant circuit rather than typical RA flutter was confirmed by (1) entrainment from the coronary sinus ostium with a postpacing interval (PPI) minus tachycardia cycle length (TCL) of 0 ms compared with entrainment from the lateral cavotricuspid isthmus with a PPI-TCL of 36 ms, (2) long diastolic electrogram over the localized reentrant focus, and (3) termination with a single-ablation application at this site. Overall, the investigational mapping algorithm was superior to the standard mapping algorithm for identifying the correct mechanism (99.2% versus 66.7%;  $P < 0.001$ ) and for identifying the successful ablation site (92.5% versus 69.2%;  $P < 0.001$ ). In addition, the investigational mapping algorithm was able to describe the mechanism of the tachycardia more clearly because as the agreement between the blinded reviewers was higher (97.5% versus 75%;  $P = 0.007$ ). Table 1 shows the comparative analysis of the correct identification of the mechanism and the successful ablation site between the 2 mapping algorithms. Table 2 shows the comparison of consistent assessment of the correct identification of the mechanism and the successful ablation by the 2 independent reviewers.

### *Prospective Evaluation of the Investigational Mapping Algorithm*

The investigational algorithm was prospectively evaluated in 20 patients with postablation AT and was used to guide the ablation. It identified 12 macroreentry, 6 localized reentry, and 2 focal tachycardias. The most common macroreentrant tachycardias were mitral annular flutter (n=8) followed by double-loop mitral annular, roof-dependent flutter (n=2), and biatrial reentry (n=2). Localized reentry was identified at the coronary sinus ostium (n=2), base of the left atrial appendage (n=2), left atrial septum (n=1), and below the left inferior PV (n=1). Two focal tachycardias were identified in the mitral annulus (n=1) and the coronary sinus ostium (n=1). The investigational mapping algorithm guided successful ablation in all 20 ATs with a mean RF time of  $3.2 \pm 1.7$  minutes. Ablation guided by the investigational mapping algorithm resulted in a significantly shorter time required for arrhythmia termination in comparison with ablation guided by the standard mapping algorithm as evaluated during the retrospective cohort ( $3.2 \pm 1.7$  versus  $17.3 \pm 6.6$  minutes;  $P \leq 0.001$ ).

The investigational mapping algorithm allowed correct identification of the mechanism in 19 of 20 ATs. Confirmation of the mechanism was performed by pacing maneuvers in all 20 cases and also with adenosine in 9 patients.

#### *Focal ATs*

Two ATs had activation pattern suggestive of a focal mechanism as the vector map showed a centrifugal spread from a single origin. In 1 case, resetting with single extrastimuli showed a flat response curve and adenosine resulted in transient slowing without termination, consistent with automaticity. Ablation at the earliest activation site resulted in immediate termination. In the second case, resetting with single extrastimuli showed a decreasing response curve, and adenosine resulted in termination, consistent with a delayed afterdepolarization triggered activity mechanism. The AT was reinduced and terminated with

2 RF applications at the site of the earliest activation. In both cases of focal ATs, electrograms at the site of termination were of normal amplitude, duration, and configuration, occurring  $\leq 50$  ms before the surface P wave. Figure 5 show san example of a localized focal AT as displayed with both the standard and the investigational mapping algorithms.

### *Localized Reentry*

In 6 ATs, the investigational activation map was consistent with a localized reentrant mechanism, demonstrating a small highly curved excitatory circular pathway. In contrast, the standard activation map showed focal tachycardia rather than localized reentry in 3 of 6 ATs, uninterpretable activation maps with multiple areas of early meets late in 2 of 6 ATs, and accurate diagnosis of a localized reentry in only 1 of 6 ATs. In these cases of localized reentry, differentiation between a focal and reentrant mechanism was performed by (1) examination of the underlying electrograms composing the circuit (6 of 6), (2) the response to resetting (4 of 6) or entrainment (5 of 6), and (3) the response to adenosine (5 of 6). In all localized reentrant circuits, electrograms comprising the circuit were abnormal, consisting of prolonged, fractionated low-amplitude potentials that occurred during the diastolic phase ( $\geq 50$  ms before the surface P wave). Resetting of the tachycardia with single extrastimuli at progressively shorter coupling intervals from a remote site resulted in evidence of intracardiac fusion with progressively longer return cycles with a predominantly increasing curve and a minimal flat component, suggestive of a small fully excitable gap. Entrainment from areas in close proximity to the circuit had shorter PPI-TCL ( $12 \pm 7$  ms) compared with entrainment from areas remote from the circuit ( $38 \pm 16$  ms), whereas entrainment from within the circuit resulted in a PPI-TCL of  $13 \pm 6$  ms. In 2 of 5 cases, attempt to entrain the tachycardia from within the circuit resulted in its termination. Adenosine administration at a

sufficient dose to cause AV block had no effect on 3 of 5 localized reentrant circuits and transiently accelerated 2 of 5 localized reentrant circuits. These findings are consistent with reentry and suggestive of circuits with a small excitable gap as shown by the investigational mapping algorithm. Figure 5 shows an example of a localized re-entrant AT as displayed with both the standard and the investigational mapping algorithms. Note that the investigational mapping algorithm shows a localized reentry circuit with highly curved vectors of propagation, whereas the standard activation algorithm displays the same tachycardia as a focal mechanism.

### *Macroreentry*

In all 15 patients with an activation map suggestive of a macroreentry, entrainment was performed from at least 3 sites inside or outside the circuit ( $3.2 \pm 2.6$  sites). The PPI-TCL in sites within the circuit as suggested by the investigational activation map was  $8 \pm 6$  ms (n=21 [0-3]). In 2 cases, pacing was not performed from the circuit but only from outside the circuit and resulted in PPI-TCL  $\geq 30$  ms. Ablation of macroreentrant tachycardias was performed using a strategy to connect 2 anatomic barriers and resulted in termination of all ATs.

The investigational mapping algorithm identified 3 macroreentry, 3 localized reentry, and 1 focal AT that were not well characterized by the standard mapping algorithm. All of these cases occurred in patients with scarred atria, whereas the standard activation map displayed complex and uninterpretable maps. The advantages of the investigational mapping algorithm for mapping these scar-related ATs can be illustrated using the following examples.

The investigational mapping algorithm showed a clockwise mitral annular flutter with a nonconductive zone between 9 and 12 o'clock on the mitral annulus, forcing the circuit

to bypass this area and extend to the base of the appendage as a pathway to get back into the lateral mitral annulus. The AT terminated with ablation at the lateral mitral annulus. In contrast, the standard activation map showed a confusing activation pattern with multiple areas of early meets late, precluding identification of both the arrhythmia mechanism and its location.

Figure 6 shows another example of a scar-related macroreentrant AT with bystander sites as displayed by the investigational and the standard mapping algorithms. The TCL was variable and ranged between 305 and 320 ms and had a proximal-to-distal coronary sinus activation pattern.

The investigational mapping algorithm identified a large LA macroreentrant circuit and a smaller secondary circuit. Entrainment confirmed that the larger circuit around the lateral mitral annulus was the active circuit, whereas the smaller circuit was a bystander. A single ablation lesion in the lateral mitral annulus terminated this tachycardia. The standard activation map was not able to identify the circuit or the successful ablation site.

Overall, the investigational mapping algorithm was superior to the standard mapping algorithm for identifying the correct mechanism (93.3% versus 66.7%;  $P < 0.001$ ) and for identifying the successful ablation site (98.3% versus 65%;  $P < 0.001$ ; Table 1). In addition, the investigational mapping algorithm was able to describe the mechanism of the tachycardia more clearly because the agreement between the blinded reviewers was higher (95% versus 80%;  $P = 0.08$ ; Table 2).

## **Conclusion**

Activation mapping of scar-related atrial ATs can be difficult to interpret because of inaccurate time annotation of fractionated electrograms, passive diastolic activity,

and the presence of a mapping window with an arbitrary designation of the earliest and latest activation assuming macroreentry. The addition of a vector map and integration of physiological constraints of electrical propagation in human atria improves the ability to describe complex patterns of propagation and for guiding ablation.



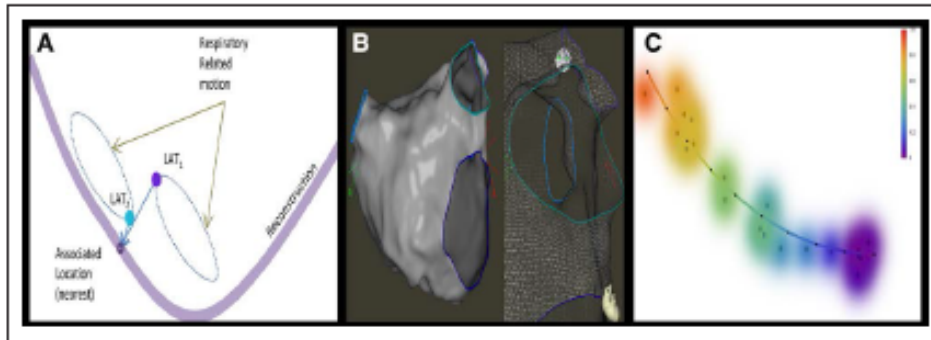


**Figure 1. Inherent limitations related to chamber reconstruction and data projection.**

**A.** Display of association of different local activation time (LAT) measurements with the same location. **B.** The reconstructed chamber divided into a triangulated mesh composed of small triangles ( $\approx 0.5$  mm) allowing a more accurate assignment of measurements. **C.** A sagittal section of the reconstructed chamber with a line colored based on the calculated LAT, with each individual measurement affecting the calculated LAT proportionally to its distance from it (the halo represents the fading effect with distance).

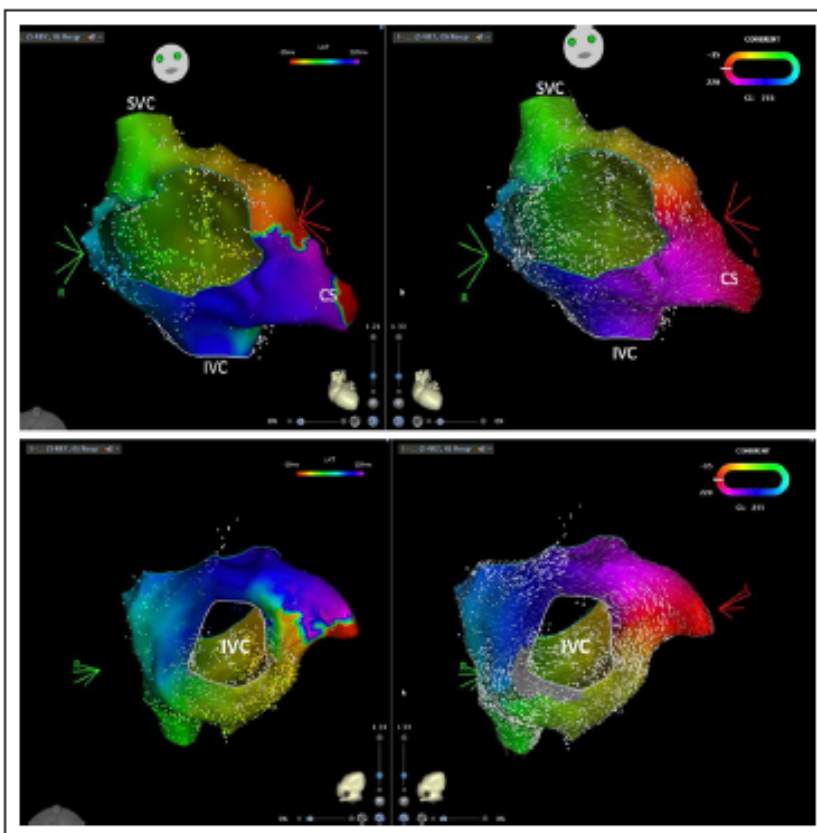


**Figure 2. Comparison between the standard and the investigational mapping algorithms.**

Right counterclockwise atrial flutter represented by the standard (**left**) and investigational (**right**) activation algorithms in 2 projections (**top** and **bottom**). Vectors are depicted by thin white lines with a propagation orientation from the thin tail to the thick head. Relative differences in conduction velocity are shown by differences in the overall thickness of the vector line, with thicker arrows representing faster velocities. Note that the investigational algorithm also shows a clockwise rotation around the inferior vena cava (IVC) not clearly evident by the standard algorithm. In addition, note the highly curved zone between the coronary sinus (CS) and the IVC. SVC indicates superior vena cava.

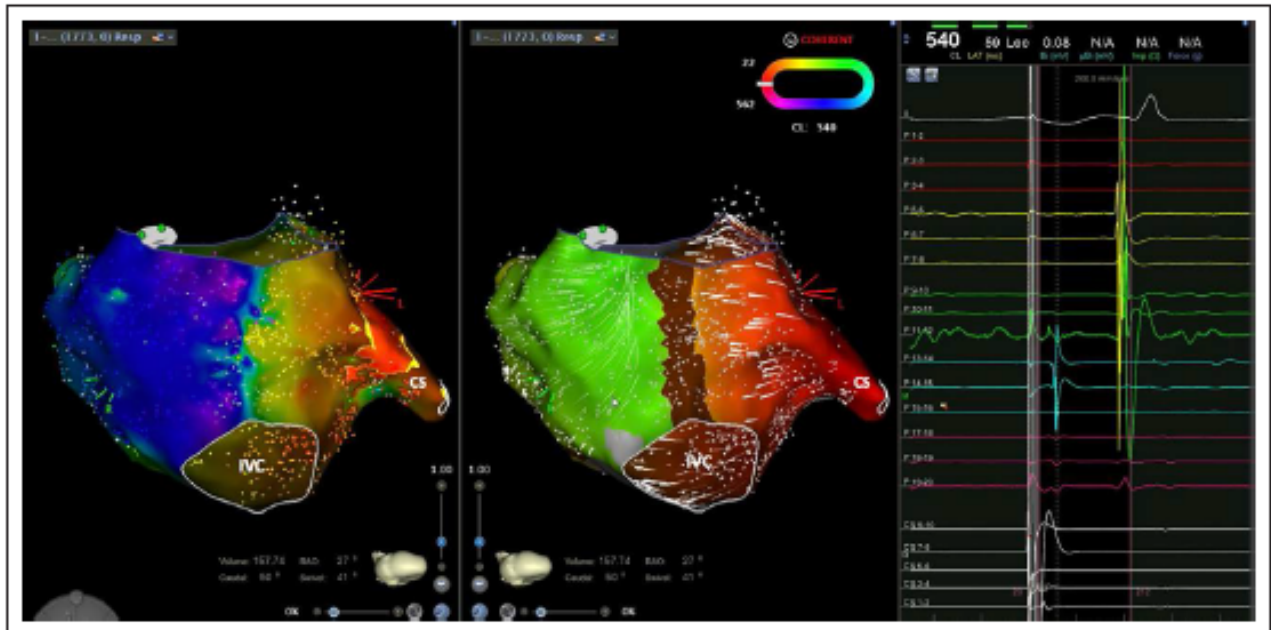


**Figure 3. Identification of discontinuous conduction.** This figure shows the right atrial mapping during proximal coronary sinus (CS) pacing after completion of a cavotricuspid Isthmus line with documented bidirectional block across the line by electrogram and pacing maneuvers. **Left**, The standard activation map, whereas the **(right)** shows the investigational activation map. **Right**, Electrograms recorded with a Pentaray catheter across the line of block with double potentials separated by 176 ms. Please see text for details. IVC indicates inferior vena cava; N/A, not available.

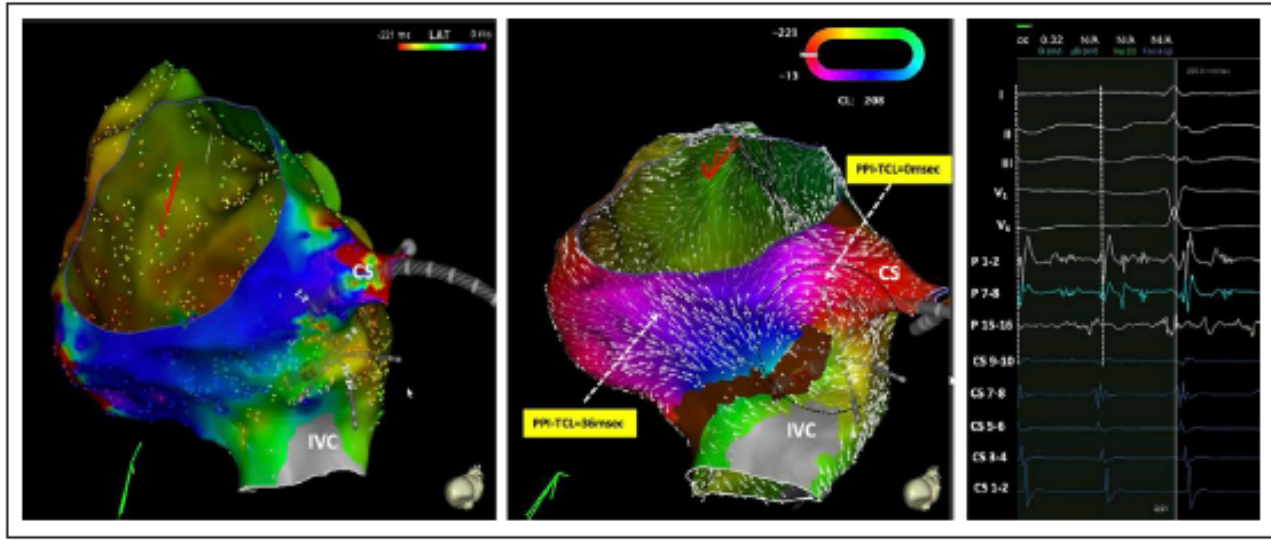


**Figure 4. Identification of a localized reentrant circuit.** Right atrial activation map in a patient with a localized reentry at the coronary sinus (CS) ostium as determined by pacing maneuvers and response to ablation (see text for details). The standard activation algorithm shows several areas of early meets late and fails to identify the mechanism and location of the tachycardia (**left**). The investigation algorithm identifies a localized reentrant circuit with a highly curved propagation wave front at the floor of the CS ostium at the site of termination (**middle**). The **(right)** shows 3 bipolar electrograms recorded simultaneously along the excitatory wave front of this small circuit. It demonstrates long diastolic electrograms propagating in a similar direction to the vector map, consistent with the diagnosis of a small reentrant circuit. IVC indicates inferior vena cava; LAT, local activation time; N/A, not available; PPI, postpacing interval; and TCL, tachycardia cycle length.

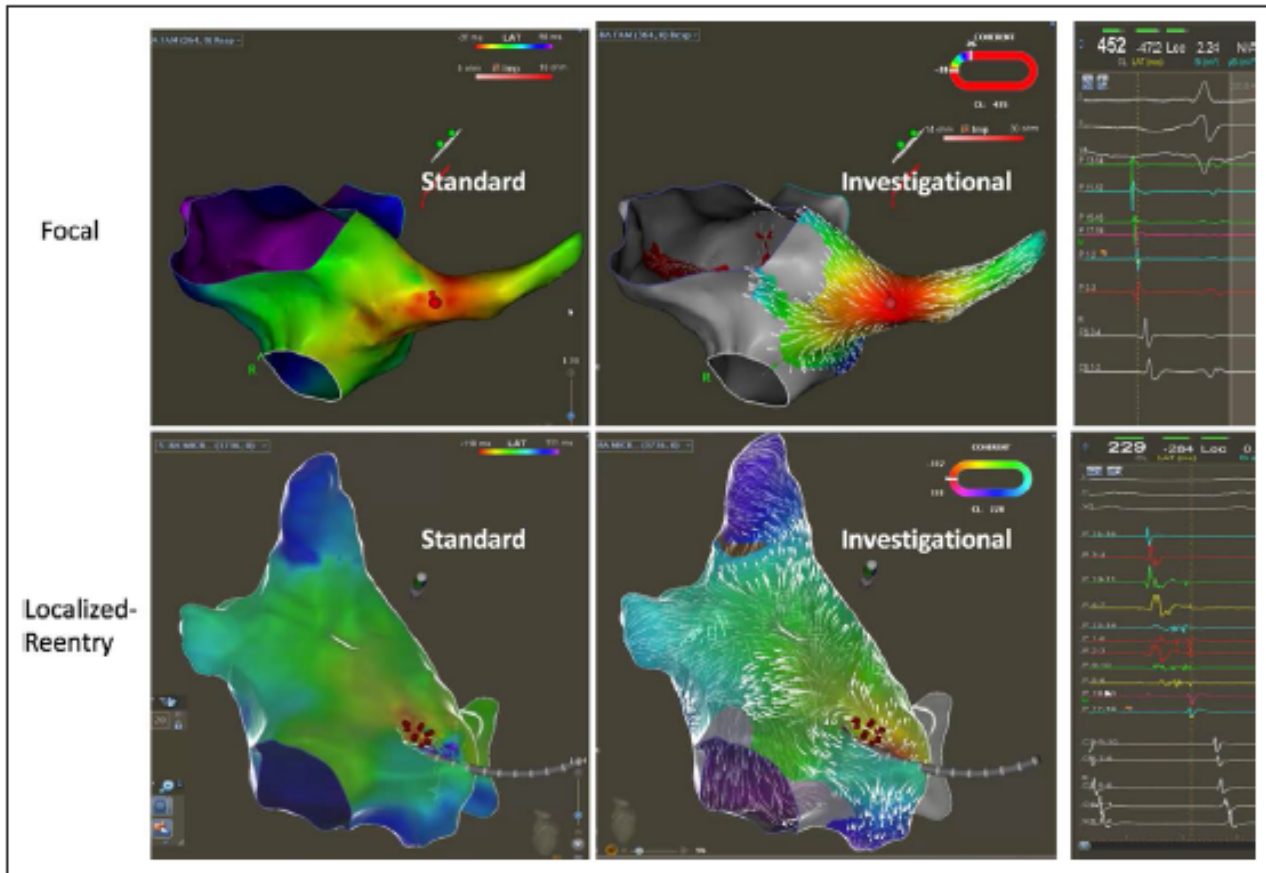


**Figure 5. Differentiation between focal and localized reentrant atrial tachycardia.**

**Top.** A case of focal tachycardia with an automatic mechanism displayed by the standard (**left**) and Investigational (**middle**) mapping algorithms. Note that both maps show an area of early activation (red color) at the proximal coronary sinus. However, the Investigational map additionally shows the vectors propagating away in a centrifugal direction from a well-defined source of activation. **Bottom.** A case of a localized reentry identified by the Investigational algorithm (**middle**) but not by the standard algorithm (**left**). **Right.** The electrograms recorded with Pentaray at the area of successful ablation. It shows that in focal ATs, electrograms often precede the P wave by  $\leq 50$  ms and have normal characteristics, whereas in localized reentrant ATs, electrograms are long and fractionated and occur earlier in diastole. LAT indicates local activation time; and N/A, not available.

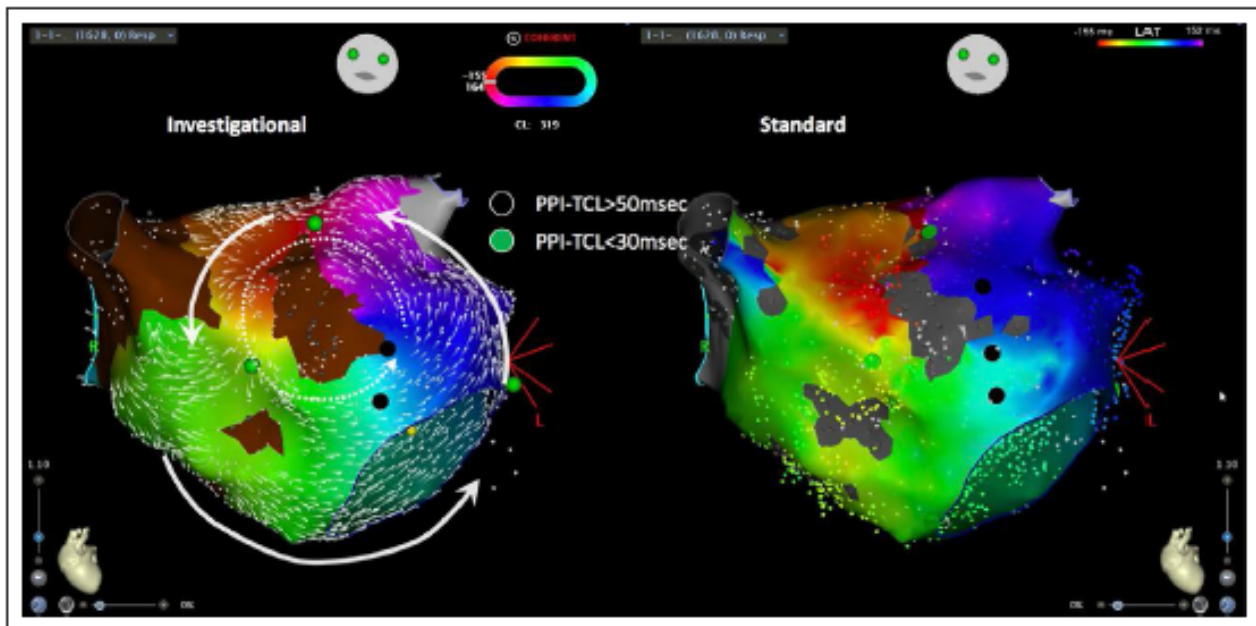


**Figure 6. Utility of vector map for describing complex circuits.**

A scar-related AT mapped and ablated using the Investigational mapping algorithm. **Left**, Activation map using the Investigational mapping algorithm. The map shows a complex circuit with a wave front propagating around the lateral mitral annulus in the counterclockwise direction, and over the base of the appendage toward the anterior roof, turning inferiorly between the right superior pulmonary veins and a patch of nonconductive tissue, and returning to the inferior mitral annulus (white solid arrows). In addition, a secondary smaller circuit is present rotating in a counterclockwise direction around the anterior wall patch of nonconductive scar tissue (white dotted arrows). Entrainment confirmed that the larger circuit around the lateral mitral annulus was the active circuit, whereas the smaller circuit was a bystander. A single-ablation lesion in the lateral mitral annulus terminated this tachycardia. The standard activation map did not show a mitral annular flutter but highlighted the passive localized circuit (**right**). LAT indicates local activation time; PPI, postpacing interval; and TCL, tachycardia cycle length.



**Table 1. Comparative Analysis of Correct Identification of the Mechanism and the Successful Ablation Site**

	Correct Identification of Mechanism			Correct Identification of Ablation Site		
	Standard	Investigational	<i>P</i> Value	Standard	Investigational	<i>P</i> Value
Retrospective cohort (n=40)						
Raw estimate	66.7%	99.2%	<0.001	69.2%	92.5%	<0.001
Odds ratio*	78.2 (10.3–592.5)		<0.001	60.8 (7.9–470.4)		<0.001
Prospective cohort (n=20)						
Raw estimate	66.7%	93.3%	<0.001	65%	98.3%	<0.001
Odds ratio*	12.5 (3.2–48.3)		<0.001	62.2 (6.7–580.3)		<0.001

\*Conditional logistic regression to account for clustering of patients; numbers in parenthesis are 95% confidence intervals

**Table 2. Comparison of Consistent Assessment by the 2 Independent Reviewers**

	Percentage of Consistent Assessment on Mechanism by 2 Reviewers			Percentage of Consistent Assessment on Ablation Site by 2 Reviewers		
	Standard	Investigational	<i>P</i> Value	Standard	Investigational	<i>P</i> Value
Retrospective cohort	75.0%	97.5%	0.007	95.0%	95.0%	1
Prospective cohort	80.0%	95.0%	0.08	85.0%	95.0%	0.16

## Chapter 14

### Journal Pre-proof

A Prospective Evaluation of Entrainment Mapping as an Adjunct to New Generations High-Density Activation Mapping Systems of Left Atrial Tachycardias

Teresa Strisciuglio, MD, Nele Vandersickele, PhD, Giuseppe Lorenzo, MSc, Enid Van Nieuwenhuyse, Msc, Milad El Haddad, MSc, PhD, Jan De Pooter, MD, PhD, Maria Kyriakopoulou, MD, Alexandre Almorad, MD, Michelle Lycke, MSc PhD, Yves Vandekerckhove, MD, René Tavernier, MD, PhD, Mattias Duytschaever, MD, PhD, Sebastien Knecht, MD, PhD



## **Introduction**

Complex left atrial tachycardia (AT) are frequent after ablation of persistent AF. New generation activation mapping systems, sometimes using multi-electrode mapping catheters and automatic annotation of local activation time (LAT), have shown promising results.

Recently, a novel mapping algorithm (Coherent, CARTO Biosense Webster) has been demonstrated to have higher accuracy in identifying complex scar-related macro-reentrant circuits, as it integrates information about conduction velocities. In recent studies, authors did not systematically use entrainment manoeuvres to confirm the diagnosis. Nonetheless, in case of very diseased left atrium (LA) (spontaneously or after extensive ablation), the interpretation of these high-density activation maps (HDAM) can remain challenging.

On the other hand, even when using new generation HDAM technologies, entrainment mapping (EM) has still shown its usefulness during complex right AT, mostly to discriminate active and bystander circuits. However, the exact added value of EM has not yet been investigated yet during complex left AT.

In this prospective single centre study, we sought to investigate whether EM is valuable even when the newest technologies for the identification of complex left ATs after persistent AF ablation are being used. **Methods.** Thirty-six consecutive complex ATs occurring after ablation of persistent AF were prospectively analysed. The AT mechanism was diagnosed in two steps by two experts: 1) based on HDAM only (Coherent, CARTO Biosense Webster) and 2) with additional analysis from EM.

## **Methods**

### *Study population*

Patients undergoing catheter ablation for left AT were prospectively included in the study,

only if previous persistent AF ablation procedures were considered as “complex”. The previous ablation procedures were considered as complex if, in addition to pulmonary vein isolation, a set of two ablation lines (roof, mitral isthmus) and additional substrate ablation (CFAE ablation) had been performed during the first procedure.

### *Study design*

AT maps were prospectively analysed by two expert electrophysiologists during the ablation procedure. For each AT, they were asked to make a diagnosis of the mechanism following a two-steps procedure: 1) firstly by looking at the HDAM (blinded to EM results) and with electrogram (EGM) analysis and then secondly 2) with additional analysis from EM added on the HDAM. For the two steps, they had to reach a consensus on the AT mechanism and its precise location/circuit. The diagnosis was considered correct if the ablation led to AT termination (to sinus rhythm or to another AT as suggested by a different cycle length/activation pattern).

### *AT mechanism definitions*

Macro-reentries were defined as roof dependent circuits when turning around the right pulmonary veins (RPV) or left pulmonary veins (LPV), or perimitral when turning around the mitral annulus. A double loop AT was defined as two simultaneous macro-reentry circuits with a common isthmus.

AT was defined as a micro-reentry circuit in the case of centrifugal activation from one atrial segment with at least 75% of the AT cycle length within the earliest region.

### *High Density Activation mapping*



The Coherent module (CARTO®, Biosense Webster Inc., Irvine, CA, USA) has been previously described<sup>5</sup>. Basically, the new algorithm takes into account three descriptors, i.e. LAT value, conduction vector, and the probability of non-conductivity, that are used to generate an integrative activation map displayed as a vector map. This algorithm then identifies the optimal conduction mechanism, considering physiological barriers manifested by scar and double potentials. Colouring is based on the best fit solution of all LAT values of the map identifying the conduction mechanism.

### *Entrainment mapping*

Entrainment was performed at predefined LA sites around both pulmonary vein (PV) circles and the mitral annulus, as well as at sites located in proximity to the observed circuits, at a cycle length of 10 ms less than the tachycardia cycle length (TCL). A post-pacing interval (PPI), measured from the stimulation artefact to the return atrial EGM on the pacing catheter and not exceeding the tachycardia TCL by more than 30 ms in three opposite atrial locations corroborated the diagnosis of macro-reentry. A colour code was used to illustrate the PPI results: a green point corresponded to a PPI-TCL < 30 ms, a yellow point to a PPI-TCL between 30 and 50 ms and a black point to a PPI-TCL > 50 ms.

If PPI-TCL was unexpectedly long based upon the diagnosis from the HDAM, the entrainment manoeuvre was repeated to ensure correct capture, after having checked the TCL and activation pattern in order to exclude any changes in the AT mechanism.

### *Radiofrequency Ablation*

RF ablation (20- 40 Watts, 30 cc irrigation rate) was performed depending on the AT mechanism and the ablation lines that had previously been performed. In the case of a micro

reentry circuit, ablation was focused mostly on the earliest area where local electrogram filled >75% of the TCL. The diagnosis of the AT mechanism was considered correct if the AT terminated during radiofrequency ablation (to sinus rhythm or to another AT). In every patient, the operators aimed to reach the non-inducibility of any AT at the end of the procedure.

## **Results**

### *Study population and procedural characteristics*

Sixty-one consecutive patients underwent AT ablation during the index period. Thirty six out of 72 AT in 32 patients fulfilled complex AT criteria as mentioned above. In one patient, EM resulted in AF after HDAM. In this patient, a direct current cardioversion (DCCV) was carried out, however an AT could not be induced anymore and the patient was excluded. Clinical characteristics of the remaining 31 patients (35 ATs) are shown in Table 1. The majority of patients (63%) were male with a mean age of  $69\pm 11$  years and a mean CHA<sub>2</sub>DS<sub>2</sub>VASc of  $2\pm 1$ . The median number of previous ablations was 1 (IQR 1-2). There was a median of 1031 points (IQR 830 – 1625) per map and a mean number of  $8\pm 4$  pacing sites during EM.

### *Accuracy of HDAM and added value of EM*

#### *Macro-reentries (single or double loop)*

Eleven single loop macro-reentries were identified by HDAM (31%): seven roof circuits (four around RPVs and three around LPVs), and four perimitral circuits (figure 1 and 2). EM confirmed the mechanism and the circuit in all cases except for one AT where EM

enabled the diagnosis of a perimitral circuit with a breakthrough at the left atrial appendage (LAA) base through the vein of Marshall, whereas analysis of HDAM misclassified it as a roof circuit around LPVs. In total, HDAM established a correct diagnosis in 10 out of 11 (91%) maps showing single loop macro-reentry.

Fourteen double loop ATs were identified by HDAM (40%): three roof dependent macro-reentrant ATs with two simultaneous circuits around both right and left PVs, and 11 simultaneous perimitral and roof circuits (four around RPVs and seven around LPVs). With EM, only 4 out of 14 double loop ATs (28.5%) were confirmed, while in the other 10 cases, EM unmasked a passive activation of one visual circuit (figure 3 and 4). For these 10 ATs with a passive activation of a visual circuit, the final diagnosis was thus single loop macro-reentries: five roof circuits (three around the RPVs and two around the left PVs) and five perimitral circuits.

#### *Micro-reentry circuits*

One sole micro-reentry circuit (located at the anterior LA wall) was identified by HDAM (3%) and then confirmed by EM.

#### *Combination of macro- and micro-reentry circuits*

HDAM showed a combination of a macro- and micro-reentry circuits in three ATs (9%): two perimitral circuits in combination with an anterior micro-reentry, and one roof circuit around RPVs in combination with a posterior micro-reentry. In the first two cases, EM revealed a passive activation of the visual perimitral circuit while the anterior micro-reentry circuit was confirmed. Ablation of the anterior micro-reentry resulted in sinus rhythm restoration. In the third case, EM confirmed that both macro- and micro-reentry circuits were

active.

#### *No diagnosis possible from troubleshooting HDAM*

In the remaining 6 out of 35 ATs (17%), it was not possible to depict at least one univocal AT mechanism using HDAM alone. In these cases, EM finally enabled the diagnosis of five micro-reentry circuits (two located at the anterior wall, one at the septum, one at the roof and one at the base of the appendage) (figure 5) and one roof dependant macro-reentrant AT turning around LPVs.

#### *AT final characteristics as confirmed by ablation*

AT characteristics are summarized in Table 2.

The median AT TCL was 275 ms (IQR 240-320). Ablation converted AT to sinus rhythm in 23 patients (66%) and to another AT in 12 (34%) cases. EM on top of HDAM enabled the correct AT diagnosis (location and circuit) in all cases, as confirmed by ablation (figure 1).

There were finally 22 single loop macro-reentries (63%) (figure 2): 10 perimitral circuits (four counter-clockwise and five clockwise) for which a mitral line was conducted; and 12 roof dependant circuits for which a roof line was performed [(seven around RPVs (four counter-clockwise and three clockwise) and five around LPVs (two counter-clockwise and three clockwise))]. In 5 out of 10 patients with a putative double loop at HDAM but not confirmed by EM, ablation was performed at a common isthmus (mitral line or roof line), which resulted in sinus rhythm restoration in all cases. In the remaining five patients, ablation 223 of the active circuit resulted in AT transformation to the initially passive loop in three patients and in sinus rhythm restoration in two patients.

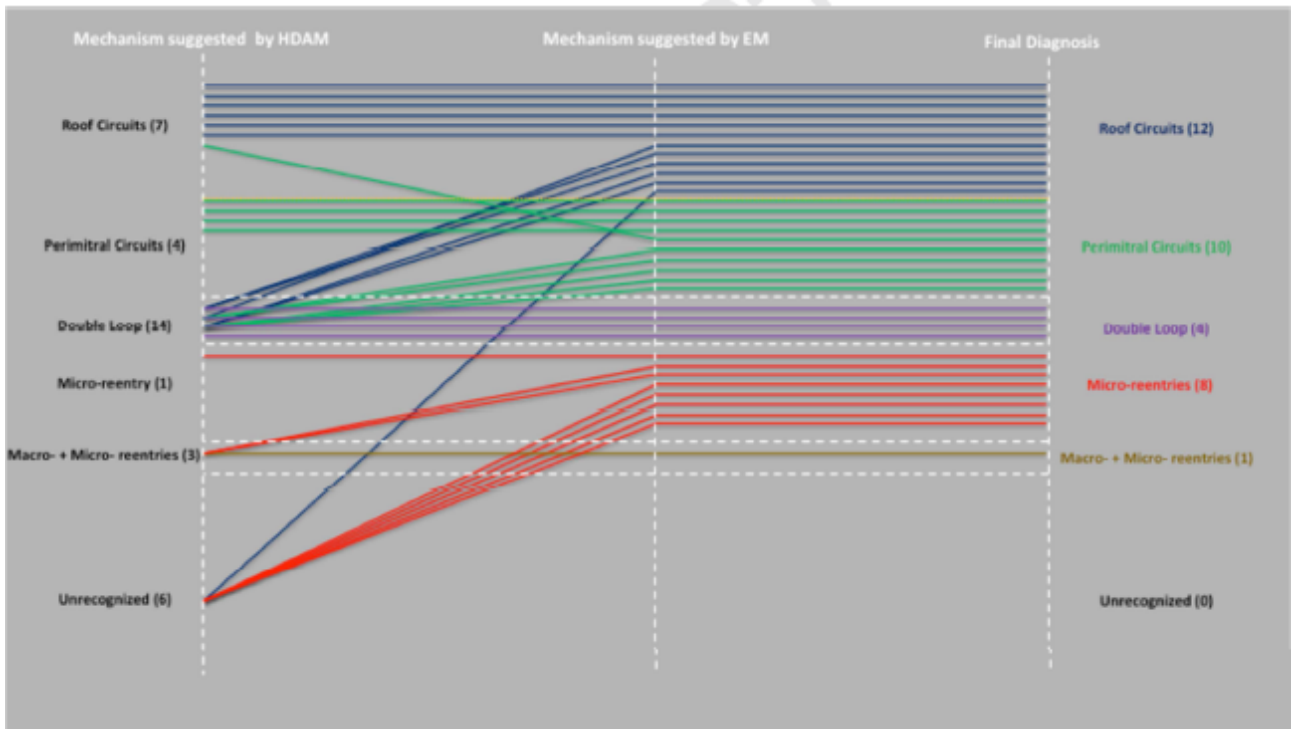
Four double loop macro-reentries (11%) were diagnosed: one double 226 roof circuit

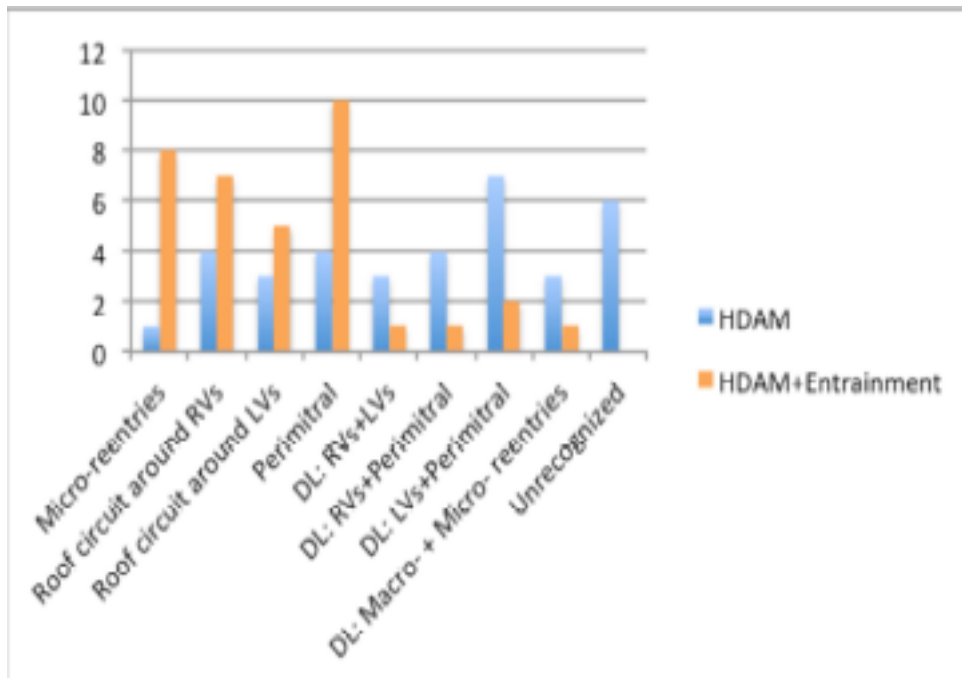
around RPVs and LPVs for which ablation at the roof was performed, and three simultaneous perimitral and roof circuits (two around LPVs and one around RPVs) for which ablation was first performed at the roof line and then at the mitral line. Eight micro-reentry circuits (23%) were diagnosed: five located at the anterior wall, one at the septum, one at the roof and one at the base of the appendage.

In one case (3%), there was a combination of one macro-reentry around RPVs and one micro-reentry around a posterior scar area.

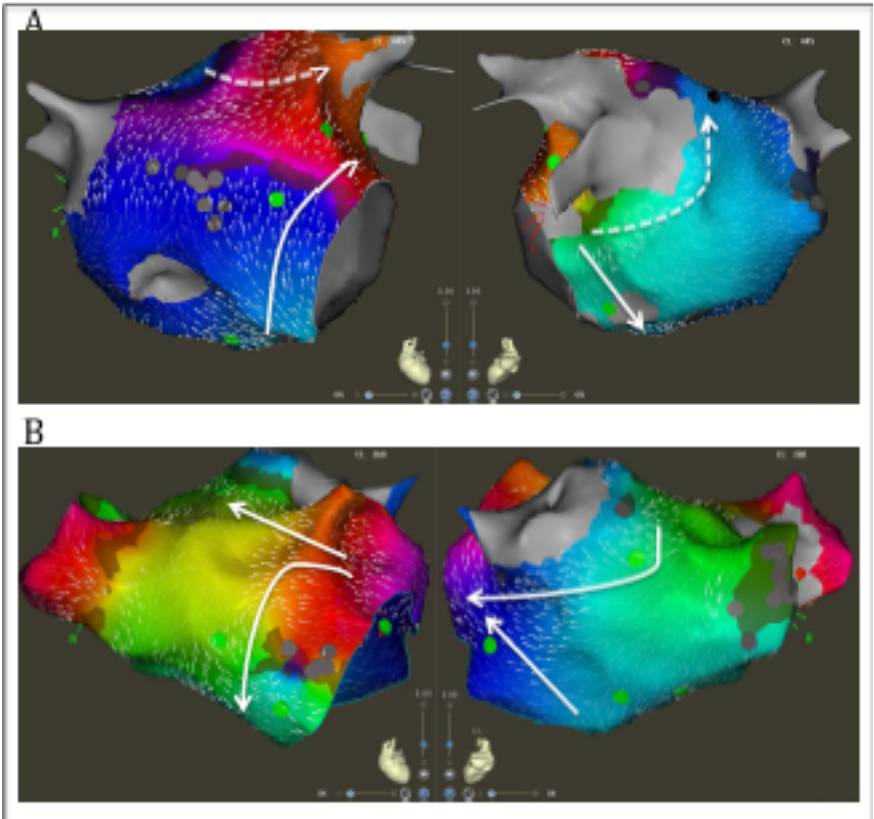
### **Conclusion**

Entrainment manoeuvres are still useful during mapping of complex left atrial tachycardia, mostly to differentiate active from passive macro-reentrant loops and to demonstrate micro-reentry circuits.

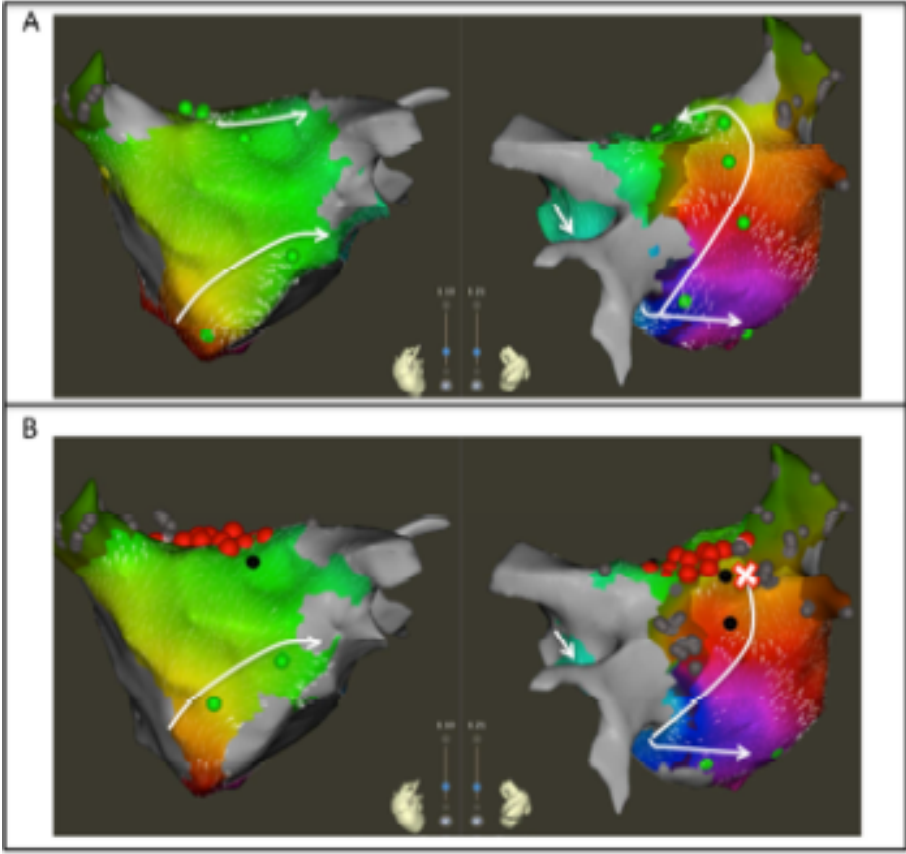




AT Mechanism	HDAM	HDAM+Entrainment
Micro-reentries	1	8
Roof circuit around RVs	4	7
Roof circuit around LVs	3	5
Perimitral	4	10
DL: RVs+LVs	3	1
DL: RVs+Perimitral	4	1
DL: LVs+Perimitral	7	2
DL: Macro- + Micro- reentries	3	1
Unrecognized	6	0







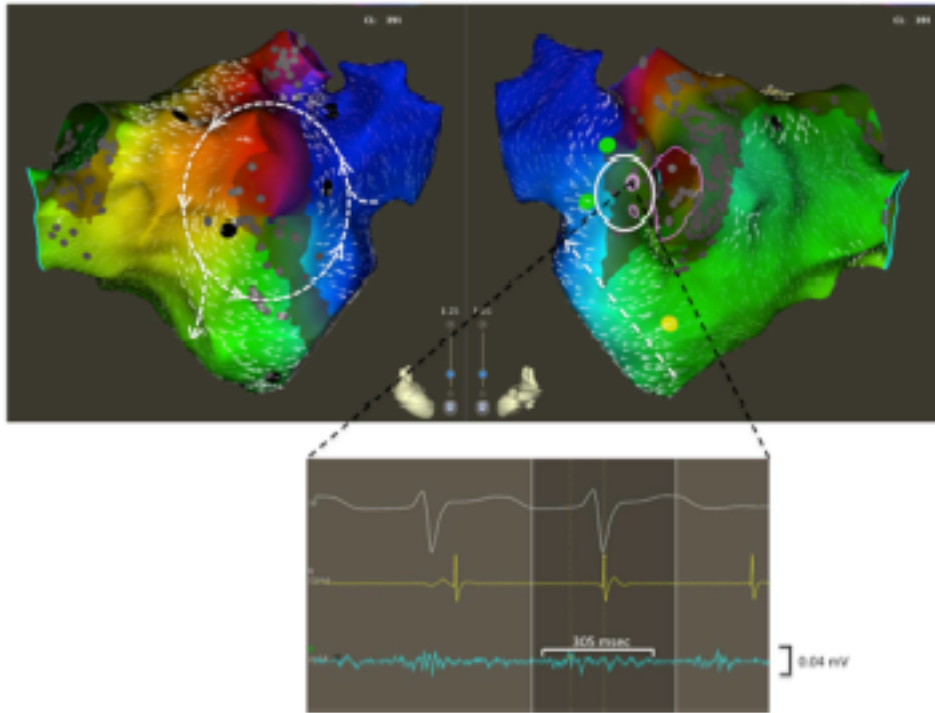


**Table 1. Patients' clinical characteristics**

Clinical characteristics	
Male, N(%)	22(63)
Age, years	69±11
CHAD <sub>2</sub> VASc, mean	2±1
AADs Class1c, N(%)	18(51)
Sotalol, N(%)	3(9)
Amiodarone, N(%)	2(6)
No AADs, N(%)	4(13)
Anti vit K, N(%)	4(11)
OAC, N(%)	19(54)
No AC, N(%)	4(13)
N previous ablation, median	1(1-2)

AADs: anti arrhythmic drugs; OAC: oral anti coagulants:

**Table 2 ATs' mechanism and characteristics**

<b>AT mechanism</b>	<b>TCL</b>	<b>HDAM points</b>	<b>EM points</b>
<b>Macro-reentrant ATs (N 22)</b>	288(238-313)	1076(898-1498)	7.5±4.7
Roof circuits (N 12)			
• around LVs (N 5)	290(245-293)	916(612-1827)	8±6.5
• around RVs (N 7)	270(215-320)	991(931-1316)	5±2.7
Perimitral circuits (N 10)	290(238-328)	1263(738-1513)	7.7±3.6
<b>Double loop ATs (N 4)</b>	255(243-260)	1535 (1067-1905)	7.5±2.5
<b>Macro- + Micro- reentries (N 1)</b>	230	344	12
<b>Micro-reentry circuits(N 8)</b>	270(226-373)	939(414-2490)	9±3.4

AT: atrial tachycardia; EM: entrainment manoeuvres; HDAM: high density activation mapping;

LVs: left veins; RVs: right veins; TCL: tachycardia cycle length

## Chapter 15



# Directed Networks as a Novel Way to Describe and Analyze Cardiac Excitation: Directed Graph Mapping

*Nele Vandersickel<sup>1\*†</sup>, Enid Van Nieuwenhuysse<sup>1†</sup>, Nico Van Cleemput<sup>2‡</sup>, Jan Goedgebeur<sup>2,3‡</sup>, Milad El Haddad<sup>4</sup>, Jan De Neve<sup>5</sup>, Anthony Demolder<sup>4</sup>, Teresa Strisciuglio<sup>6</sup>, Mattias Duytschaever<sup>4,6</sup> and Alexander V. Panfilov<sup>1,7</sup>*

OPEN ACCESS

## **Introduction**

Networks provide a powerful methodology with applications in a variety of biological, technological and social systems such as analysis of brain data, social networks, internet search engine algorithms, etc. To date, directed networks have not yet been applied to characterize the excitation of the human heart. Directed networks naturally occur in the analysis of excitation patterns recorded by electrodes. When connecting discrete points of measurement in proximity to each other based on their local activation times (LAT), a directed network is created. This network of cardiac excitation appears suitable for directed network analysis. By applying network theory, conduction paths can be identified in a new and different way based on local activation times and by taking the physiological conduction velocity into account. During the analysis, the algorithm identifies potential ablation targets such as rotational activity, spreading from electrode to electrode creating a closed loop, or focal activity, manifesting as a divergence of excitation from a given point (region). We refer to this method as directed graph mapping (DG mapping). In graph theory, very efficient methods have been developed to find closed loops in directed networks. Using these methods, one can easily find all possible loops in these data within mere seconds. Since this approach analyzes all possible loops automatically, it forms a robust method even in the presence of noise or incorrect electrode recordings, making it much more reliable than current existing methods. Furthermore, it allows the determination of additional properties of excitation as well, which can be essential for the characterization of the arrhythmia. By using directed networks and DG mapping, we believe that a more reliable, faster and fully automatic analysis of activation patterns can be performed with a higher accuracy than in current daily practice.

The goal of this study is to demonstrate the wide applicability of directed networks to the heart for each driving mechanism of cardiac arrhythmias in both the atria and the ventricles. Therefore, we tested the accuracy of DG mapping in in-silico (ventricular) models of functional and anatomical reentry and focal activity. To determine the accuracy of DG mapping in the atria, we analyzed 31 clinical cases of atrial tachycardia. Regular AT is a clinical tachyarrhythmia in which the operator can be sure about the location of the tachycardia since ablation of the correct target almost always results in immediate success. Therefore, AT was used as the gold standard for validating DG mapping in a clinical setting. In addition, DG mapping was compared to phase mapping (Gray et al., 1998) via in-silico simulations, a widely used technique for detecting the center of a rotor.

## **Methods**

### *In-silico Generated Datasets*

All simulations were performed using the TNNP-computer model for human ventricular cells (ten Tusscher and Panfilov, 2006) utilizing the explicit-Euler integration scheme (Vandersickel et al., 2014) on a GeForce GTX 680 and a GeForce GTX Titan, with single precision. The following different scenarios were simulated: (1) Functional reentry was simulated in 2D (in a domain of 512 by 512 grid points with interspacing of 0.25 mm) and 3D (a simplified model of the human ventricle and an anatomically accurate model of the human ventricle Tusscher et al., 2007). (2) Anatomical reentry was also simulated in 2D and 3D (anatomically accurate model of the human ventricle). In both scenarios, the S1S2-protocol was applied to obtain rotational activity (Tusscher and Panfilov, 2003). (3) Focal activity was simulated in 2D and 3D (anatomical model of the human ventricle) by applying 3 stimuli at 3 different locations of 500 ms each.

All simulations were performed for a duration of 20s. In all simulations, the rotors were stable in space and time. For each different setup, we implemented either 64 surface electrodes (mimicking 64 electrode-basket catheters, Narayan et al., 2012), 256 surface electrodes with an interspacing of 0.8 mm (mimicking experimental grid sizes, de Groot et al., 2010) or 500 intramural electrodes (in the 3D anatomical model) in analogy with the experimental setup by Taccardi et al. (2005) In Figure 2, an example of a rotor with 64 electrodes is shown.

### *Clinical Datasets*

Between April and August 2017, 29 patients undergoing ablation of symptomatic ATs at AZ Sint-Jan BrugesHospital were enrolled in the study, resulting in 31 activation maps (30 left atrium 1 right atrium).

Automated and continuous acquisition of points was performed by the CONFIDENSE mapping module (Carto 3 v. 4, Biosense Webster Inc.) using the novel hybrid LAT annotation method (LATHybrid) (Pooter et al., 2018). Each AT case was analyzed offline by DG mapping after exporting all local activation times (LATs) and the corresponding 3D coordinates. In Figure 3A, an example of the left atrium is shown, with the corresponding LAT map and annotated points.

The tachycardia mechanism was confirmed when ablation resulted in sinus rhythm or in conversion of a second tachycardia. In case of multiple hypotheses of the AT mechanism, the hypothesis which agreed with the ablation endpoint was chosen.

### *Directed Graph Mapping Protocol*

This section explains the DG mapping algorithms, as shown in the blue panels in Figure 1.



### *Determine the Neighbors in a Given System*

First, for a given configuration of electrodes, possible neighbors for each electrode are determined. These neighbors cover all possible paths where the wave can travel to, starting from a certain electrode. For regular grids, the neighbors are found by setting a spheric distance around a single point. Hence, a single point incorporates up to 8 neighbors in case of the 2D grid (see Figure 2B) and up to 26 neighbors in case of a regular 3D grid. For an irregular configuration of electrodes, like the clinical AT cases, Delanauy triangulation is applied to determine for each electrode its possible neighbors (see Figure 3B).

### *Creating Network of Cardiac Excitation*

We chose a certain time  $t$ . Starting from this time, we find  $LAT_1, \dots, LAT_n$  which are the first LAT larger than  $t$  for each electrode in our system of  $n$  electrodes. We then draw arrows as follows. Suppose electrodes 1 and 2 form a pair of neighbors. Assume electrode 1 has  $LAT_1$  and electrode 2 has  $LAT_2$ , with  $LAT_2 > LAT_1$ , meaning the difference between the two electrodes is  $LAT = LAT_2 - LAT_1 > 0$ . We allowed a directed link from electrode 1 to 2 if (Vandersickel et al., 2017):

$$CV_{min} < \frac{d}{dLAT} < CV_{max}. \quad (2)$$

In this equation,  $CV_{min}$ ,  $CV_{max}$ , and  $d$  represent minimal conduction velocity, maximal conduction velocity and the euclidean distance between the two electrodes, respectively. For the simulated examples for ventricular tissue (2D and 3D) we took  $CV_{min} = 0.2$  mm/ms, and  $CV_{max} = 2.00$  mm/ms. For the clinical AT cases,  $CV_{min}$  was set at 0.08 mm/ms, according to the lowest physiological conduction velocity in human atria determined by Konings et al. (1994),  $CV_{max}$  was set to maximal

2.0 mm/ms (Harrild and Henriquez, 2000). In Figures 2C, 3C, the directed arrows from a single electrode are shown. Once this first graph was created, a second graph at a time  $t + t$  was created in exactly the same way as the first graph. We set  $t = 40$  ms. Finally, these two graphs were merged, whereby arrows of the second network were added to the first network if the LAT of the node where the arrow originates from was the same. This was necessary as in the first network, no closed cycles will be present, which represent the rotational activity of the arrhythmia, and they are exactly the arrows of the second graph, which will create cycles in the network. The resulting graph is the final directed network. For example, in Figures 2D, 3D, the complete network is shown for a simulated case and a regular AT.

### Rotational Activity

Once the network is created, any type of rotational activity can be found by detecting cycles in the network. A cycle is a closed directed walk without repetition of nodes. In order to find the cycles, a standard breadth-first search algorithm was used. Since the constructed network generally turns out to be rather small and very sparse, this can be done very efficiently. It turns out that detecting all (smallest) cycles through each node can be done almost instantaneously. We ran theoretical simulations on networks with 1,000,000 nodes, and even in these cases all cycles were found in the range of seconds. Clearly, the physical bounds on the number of electrodes that can be placed will be more limiting than the computational work that is needed to process the data. In Figures 2E, 3E, the resulting cycles of the network of a simulated rotor and a regular AT case are shown. In order to find the core of any type of rotational activity,

we looked for the smallest cycles in the network and computed the geometric center. This was performed by grouping all found cycles based on their proximity to the geometric center. If the centers lie closer to each other than a specified threshold, the cycles were considered to belong to the same core. In this study, we took 1 cm as threshold, as we estimated that the cores of the reentry loops considered in this work were always apart > 1 cm. Afterwards there was an optional pass which merges bundles of cycles if they shared nodes. Finally, the centers of each bundle were defined as the core of rotational activity. In Figures 2F, 3F, the selected cycles are shown.

### Focal Activity

Focal activity was detected as a source node, i.e., a node which has a non-zero out-degree, and an in-degree equal to 0. These can be found immediately by doing a single pass over all nodes. Then, the LATs were bundled in certain intervals to reduce the inter-variability in the LAT values. Afterwards, we reconstructed the network with these bundled values. We then checked if regions with only outgoing arrows were present. The middle of these regions corresponds to the source of the focal activity.

## Results

### *In-silico Models of Functional and Anatomical Reentry and Focal Activity*

The accuracy of DG mapping was tested in different in-silico models as described in the methods section. First, for functional reentry (see Figure 4A), we simulated a 2D rotor with a configuration of 64 electrodes (A1) and 256 electrodes (A2). In 3D, functional reentry was induced in a simplified model of the ventricles with 64 surface electrodes (A3) and in an anatomical model of the ventricles with 500 intramural electrodes (A4).

In all four setups, DG mapping was able to accurately detect functional reentry and correctly determine the location of the core of the rotor for the entire length of the simulation (20 s duration). The smallest cycle and corresponding core are shown in yellow for each setup. Second, DG mapping was validated in two models of anatomical reentry (Figure 4B): a 2D anatomical circuit with 64 electrodes (B1) and a 3D anatomical reentry with 500 intramural points in the model of the ventricles (B2). In both models, DG mapping correctly identified the reentrant path around the obstacles for the entire length of the simulation (20s). The shortest reentry loops are again depicted in yellow. Third focal activity was simulated in 2D (64 electrodes) and 3D (500 intramural electrodes) (Figure 4C) by repetitively stimulating 3 different locations. Again, DG mapping identified the electrodes most closely to the site of stimulation, see C1 (yellow arrows) and C2 (black circles).

### *Clinical Dataset*

To establish proof of concept in the clinical setting, we retrospectively and blindly analyzed 31 cases of regular atrial tachycardia (AT). For clarity, in Figure 3, all the steps of the DG mapping protocol were demonstrated on an AT case of a localized reentry. In general, the atria have a complex structure. In case of reentry during AT, the electrical waves circle around obstacles such as the valves, the veins or scar tissue, creating a (sustained) reentry loop. Ablation aims to terminate the reentry loop so that the circular electrical conduction can no longer be sustained. Therefore, it is important to precisely determine the location of the activation pathway. The accuracy of DG mapping was compared to the standard diagnosis, i.e., type of arrhythmia and location of the circuit/focal activity as determined by the

electrophysiologist (EP) based on the activation map and the ablation result. The overall results are summarized in Figure 5. Out of 31 cases, 20 were due to macro-reentry, 6 due to localized reentry and 5 due to focal activity. In 9 cases with reentry, the operator was not sure about the reentry mechanism purely based on the LAT activation map, formulating several hypotheses. The gold standard was taken as the diagnosis. matching the ablation endpoint. Compared to this gold standard diagnosis, DG mapping identified the exact same mechanism and location in 28 out of 31 cases (90.3%, 95% exact binomial confidence interval 74.2% - 98%). In 3 out of 31 cases, the diagnosis of DG mapping did not fully match with the gold standard. In 2 cases of double loop reentry (cases 6 and 14), DG mapping identified only one single loop. In the other case (case 22), the mapping data indicated focal tachycardia, whereas DG mapping identified localized reentry at the same location.

However, in all 3 cases, DG mapping would have pointed to the correct ablation target, meaning that DG mapping correctly identified the ablation target in 31/31 cases.

Representative cases are shown in Figure 6. Panel A depicts a macro-reentrant AT around the right pulmonary veins in the LA conducting over the roof. Ablation of the roof resulted in prompt termination of the AT. Blinded analysis by DG mapping revealed a selected loop at the same location (middle panel).

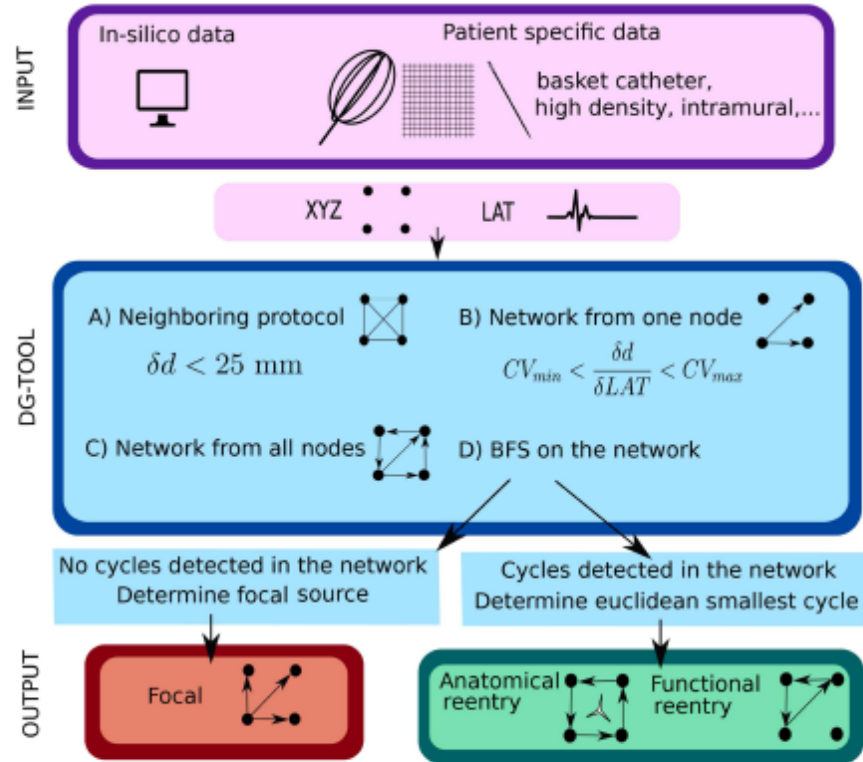
Panel B shows a localized reentry at the anterior wall, rotating around local scar tissue.

Ablation from the scar to the mitral valve terminated AT. DG mapping (middle) as well as wave averaging (bottom) identified the same location of the localized reentry. In panel C, activation mapping and ablation conformed with focal tachycardia at the septum. DG mapping (in the absence of loops) pointed to focal activity as well (middle panel). We also tested the wave algorithm for each case, as shown in the bottom panels of Figure 6. Wave averaging was for all

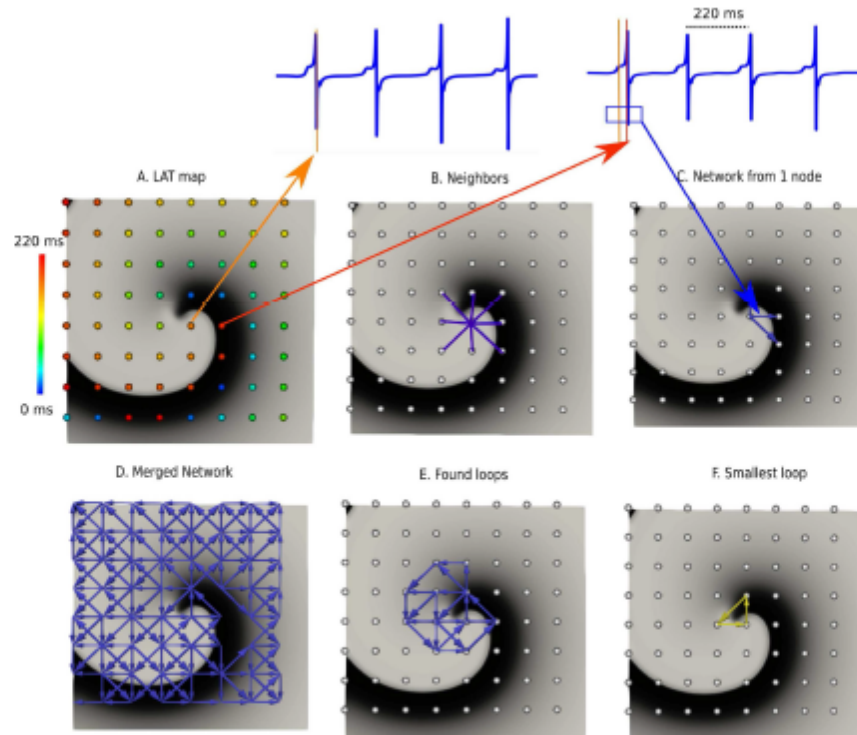
the cases compatible with the results of the DG mapping. Representative examples are shown in Figure 6: macro reentry (A), localized reentry (B), and focal activation (C).

## **Conclusion**

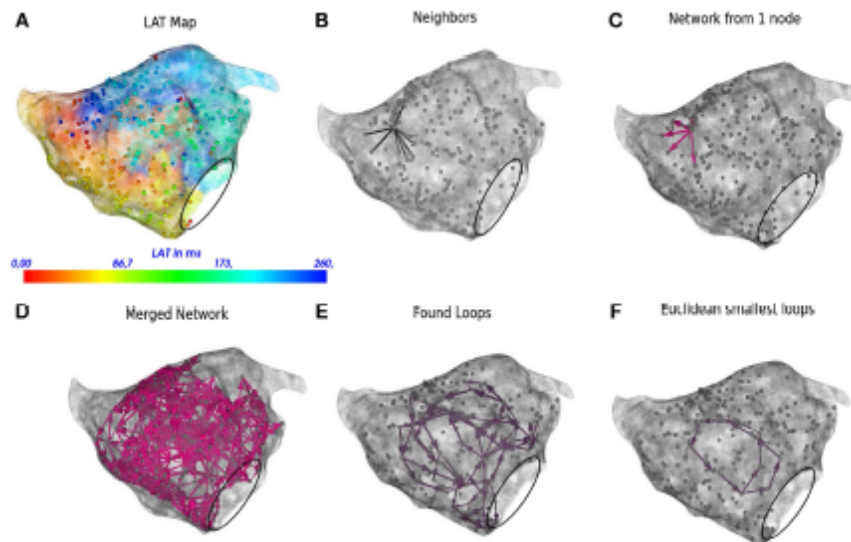
We demonstrated that tools used in network theory analysis allow determination of the mechanism and location of certain cardiac arrhythmias. We show that the robustness of this approach can potentially exceed the existing state-of-the-art methodology used in clinics. Furthermore, implementation of these techniques in daily practice can improve the accuracy and speed of cardiac arrhythmia analysis. It may also provide novel insights in arrhythmias that are still incompletely understood.



**FIGURE 1** | Illustration of the work flow of the DG mapping tool. As input, the DG-tool requires for a given setup of electrodes the LAT values with the corresponding XYZ coordinates, which can be extracted from either simulation studies or a clinical setup. The input is then processed as follows in the DG-tool as presented in the flowchart. Next, we apply a loop-finding algorithm to detect cycles in the network. If cycles are not detected, we locate the source of focal activity. In case cycles were detected, the loops are merged and its center is determined. At the end, the output is visualized. In case of a focal source, arrows pointing away from a (group of) node(s) are shown, while for reentry, arrows will be plotted to visualize the reentry path.

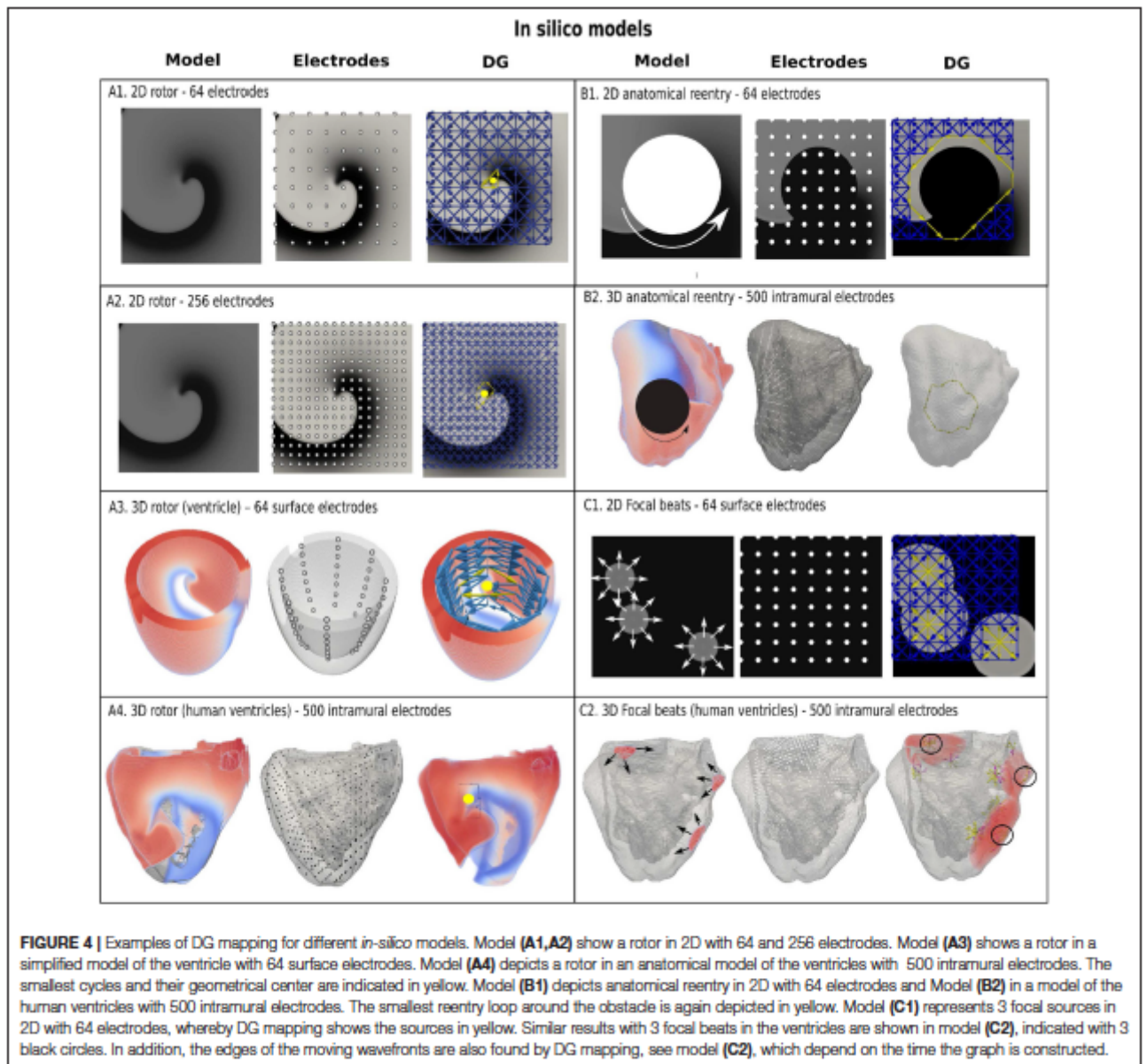


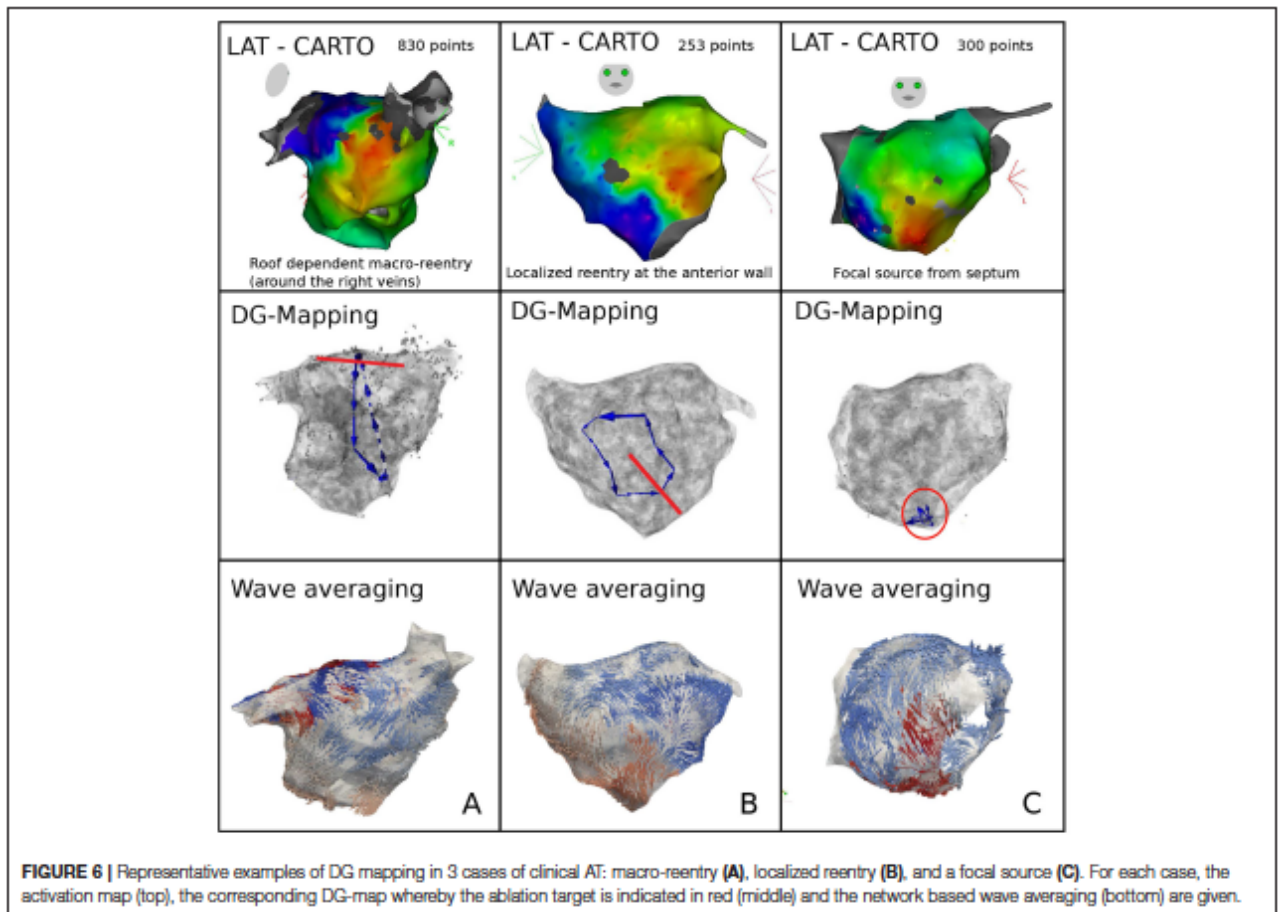
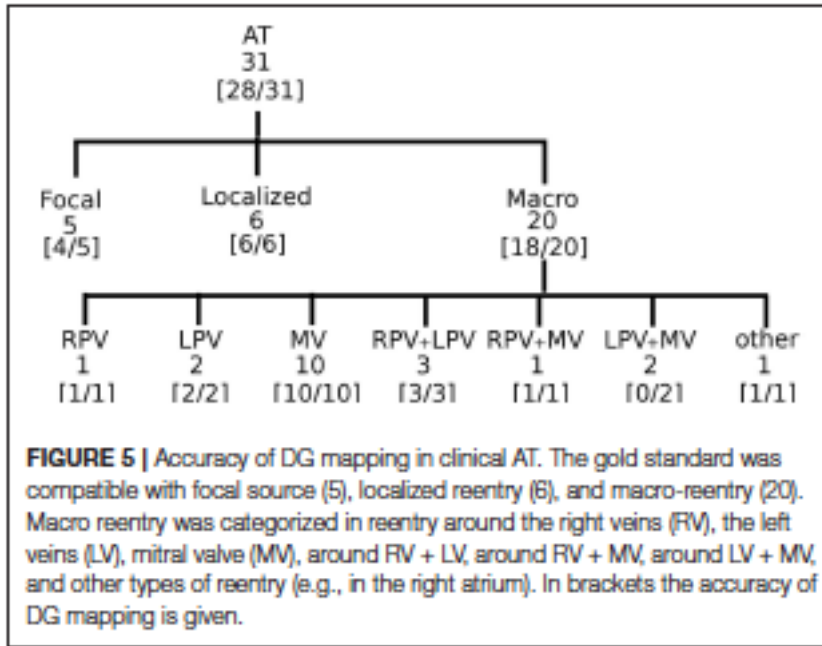
**FIGURE 2** | DG mapping for a simulated rotor with a regular measuring grid. **(A)** The points are colored according to their LAT. **(B)** Shows an example of the 8 possible neighbors for a single grid point. **(C)** Represents the corresponding network for the same location. **(D)** The complete network is drawn from which all detected loops in the network are derived, as shown in **(E)**. The selected (smallest) loop among the bundle is shown in **(F)**.



**FIGURE 3** | DG mapping for a regular AT case of localized reentry. The gray dots represent the mapping points while the black circle denotes the mitral valve. The LAT annotation map in ms is given in **(A)**. **(B)** Shows an example of all possible neighbors for a single annotated location. **(C)** Represents the corresponding network for the same single annotated location. **(D)** The complete network is drawn from which all detected loops in the network are derived, see **(E)**. The loop corresponding to the smallest cycle in the network among the bundle is shown in **(F)**.







## Chapter 16

### **Evaluation of Directed Graph-mapping in complex Atrial Tachycardias**

Enid Van Nieuwenhuyse<sup>1,†</sup>, Teresa Strisciuglio<sup>2,3,†</sup>, Giuseppe Lorenzo<sup>4,\*</sup>, Milad El Haddad<sup>2,‡</sup>, Jan Goedgebeur<sup>5,8</sup>, Nico Van Cleemput<sup>5</sup>, Christophe Ley<sup>5</sup>, Alexander V. Panfilov<sup>1,7</sup>, Jan de Pooter<sup>2,6</sup>, Yves Vandekerckhove<sup>2</sup>, Rene Tavernier<sup>2</sup>, Mattias Duytschaever<sup>2,6,‡</sup>, Sebastien Knecht<sup>2</sup> and Nele Vandersickel<sup>1</sup>

*Under peer review*

## **Abstract**

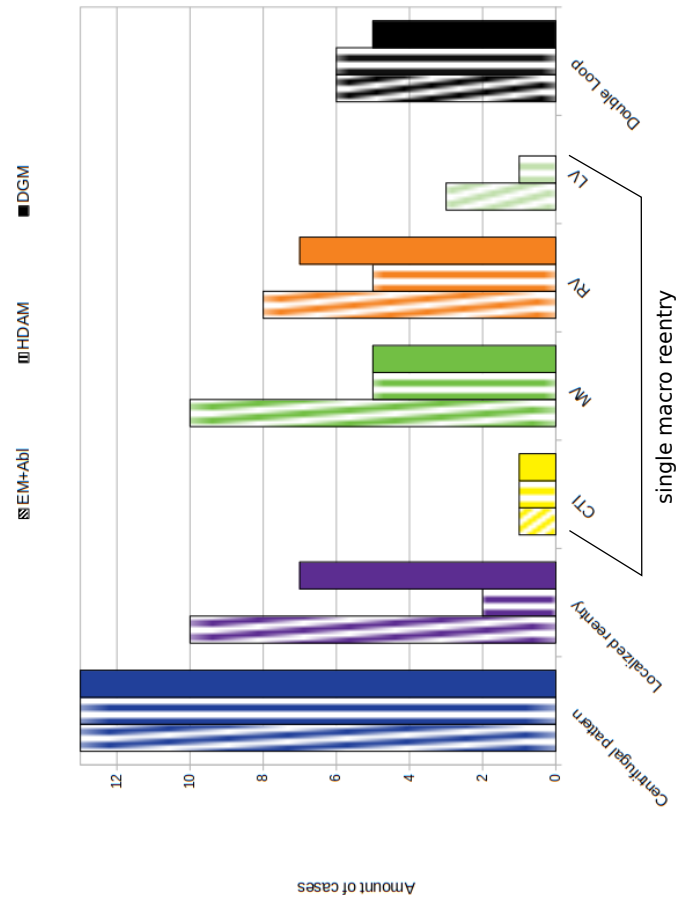
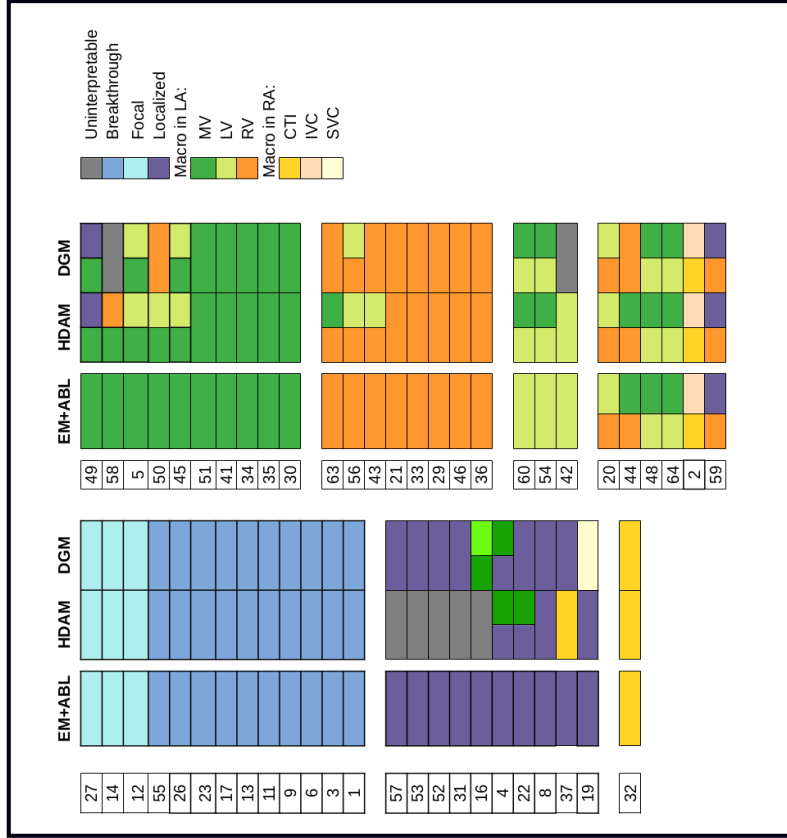
**Background** Catheter ablation of atrial tachycardias (ATs) still represents a challenge as the identification of the correct mechanism can be difficult. New algorithms for high density activation mapping (HDAM) render an easier acquisition of more detailed maps, however the understanding of the mechanism is still strongly operator-dependent.

**Aims** DGM is an automatic tool that can be applied to the identification of the AT mechanism. In the present study we sought to evaluate the diagnostic accuracy of DGM in complex ATs.

**Methods** HDAMs acquired with the latest generation algorithm (CoHerent v7, Biosense Webster) were interpreted off-line by four expert electrophysiologists and by DGM (also offline development). Entrainment manoeuvres (EM) were performed to understand the correct mechanism, then confirmed by successful ablation (13 cases were focal/breakthrough, 10 cases were localized reentry, 22 cases were macro reentry and 6 were double loops). In total 51 ATs were retrospectively analyzed. We compared the diagnoses made by DGM with those of the experts and with EM results.

**Results** Experts and DGM diagnosed the correct AT mechanism and location in 33 and 38 cases respectively. The diagnostic accuracy varied according to different AT mechanisms. The 13 centrifugal activation patterns were always correctly identified by both methods. 2/10 localized reentries were identified by the experts, whereas DGM diagnosed 7/10. For the macro reentries, 12/22 were correctly identified with HDAM versus 13/22 for DGM. Finally, 6/6 double loop were correctly identified by the experts, versus 5/6 for DGM.

**Conclusion** DGM is an automatic, fast and operator-independent tool to identify the AT mechanism and location and could be a valuable addition to current mapping technologies.



## General Discussion

### *The optimization journey of catheter ablation for paroxysmal AF*

Despite the great interest in the newest technologies (1-2), the radiofrequency ablation with a linear catheter and a point-by-point approach represents the most widely used strategy (3).

In the past, while the target of the ablation procedure, i.e. the electrical disconnection between the PV ostia and the LA, was clear, however the way to reach a durable result has been a matter of debate, and the reconnection of PV as cause of AF recurrence has been the major concern for years. The recovery of PV conduction has been attributed to the inadequacy of lesion formation (4-5), and in particular to the lack of transmural damage that causes temporary electric uncoupling but not cell death. Thus, the line of ablation is not complete and these lesion gaps, that often go undetected during the index procedure, may determine late PV reconnection. Of note, the introduction of an automated algorithm for the objective annotation of the RF applications enhanced the detection of ineffective energy delivery and gaps, thus reducing the incidence of conduction recovery (6). On the other hand, in the absence of real-time assessment of lesion development and transmurality, surrogate measures of lesion quality have been commonly utilized. Before the advent of contact force catheters the most used were the fall in local impedance during ablation and the reduction in local electrograms' amplitude during ablation (7-9), then the force-time integral, which multiplies contact force by radiofrequency duration, has been extensively used. The FTI correlated with either impedance drop and electrograms attenuation (10). Of interest, a low contact force and a low FTI have been associated after PVI with early recovery and dormant conduction demonstrated with the adenosine proof (11).

Furthermore, the value of the FTI as a marker of lesion quality has been corroborated by the EFFICAS I and II studies. The first demonstrated that the FTI was predictive of PVI segment

reconnection at repeat study (12), and the second that the ablation guided by a minimum FTI target reduced significantly the rate of reconnected veins, although this was still high (13). Afterwards, it became clear that the FTI has two major limitations: 1) it doesn't take into account the power, 2) it is derived by the simple multiplication of the force by the duration of lesion formation. The first point implies that the same FTI value can be obtained with low power for longer time or with high power for shorter time, however we know that power plays a major role and a higher power is associated with a larger lesion size (14). As for the second point it means that the two variables force and duration have the same weight, however from the animal models we know that after 20 seconds of radiofrequency energy delivery the size of the lesion doesn't change much (15), whereas the force have a greater contribution to lesion formation. From these evidences arose the need to find a new marker for lesion quality, and this is what Nakagawa and colleagues did. They elaborated a new formula incorporating power, time and contact force in a weighted formula, the force-power-time index (FPTI) then called ablation index (AI), and they found that this formula accurately ( $\pm 1\text{mm}$ ) predicted lesion depth in the canine beating heart (16-17). A step forward has been made with the study by Das et al. (18) demonstrating that in patients with paroxysmal AF at the repeat electrophysiological study 2 months after a first PVI the minimum AI was predictive of PV segment reconnection and that higher AI values were required to prevent reconnection in the anterior/roof segments.

Beyond being transmural the lesions created by RF energy should also be enough close to create a complete ablation line without gaps. The study by El Haddad et al. (19) investigated the determinants of acute and late PV reconnection after contact force guided PVI. For each annotated RF lesion (tag), the data reflecting lesion depth (time, power, contact force, FTI and AI) and the inter-lesion distance (ILD) were collected. They found that the lack of

transmurality (low AI) and contiguity (large ILD) were independent predictors of the recovery of PV conduction. The optimal cut-off values were 550 and 400 for the AI on the anterior and posterior wall respectively, and  $\leq 6$ mm for the ILD.

These represented the key ingredients of the CLOSE protocol recipe.

### *Efficacy and Reproducibility*

The CLOSE-guided PVI, consisting of the encirclement of the PVs following strict criteria of transmurality and contiguity represents an objective and reproducible endpoint that enables: 1) to reduce procedure and RF time 2) to reach high rates of procedural success (97-98%) 3) to reach high rates of 1-year freedom from AF (91-94%) (20-21). Previous studies reporting on RF ablation showed less favorable results.

The FIRE AND ICE (FIRE AND ICE: Comparative Study of Two Ablation Procedures in Patients With Atrial Fibrillation) study described a 64% single-procedure freedom from AF after point-by-point RF ablation (22), however only 2/3 of patients were ablated with contact force (CF) catheters.

Since the introduction of CF-sensing technology, several studies suggested enhanced acute durability of PVI and 1-year freedom from paroxysmal AF (23–26). In a parallel cohort study, CF guidance was associated with lower incidence of dormant conduction (8% vs. 35%) and better 1-year arrhythmia-free survival (88% vs. 66%) (23). In a single-center controlled study, CF guidance was associated with higher acute procedural success (80% vs. 36%) and 1-year AF freedom (90% vs. 67%) (24).

Although randomized controlled studies failed to demonstrate a beneficial effect of CF-guidance on AF free survival at 1 year (27-28), the study by Philips et al (21), in which CLOSE



guided PVI was compared to a CF-guided ablation (conventional ablation) confirmed the 80% single-procedure freedom of AF in the latter group.

More importantly, the data by Philips et al. suggest that further optimization of CF-guided ablation by adding objective criteria (the 'CLOSE' criteria of ILD and AI) further improves acute durable isolation rates and 1 year single-procedure outcome. Several observations speak for the reliability of the currently reported >90% single-procedure freedom of AF after 'CLOSE'-guided PVI. First, this high success rate is in line with the hypothesis that avoiding weak links within the deployed RF circle is the key to durable PVI and clinical success (19). Second, also other research groups, respecting a contiguous encircling, reported a >90% single-procedure arrhythmia-free survival in CF-guided PVI. A recent sub-analysis of SMART-AF in 40 paroxysmal AF patients showed 93% freedom from arrhythmia in those patients with short ILD (29). Likewise, Itoh et al. (30) reported single-procedure freedom of 96% at 1 year after a procedure in which CF-guided PVI was performed using catheter tip dragging in steps of about 2mm.

Beyond these single-center experiences, the efficacy of the CLOSE protocol needed also to be confirmed in larger cohorts of patients and in multicenter studies in order to be widely adopted.

In [Chapter 3](#) we showed that using a standardized AI guided workflow and integrated 3D angiography-derived models enables predictable procedural efficiency. Procedure and fluoroscopy times under the standardized workflow were markedly shorter and less variable when compared to prior studies of CF-sensing technology (26, 31). For example, comparing the PAF cohort in our study to the published SMARTAF cohort, a > 2-fold average procedure time reduction was observed (96 min vs. 222 min) (31). Perhaps even more important from a standardization perspective is the observed reduction in the variability of procedure

times in a real-world setting of consecutive cases (standard deviation of procedure time: 26 min vs. 84 min in SMART-AF) (31). Serious procedure-related complications were infrequent and within previously reported ranges (31), indicating that efficiency and effectiveness gains did not compromise patient safety. Freedom from atrial arrhythmia recurrence among PAF patients was higher than typical of previously published studies on CF-sensing technology (31). Although procedural efficiency and effectiveness were greater in the PAF cohort compared to the PsAF cohort, the PsAF cohort also demonstrated good efficiency and long-term effectiveness, consistent with previous reporting of CF ablation compared to pre-CF ablation technology (32).

Reproducibility of AF catheter ablation safety and efficacy still remains an unsolved issue. RF ablation of AF is a technically complex procedure, with a long learning curve, and its results seem to largely depend on center's experience. In recent years, cryoballoon ablation of AF has been introduced as an alternative “single - shot” approach for PV isolation. Several multicenter studies (33,34) showed the higher reproducibility of cryoballoon ablation compared with standard RF ablation as regards midterm outcomes of catheter ablation of AF, with lower inter - operator and inter - center variability.

In Chapter 4 we report the 1-year results of the AIR registry, a prospective, multi-centric study designed to evaluate the reproducibility of PV isolation guided by the AI. A total of 44 operators, in 25 centers, performed the 490 ablation procedures in patients with paroxysmal (80.4%) and persistent AF underwent first time PV isolation. Twelve operators performed at least 15 ablation procedures. Patients were divided in four study groups according to operator's preference in choosing the ablation catheter (a contact force (ST) or contact force surround flow (STSF) catheter) and the AI setting (330 - 450 or 380 - 500 at anterior wall or

posterior wall, respectively). In our multicentre study we observed about 90% rate of freedom from AF recurrence. Moreover, we reported a high (>80%) 1 year success rate also in patients with persistent AF. In our study AI guided PV isolation seems to perform equally well, acutely (35) and at 1-year, when ablation is performed by high - volume operators as compared with low - volume operators with different skills.

These excellent results have been corroborated by the recently published VISTAX study, a multicentre, prospective, non-randomized study conducted at 17 European sites, that enrolled 340 patients with drug-refractory paroxysmal AF. This study showed that different centers by using a standardized PVI workflow (CLOSE protocol) reached a high rate of first pass isolation and a 12-months freedom from arrhythmia approaching 80% (36).

#### *The outcomes of ablation: AF burden reduction and PVI durability*

Efficacy of catheter ablation (CA) is commonly expressed as single-procedure freedom from any ATA (>30s) (37). This definition (in which one single, even short episode implies permanent failure) most likely underestimates clinically relevant success after CA. In this regard, ATA burden, defined as % of time spent in ATA, seems a more reliable estimate of clinically relevant success after CA (38-39) Indeed, prior studies suggested a dose-effect relation between ATA burden and symptoms, heart failure and stroke(40-44). Glotzer et al showed that a  $\geq 20\%$  ATA burden was associated with a double stroke risk(42), whereas Go et al. showed that only a  $\geq 11.4\%$  AF burden was associated with a >3-fold higher adjusted rate of thromboembolism in PAF patients(43).

A limited number of prospective studies reported on patient-controlled ATA burden after CA.

In the DISCERN AF study, CA reduced mean ICM-detected ATA burden from 8.3% to 1.25% after 18 months (45). In MANTRA-PAF, CA reduced estimated ATA burden from a 90th ATA burden of 30% to 13% throughout the first 24 months.(46) In the CAPTAF study, CA reduced ICM-detected ATA burden from 24.9±37% to 5.5±18.1% at 12 months (p<0.001), not different from medical therapy.(47)

In Chapter 5, we showed that optimized CA had a marked and maintained impact on ATA burden (with a low number of repeat procedures and without ADT). In a PAF population in which one quarter of the patients presented with ATA burden >15.02%, median ATA burden in the 1st two years after CA was 0 [IQR 0-0] % and also in patients with some ATA recurrence, ATA burden was significantly reduced (because episodes were short-lasting and isolated in nature). Probably an early intervention strategy during the first year from AF diagnosis (although performed in only 26% of patients) might contribute to improved outcome. Whether reduction in ATA burden by CA might impact AF-related morbidity and mortality requires further study, especially in a sicker population.

Marrouche et al recently showed that reduction of burden improves outcome in heart failure patients(44). Likewise, reduction of burden might improve symptoms (40,41), and reduce stroke(42,43).

The relation between atrial tachyarrhythmia (ATA) burden in paroxysmal atrial fibrillation (AF), atrial remodelling, and efficacy of catheter ablation (CA) has never been investigated before, thus in Chapter 6, that is a sub-analysis of the CLOSE to CURE study, we investigated whether high vs. low-burden paroxysmal AF patients have distinct clinical characteristics or

electro-mechanical properties of the left atrium (LA) and whether burden impacts outcome of CA.

We observed a large variation in ATA burden with a median burden of 2.7%, and one-third of patients presenting with a burden threshold of more than 9.3%. The reported burden and its variation is in line with prior studies reporting a burden of 4.4 (1.1–17.23%) (43), 8% (3–53%) (48), 3.7% (0.6–33.1%) (47).

Also the value for high burden (arbitrarily defined as the highest tertile) is in close proximity to the value reported in the large paroxysmal AF cohort in the study by Go et al. (43).

Those high-burden patients were not characterized by specific clinical characteristics, with no trend towards more obesity or hypertension.

We did not observe any association between ATA burden and atrial refractoriness or conduction velocity. Although several experimental and clinical studies confirmed that maintained AF leads to shortening of atrial refractoriness (electrical remodelling) (49-50), lack of changes in refractoriness can be explained by the self-terminating nature of paroxysmal AF and the rapid time course of reversed electrical remodelling.

We did observe that higher AF burden (together with a longer AF history) is associated with structural and functional changes of the LA resulting in atrial dilatation and impaired function. Most likely higher burden is both the cause and consequence of mechanical alterations of the atria (inducing a vicious circle promoting the progression of AF).

In animal models, maintained AF was associated with contractile and structural remodelling of the atria (49). Mechanical alterations of the atria in high-burden patients might be due to AF-induced metabolic and functional changes (reduction in Ca<sup>2+</sup> inward current, I<sub>CaL</sub>) (49).

Indeed, many studies have pointed out a relation between impairment of atrial function

and markers of fibrosis either assessed either by magnetic resonance imaging (51), atrial histology (52), or low-voltage mapping (53). Of note, however, the current observation that high-burden patients have no apparent increase in low-voltage characteristics, suggests that AF itself (without structural heart disease) does not lead to atrial fibrosis in paroxysmal AF patients. As for the relation between burden and efficacy of CA, we observed in patients with high burden—despite the presence of larger atrial size and depressed atrial function—a high efficacy of CA. After optimized PV isolation aiming for durable isolation, single-procedure freedom from ATA was 83% with a low residual burden [0 (0–0)%] throughout the 1st year after CA. The discrepancy between the  $\approx 20\%$  recurrence rate and  $\approx 0\%$  residual burden suggests that CA does not completely eliminate all triggers, but reduces atrial vulnerability to residual triggers. Our data fuel the debate on the optimal timing for CA in patients with paroxysmal AF. The observation that high burden leads to (potentially irreversible) mechanical remodeling together with the low efficacy of CA in persistent AF speaks to an early ablation strategy. On the other hand, our data on the high efficacy in high-burden patients suggest that there is no need to rush the decision to ablate.

So far we have seen that the CLOSE protocol is associated with excellent outcome in terms of freedom from AF recurrence and of ATA burden reduction, however in [Chapter 7](#) we investigated if the low rate of patients with recurrence had still durable PVI at repeat procedure. The durability is very important as this is an objective parameter, as it is referred to patients coming back to the cathlab for clinical recurrence., therefore it is a clinically indicated repeat procedure. We found that 62% of repeat patients revealed a status of complete isolation and this confirms that CLOSE-guided PVI, by avoiding weak links in the ablation chain, is associated with durable isolation.

It is generally accepted that AF recurrence after PVI is due to reconnection of 1 or more PV. This is based on the good outcome after isolation of reconnected veins with repeat ablation for AF and numerous observations that recurrence after PVI is almost invariably associated with reconnection of the vein(s). Prior studies, predominantly in patients with paroxysmal AF, reported indeed a low incidence of a status of complete vein isolation at repeat ablation for AF recurrence (54-60).

In the earlier years (using non irrigated or irrigated non-CF RF or first-generation cryoballoon to isolate the veins) the likelihood of complete isolation was as low as 0% and certainly not exceeding 20%. The likelihood of finding 4 isolated veins at repeat ablation for AF recurrence after predominantly second-generation cryoballoon PVI ranged from 26% to 41% (54-60).

More recent data on RF-guided PVI still show high reconnection rates (61,62). Shah et al. (62) showed that the incidence of isolated veins in patients with late AF recurrence (>36 months after first PVI) was 19%. Of interest, although CF-guided ablation is associated with higher percentage of complete isolation in study patients undergoing invasive re-evaluation at 3 months regardless of symptoms (63,64), Buist et al. (61) reported a low incidence of finding 4 veins isolated at repeat for CF-guided RF (only 3%). Finally, a recent meta-analysis by Nery et al. (65) reported an overall 14% likelihood of finding 4 isolated veins in case of a clinically indicated repeat ablation after PVI.

#### *How to further improve the ablation results?*

During point-by-point RF ablation, lesion size is determined by different parameters including the catheter stability (66). However, the stabilization of the catheter on the atrial wall during

application is difficult to achieve depending on (i) movements of the beating heart, (ii) respiratory movements whether spontaneous or due to mechanical ventilation under general anaesthesia, and (iii) stability of the catheter itself in the atrium. To overcome these potential stability problems during AF ablation, different techniques have been proposed. Rapid ventricular pacing has been shown to reduce catheter-tissue contact variability, and therefore, increase the probability of achieving pre-specified catheter-tissue contact endpoints, resulting in higher impedance reduction during ablation (67). Deep sedation (68), adaptative servo ventilation (69), general anaesthesia (70-71), and high frequency jet ventilation (72) are also associated with more efficient procedures. Using a long sheath, potentially a steerable one, also seems to improve catheter ablation results (73-74). Finally, studies about high power and short duration applications have also shown some potential benefits (75-77).

Despite potential manoeuvres used to increase catheter stability, some complex anatomical structures of the left atrium remain unfavourable to ablation and result in a higher risk of catheter dislocation. The anterior part of the left PVs is very complex since it combines two different ridges: the ridge between the left PVs and the LAA and the carina between the two veins. As mentioned in previous manuscripts, 67% of the patients have two separate left PVs (78-79) with a mean distance between the ostia of up to 4.5mm.

In their manuscript, Cabrera et al. nicely showed that there was no common ostium in the majority of patients, and therefore, the anterior line of the left PV encirclement needed to be placed on the crest of the ridge or in its vicinity. As the ridge itself is generally narrow (<5mm), catheter stability is difficult to obtain and it is challenging to ensure contiguous and optimized ablations lesions. In [Chapter 8](#) we described a new simple technique, the “loop technique, for stabilizing the ablation catheter during anterior pulmonary vein (PV) encirclement in patients ablated for paroxysmal atrial fibrillation. This consists in bending the



ablation catheter in the left atrium, creating a loop that is then cautiously advanced together with the long sheath towards the ostium and then within the left superior PV. The use of the loop technique helps stabilizing the ablation catheter on the thin ridge. This technique was also associated with a significantly higher impedance drop as compared to a direct approach, in addition to the favorable time and RF outcomes. Therefore, it could be used as a systematic approach or in the case of recurrent dislocation using a more conventional technique.

In addition to catheter stability, another important parameter for lesion formation is the power. We know that, for different RF durations, the lesion size invariably increases with increasing power (80).

Several studies have compared different power RF ablation strategies for PV isolation, mostly without relying on the AI formula (81-84). Higher power ablation has been shown to be associated with a reduction in the duration of the procedural parameters (ablation procedure time, PV isolation time, fluoroscopy time, and radiation dose)(81-84), reduced AF recurrence (84), and PV reconnection (83), but sometimes with an increased risk of steam pops along with a higher incidence of pericardial effusion and gastrointestinal symptoms (especially during longer RF application) (84).

A recent multicenter registry compared two different RF power setups and two different irrigated catheters (83). As compared to the conventional group (25 - 30 W), the high power group (30 - 40 W) was associated with better efficiency, lower acute PV reconnection, without increased side effects (83). In [Chapter 9](#) we compared patients ablated with the CLOSE protocol and 40 W with patients ablated with the CLOSE protocol and 35 W. Our study confirmed prior data as all procedural parameters were improved, and moreover we did not observe any steam pop or esophageal injury in the few patients with significantly increased

esophageal temperature who received a gastroscopy. Also, the postprocedural recurrence of ATA at 1 year was not significantly different in the high power group of this study.

However, this was a monocentric nonrandomized study with a limited amount of patients, and therefore caution has to be taken regarding the risk of complications. To overcome these limitations we conducted a randomized prospective study, the POWER-AF study described in [Chapter 10](#), that confirmed the efficacy and safety of higher power.

### *Safety of the CLOSE-guided PVI*

In every ablation strategy safety should run parallel with the efficacy. One of the major concern during ablation is the esophageal damage, due to the close proximity of the esophagus with the posterior wall of the left atrium. Esophageal injury and atrio-esophageal fistula are obstacles in the search for durable PVI. In order to avoid thermal esophageal lesions, the 2017 expert consensus statement advises (1) reduction of RF power along the posterior wall (class I indication); and (2) use of an intraluminal temperature probe to monitor intraesophageal temperature rise (ITR) and help guide energy delivery (class IIa indication) (85). However, reduction of RF power might lead to nondurable PVI and more repeat ablations. Moreover, during the procedure itself, lower power might lead to non-adenosine-proof or non-first-pass isolation with the ensuing need for touchup applications (with possible accumulation of RF delivery and conductive heating at particular locations, which paradoxically increases the risk for AEF formation).

The incidence of esophageal injury is equally high after PVI in which RF delivery is guided by an esophageal temperature probe and ITR. Di Biase et al. (86) (50 patients; 35 W over the posterior wall with discontinuation of RF at ITR >39°C) reported esophageal injury in 26% of patients. Muller et al (87) (40 patients; ≤25 W posterior wall; CF target 10–40g;

discontinuation of RF delivery at ITR  $\geq 39.5^{\circ}\text{C}$ ) reported an incidence of esophageal injury of 30% (7.5% ulceration). Halbfass et al (88) (40 patients;  $<25\text{ W}$ ; CF 10–20g; RF time  $<20$  seconds on posterior wall; discontinuation of RF delivery at ITR  $>39^{\circ}\text{C}$ ) reported an incidence of 7.5% (2.5% ulceration). The high incidence is in line with a recently published largest single-center registry (89) (832 patients), in which it was demonstrated that endoscopically detected esophageal injury early after RF ablation (performed within 7 days) is as high as 18% (12% erythema, 6% ulceration) and that the only risk factor associated with the occurrence of esophageal injury is ITR  $>40.5^{\circ}\text{C}$

In [Chapter 11](#) we evaluated esophageal and periesophageal injury with endoscopy in patients revealing ITR during CLOSE-PVI and we found that at endoscopy the occurrence of esophageal or periesophageal injury is markedly low (1.2%), suggesting that this ablation strategy is safe. The discrepancy with the high rate of ulceration found by Halbfass et al. is probably due to the timing of the endoscopy. They performed it 7 days after ablation and they found that the ulcerations were already healing, whereas we performed the endoscopy later, i.e. 9 days after ablation. However, another difference is that we report very few short lasting applications at the posterior wall with no dislocations and no kissing circles, and this could also explain the markedly lower rate of esophageal injury.

#### *Catheter ablation of persistent AF and scar-related atrial tachycardias: What's new?*

The underlying mechanisms sustaining human persistent atrial fibrillation (PsAF) is poorly understood. The consequence of this is that so far different ablation strategies have been adopted but none of these was demonstrated to be more effective than the others. There is growing evidence that persistent AF is maintained by local reentrant or focal sources (90).

Invasive and non invasive mapping have been used to identify these drivers during persistent

AF (91-92). An ablation strategy targeting these drivers results in favourable AF-free survival at 1 year, albeit with a significant rate of AT recurrence requiring further management (93). Some mapping technologies have relied on mathematical transformations of the data, such as phase mapping (94), to better visualize rotational activations in particular. However phase mapping may generate false rotational activities as in the case of low voltage areas (95-96) therefore other detection algorithms have been developed such as the Cartofinder software (Biosense Webster) (97). Prior studies evaluating this software always used the 64 pole basket catheter (Constellation, Boston Scientific, Natick, MA) and were able to reliably and reproducibly identify repetitive activation patterns during AF in the majority of patients (98-100). However with the basket catheter, the interelectrode spacing is larger and there could be an issue with electrode - tissue contact and a predilection to position the basket towards the anterior wall (97,100). This can result in a suboptimal coverage of the atrial surface (54% to 72%) (97,100), with possible underestimation of RAAPs.

In Chapter 12 we aimed to identify repetitive atrial activation patterns (RAAPs) during ongoing atrial fibrillation (AF) based upon automated annotation of unipolar electrograms (EGMs) recorded with a high - density regional endocardial contact mapping catheter (Pentaray, Biosense Inc.). In our study sequential high - density mapping showed the presence of RAAP during persistent AF in all patients and in our series, focal firing was the most frequently observed pattern. We highlighted that the PentaRay high - density mapping catheter may detect a greater number of RAAPs due to better coverage and mapping density in comparison with basket catheters, indeed it has the ability to reach all atrial regions. Furthermore, the automated annotation software has the potential to provide on - line

detection of potential biatrial AF drivers annotated on the 3D - geometric biatrial shell, making patient - tailored substrate ablation possible.

Beyond the identification of drivers, several different ablation techniques have been developed to target the atrial substrate in persistent AF, including ablation of CFAEs in both atria, left atrial linear lesions, and the so - called “stepwise” approach (101).

Outcomes from ablation using these strategies have given modest results, and each approach lacks specificity, sometimes resulting in extensive ablation with potentially deleterious effects (on atrial hemodynamic function or with proarrhythmic consequences) (101). The occurrence of scar-related atrial tachycardias (ATs) is common and repeat ablation procedure after a first ablation for persistent AF is often necessary, as these arrhythmias are poorly tolerated by the patients. However the identification of the correct mechanism may be difficult especially in very diseased atria. Standard activation mapping algorithms utilizing local activation time (LAT) alone are suited for describing simple activation patterns in normal tissue. However, they are suboptimal for mapping complex patterns of propagation in the presence of abnormal electrograms. Their basic limitation stems from the fact that each electrogram receives a single-time annotation regardless of its complexity or duration. In this regard, high-resolution mapping technologies utilizing catheters with small and closely spaced electrodes may improve the accuracy of local time annotation over standard linear catheters by sampling smaller tissue size (102-103). However, their use without resolving the basic discernment of accurate electrogram annotation may further complicate interpretation of complex activation patterns. These limitations are the most evident in complex substrates and require a different approach.

Chapter 13 describes a novel mapping algorithm (Coherent mapping, Biosense Webster) that calculates vectors and applies physiological constraints of electrical excitation in human atrial tissue, thus overcoming the major limitations of standard activation mapping.

In this study, we found that the investigational mapping algorithm was superior to the standard activation algorithm, and it allowed accurate identification of the mechanism in >90% of cases as compared with 66.7% ( $P < 0.001$ ) with improved identification of the successful ablation site at a similar proportion. Finally, this new algorithm improves the ability to identify and follow complex patterns of propagation and to guide ablation.

Despite the recent improvement of high density activation mapping (HDAM) technologies, we are still far from achieving the correct diagnosis in all cases. A study by Pathik et al. (104) on right atrial ATs clarified that HDAM often shows visual reentrant circuits that are only bystanders and not part of the circuit. In Chapter 14 we investigated whether in the era of HDAM the entrainment mapping (EM) has still a role in the ablation of complex left ATs. EM is a pivotal electrophysiological technique to identify arrhythmia mechanisms as well as to define components of the reentrant circuit (105-106).

Our study highlighted the following problems encountered during HDAM alone. First of all, “false” double loop macro-reentrant ATs were frequently visualized with HDAM. Secondly, the performance of HDAM for diagnosing micro-reentrant ATs was poor. This was mostly due to the problems encountered by the system to correctly annotate multicomponent and long duration fractionated EGMs in micro-reentrant ATs as well as to correctly represent a very small micro-reentry circuit with colour coding. Furthermore, micro-reentry circuits often generate passive activations around the atrium, which can mimic larger macro-reentrant ATs and render difficult diagnosing.

Therefore, EM still represents a crucial additional tool to increase the diagnostic accuracy for left ATs, and especially to differentiate active from passive macro-reentrant loops and to demonstrate micro-reentry circuits.

Another disadvantage of the HDAM is that the understanding of the mechanism is still strongly operator-dependent as the same colour-coded map can be differently interpreted by different operators. Furthermore, the colour code is based on the arbitrary setting of the window of interest and the wrong LAT annotation may determine the presence of multiple “early” and “late” areas on the map, where the identification of the correct mechanism is not possible. When these situations occur the manual editing of the LAT annotation and the analysis of single EGMs is the solution, however this is time-consuming. In [Chapter 15](#) a novel automatic and operator-independent diagnostic algorithm, the Direct Graph Mapping (DGM), has been validated using in-silico and clinical data. DGM applies the directed network analysis to characterize the cardiac excitation. In clinical practice, cardiac excitation is recorded by multiple discrete electrodes and during (normal) sinus rhythm or during cardiac arrhythmias, successive excitation connects neighboring electrodes, resulting in their own unique directed network. DGM for instance can be used to understand the mechanism of tachycardias as it creates from the LAT map a directed network where each measured point is a node of the network. Then, based on the LAT of each single node, DGM detects the most probable circuit of propagation and therefore automatically identifies the mechanism and location of the tachycardia. In the study presented in chapter 15, the DGM reliably detected functional/anatomical reentry and focal activity in in-silico (ventricular) models. Additionally in the clinical setting of 31 cases of regular AT (also retrospective analysis), it has been demonstrated to be effective in identifying the correct AT mechanism and the site of ablation.

In Chapter 16, the added value of DGM for the ablation of complex ATs has been evaluated. The diagnostic accuracy of DGM was then compared with that of HDAM interpreted off-line by 4 expert electrophysiologists. We found that DGM was accurate for the detection of macro-reentries as well as localised re-entries and focal AT. Of note, DGM was able to overcome the wrongly annotated LAT points and therefore the editing of the LAT map was not needed. The reason thereof is that DGM does not only take into account local properties of the LATs but takes into account the global picture of the LATs.

The present study demonstrates that the use of DGM in the clinical setting of right and left ATs could be beneficial. DGM has a diagnostic accuracy similar to that of HDA maps' interpretation by experts however it has the advantage of being independent from the operator's experience and interpretation. This is the first tool that is completely automatic and operator-independent as it is based on mathematical algorithms that enable to have the correct diagnosis of the AT mechanism and location within a minute. Therefore DGM represents a unique tool to standardize ATs' ablation procedures, as operator experience will not be an influencing factor.



## **Conclusion**

In this long lasting research journey we demonstrated that the CLOSE-guided PVI, an ablation protocol following strict criteria of contiguity and transmuralty a) enables to standardize the RF ablation procedure with more predictable procedure and ablation times 2) is highly effective as demonstrated by the low rates of AF recurrence at long-term follow up, the dramatic reduction of the AF burden and the high rates of durable PVI at repeat ablation c) is safe as the rate of complications and esophageal injury is low 4) is reproducible as in multicenter studies different operators with different skills had similar good outcomes.

While our findings provide certainties to the field of paroxysmal AF ablation, we are still far from having the same confidence in the field of persistent AF ablation and ATs.

We hereby described the latest algorithms for mapping and ablation of persistent AF and ATs, and we showed that the diagnostic accuracy of these technologies is high, thus representing a valid support for ablation.

## LIST OF ABBREVIATIONS

AF: Atrial Fibrillation

PV: Pulmonary Vein

PVI: Pulmonary Veins Isolation

CF: Contact Force

FTI: orce Time Integral

FPTI: Force Powe Time Index

AI: ablation Index

ST: Smartouch catheter

SF: Surround Flow catheter

AEF: atrio-Esophageal Fistula

ITR: Intra-esophageal Temperature Rise

RAAP: Rapid atrial Activation Pattern

AT: atrial Tachycardia

HDAM: High density activation Mapping

EM: Entrainment Mapping

DGM: Directed Graph Mapping

## Bibliography

1. Rottner L, Bellmann B, Lin T et al. Catheter Ablation of Atrial Fibrillation: State of the Art and Future Perspectives *Cardiol Ther* (2020) 9:45–58
2. J.S. Koruth, K. Kuroki, J. Iwasawa, et al. Endocardial ventricular pulsed field ablation: a proof-of-concept preclinical evaluation. *Europace*, 22 (2020), pp. 434-439
3. Arbelo E, Brugada J, Hindricks J. et al. The Atrial Fibrillation Ablation Pilot Study: an European Survey on Methodology and results of catheter ablation for atrial fibrillation conducted by the European Heart Rhythm Association. *European Heart Journal*, 2014: 35(22); 1466-1478.
4. Verma A, Kilicaslan F, Pisano E, et al. Response of atrial fibrillation to pulmonary vein antrum isolation is directly related to resumption and delay of pulmonary vein conduction. *Circulation* 2005;112:627–635.
5. Kowal RC. PVI's inconvenient truths: lights out for dormant reconnection? *J Cardiovasc Electrophysiol* 2012;23:261–263.
6. Anter E, Tschabrunn CM, Contreras-Valdes FM. et al. Radiofrequency ablation annotation algorithm reduces the incidence of linear gaps and reconnection after pulmonary vein isolation. *Heart Rythm* 2014 May;11(5):783-90.
7. He DS, Bosnos M, Mays MZ, Marcus F. Assessment of myocardial lesion size during in vitro radio frequency catheter ablation. *IEEE Trans Biomed Eng* 2003;50: 768–76.
8. Avitall B, Mughal K, Hare J, Helms R, Krum D. The effects of electrode-tissue contact on radiofrequency lesion generation. *Pacing Clin Electrophysiol* 1997;20: 2899–910.
9. Reichlin T, Lane C, Nagashima K, Nof E, Chopra N, Ng J et al. Feasibility, efficacy, and safety of radiofrequency ablation of atrial fibrillation guided by monitoring of the initial impedance decrease as a surrogate of catheter contact. *J Cardiovasc Electrophysiol* 2015;26:390–6.
10. Ullah W, Hunter RJ, Baker V, Dhinoja MB, Sporton S, Earley MJ et al. Target indices for clinical ablation in atrial fibrillation: insights from contact force, electrogram, and biophysical parameter analysis. *Circ Arrhythm Electrophysiol* 2014;7:63–8.
11. le Polain deWaroux JB, Weerasooriya R, Anvardeen K, Barbraud C, Marchandise S, De Meester C et al. Low contact force and force-time integral predict early recovery and dormant conduction revealed by adenosine after pulmonary vein isolation. *Europace* 2015;17:877–83.
12. Neuzil P, Reddy VY, Kautzner J, Petru J, Wichterle D, Shah D et al. Electrical reconnection after pulmonary vein isolation is contingent on contact force during initial treatment: results from the EFFICAS I study. *Circ Arrhythm Electrophysiol* 2013;6: 327–33.
13. Kautzner J, Neuzil P, Lambert H, Peichl P, Petru J, Cihak R et al. EFFICAS II: optimization of catheter contact force improves outcome of pulmonary vein isolation for paroxysmal atrial fibrillation. *Europace* 2015;17:1229–35.
14. Guerra JM, Jorge E, Raga S, Galvez-Monton C, Alonso-Martin C, Rodriguez-Font E et al. Effects of open-irrigated radiofrequency ablation catheter design on lesion formation and

- complications: in vitro comparison of 6 different devices. *J Cardiovasc Electrophysiol* 2013;24:1157–62.
15. Wittkamp FH, Hauer RN, Robles de Medina EO. Control of radiofrequency lesion size by power regulation. *Circulation* 1989;80:962–8.
  16. Nakagawa H, Ikeda A, Govari A, Papaioannou T, Constantine G, Bar-Tal M et al. Prospective study using a new formula incorporating contact force, radiofrequency power and application time (Force-Power-Time Index) for quantifying lesion formation to guide long continuous atrial lesions in the beating canine heart. *Circulation* 2013;128:A12104 (abstr).
  17. Nakagawa H, Ikeda A, Govari A, Papaioannou T, Constantine G, Bar-Tal M et al. Prospective study to test the ability to create RF lesions at predicted depths of 3, 5, 7 and 9 mm using a new formula incorporating contact force, radiofrequency power and application time (Force-Power-Time Index) in the beating canine heart. *Heart Rhythm* 2013;10:S481 (abstr).
  18. Das M, Loveday JJ, Wynn GJ. et al. Ablation index, a novel marker of ablation lesion quality: prediction of pulmonary vein reconnection at repeat electrophysiology study and regional differences in target values. *Europace* 2017: 19; 775–783.
  19. El Haddad M, Taghij P, Philips T. et al. Determinants of Acute and Late Pulmonary Vein Reconnection in Contact Force-Guided Pulmonary Vein Isolation: Identifying the Weakest Link in the Ablation Chain. *Circ. Arrhythm. Electrophysiol.* 2017 Apr;10(4):e004867.
  20. Taghji P, El Haddad M, Philips T, et al. Evaluation of a strategy aiming to enclose the pulmonary veins with contiguous and optimized radiofrequency lesions in paroxysmal atrial fibrillation: a pilot study. *J Am Coll Cardiol EP* 2018;4:99–108.
  21. Philips T, Taghji P, El Haddad M, et al. Improving procedural and one-year outcome after contact force-guided pulmonary vein isolation: the role of interlesion distance, ablation index, and contact force variability in the 'CLOSE'-protocol. *Europace* 2018;20:f419–27.
  22. Kuck KH, Brugada J, Fürnkranz A, et al., for the FIRE AND ICE Investigators. Cryoballoon or radiofrequency ablation for paroxysmal atrial fibrillation. *N Engl J Med* 2016;374:2235–45.
  23. Andrade JG, Monir G, Pollak SJ, et al. Pulmonary vein isolation using contact force ablation: the effect on dormant conduction and long-term freedom from recurrent atrial fibrillation—a prospective study. *Heart Rhythm* 2014;11:1919–24.
  24. Marijon E, Faza S, Narayanan K, et al. Realtime contact force sensing for pulmonary vein isolation in the setting of paroxysmal atrial fibrillation: procedural and 1-year results. *J Cardiovasc Electrophysiol* 2014;25:130-7.
  25. Reichlin T, Lane C, Nagashima K, et al. Feasibility, efficacy, and safety of radiofrequency ablation of atrial fibrillation guided by monitoring of the initial impedance decrease as a surrogate of catheter contact. *J Cardiovasc Electrophysiol* 2015;26:390–6.
  26. Afzal MR, Chatta J, Samanta A, et al. Use of contact force sensing technology during radiofrequency ablation reduces recurrence of atrial fibrillation: a systematic review and meta-analysis. *Heart Rhythm* 2015;12:1990–6.
  27. Ullah W, McLean A, Tayebjee MH, Gupta D, Ginks MR, Haywood GA; UK Multicentre Trials

- Group et al. Randomized trial comparing pulmonary vein isolation using the SmartTouch catheter with or without real-time contact force data. *Heart Rhythm* 2016;13:1761–7.
28. Reddy V, Dukkipati S, Neuzil P, Natale A, Albenque J, Kautzner J et al. Randomized controlled trial of the safety and effectiveness of a contact-force sensing irrigated catheter for ablation of paroxysmal atrial fibrillation (Toccastar study). *Circulation* 2015;132:907–15
  29. Reddy V, Pollak S, Lindsay B, McElderry H, Natale A, Kantipudi C et al. Relationship between catheter stability and 12-month success after pulmonary vein isolation: a subanalysis of the SMART-AF trial. *J Am Coll Cardiol* 2016;2:691–9.
  30. Itoh T, Kimura M, Tomita H, Sasaki S, Owada S, Horiuchi D et al. Reduced residual conduction gaps and favourable outcome in contact force-guided circumferential pulmonary vein isolation. *Europace* 2016;18:531–7.
  31. Natale A, Reddy VY, Monir G, Wilber DJ, Lindsay BD, McElderry HT, et al. Paroxysmal AF catheter ablation with a contact force sensing catheter: Results of the prospective, multicenter SMARTAF trial. *J Am Coll Cardiol*. 2014;64(7):647–56.
  32. Hussein AA, Barakat AF, Saliba WI, Tarakji KG, Bassiouny M, Baranowski B, et al. Persistent atrial fibrillation ablation with or without contact force sensing. *J Cardiovasc Electrophysiol*. 2017;28(5):483–8.
  33. Providencia R, Defaye P, Lambiase PD, et al. Results from a multicentre comparison of cryoballoon versus radiofrequency ablation for paroxysmal atrial fibrillation: is cryoablation more reproducible? *Europace*. 2017;19:48-57.
  34. Landolina M, Arena G, Iacopino S, et al. Center experience does not influence long-term outcome and peri-procedural complications after cryoballoon ablation of paroxysmal atrial fibrillation: data on 860 patients from the real-world multicenter observational project. *Int J Cardiol*. 2018;272:130-136.
  35. Solimene F, Lepillier A, Ruvo E, et al. Reproducibility of acute pulmonary vein isolation guided by the ablation index. *Pacing Clin Electrophysiol*. 2019;42:874-881.
  36. Duytschaever M, Vijgen J, De Potter T, et al. Standardized pulmonary vein isolation workflow to enclose veins with contiguous lesions: the multicentre VISTAX trial. *Europace* 2020 Sep 3;euaa157.
  37. Calkins H, Hindricks G, Cappato R, et al. 2017 HRS/EHRA/ECAS/APHRS/SOLAECE expert consensus statement on catheter and surgical ablation of atrial fibrillation. *Heart Rhythm* 2017;14:e275-e444.

---

  38. Hindricks G, Potpara T, Dagres N, et al. 2020 ESC Guidelines for the Diagnosis and Management of Atrial Fibrillation Developed in Collaboration With the European Association of Cardio-Thoracic Surgery (EACTS): The Task Force for the Diagnosis and Management of Atrial Fibrillation of the European Society of Cardiology (ESC) Developed With the Special Contribution of the European Heart Rhythm Association (EHRA) of the ESC. *Eur Heart J* 2020;Aug 29:[Epub ahead of print].

---

  39. Chen L, Chung M, Allen L, et al. Atrial Fibrillation Burden: Moving Beyond Atrial Fibrillation as a Binary Entity: A Scientific Statement From the American Heart Association. *Circulation*. 2018;137(20).
  40. Mantovan R, Macle L, De Martino, et al. Relationship of quality of life with procedural success of atrial fibrillation (AF) ablation and postablation AF burden: substudy of the STAR AF randomized trial. *The Canadian journal of cardiology* 2013;29:1211-7.
  41. Bjorkenheim A, Brandes A, Magnuson A, Chemnitz A, Edvardsson N, Poci D. Patient-

- Reported Outcomes in Relation to Continuously Monitored Rhythm Before and During 2 Years After Atrial Fibrillation Ablation Using a Disease-Specific and a Generic Instrument. *Journal of the American Heart Association* 2018;7.
42. Glotzer TV, Daoud EG, Wyse DG, et al. The relationship between daily atrial tachyarrhythmia burden from implantable device diagnostics and stroke risk: the TRENDS study. *Circulation Arrhythmia and electrophysiology* 2009;2:474-80.
  43. Go A, Reynolds K, Yang J, Gupta N, et al. Association of Burden of Atrial Fibrillation With Risk of Ischemic Stroke in Adults With Paroxysmal Atrial Fibrillation. *JAMA Cardiology*. 2018;3(7):601.
  44. Marrouche N, Brachmann J, Andresen D, et al. Catheter Ablation for Atrial Fibrillation with Heart Failure. *New England Journal of Medicine*. 2018;378(5):417-427.
  45. Verma A, Champagne J, Sapp J, et al. Discerning the Incidence of Symptomatic and Asymptomatic Episodes of Atrial Fibrillation Before and After Catheter Ablation (DISCERN AF). *JAMA Internal Medicine*. 2013;173(2):149.
  46. Schmidt M, Dorwarth U, Andresen D, et al. German ablation registry: Cryoballoon vs radiofrequency ablation in paroxysmal atrial fibrillation—One-year outcome data. *Heart Rhythm*. 2016;13(4):836-844.
  47. Blomström-Lundqvist C, Gizurarson S, Schwieler J, et al. Effect of Catheter Ablation vs Antiarrhythmic Medication on Quality of Life in Patients With Atrial Fibrillation. *JAMA*. 2019;321:1059.
  48. Walters TE, Nisbet A, Morris GM, Tan G, Mearns M, Teo E et al. Progression of atrial remodeling in patients with high-burden atrial fibrillation: implications for early ablative intervention. *Heart Rhythm* 2016;13:331–9.
  49. Allessie M, Ausma J, Schotten U. Electrical, contractile and structural remodeling during atrial fibrillation. *Cardiovasc Res* 2002;54:230–46.
  50. Wijffels MC, Kirchhof CJ, Dorland R, Allessie MA. Atrial fibrillation begets atrial fibrillation. A study in awake chronically instrumented goats. *Circulation* 1995;92: 1954–68.
  51. Kuppahally SS, Akoum N, Badger TJ, Burgon NS, Haslam T, Kholmovski E et al. Echocardiographic left atrial reverse remodeling after catheter ablation of atrial fibrillation is predicted by preablation delayed enhancement of left atrium by magnetic resonance imaging. *Am Heart J* 2010;160:877–84.
  52. Cameli M, Lisi M, Righini FM, Massoni A, Natali BM, Focardi M et al. Usefulness of atrial deformation analysis to predict left atrial fibrosis and endocardial thickness in patients undergoing mitral valve operations for severe mitral regurgitation secondary to mitral valve prolapse. *Am J Cardiol* 2013;111:595–601.
  53. Watanabe Y, Nakano Y, Hidaka T, Oda N, Kajihara K, Tokuyama T et al. Mechanical and substrate abnormalities of the left atrium assessed by 3-dimensional speckle-tracking echocardiography and electroanatomic mapping system in patients with paroxysmal atrial fibrillation. *Heart Rhythm* 2015;12: 490–7.
  54. Nanthakumar K, Plumb VJ, Epstein AE, Veenhuyzen GD, Link D, Kay GN. Resumption of electrical conduction in previously isolated pulmonary veins: rationale for a different strategy? *Circulation* 2004;109:1226–9.
  55. Ouyang F, Antz M, Ernst S, et al. Recovered pulmonary vein conduction as a dominant factor for recurrent atrial tachyarrhythmias after complete circular isolation of the pulmonary veins: lessons from double Lasso technique. *Circulation* 2005;111:127–35.
  56. Bordignon S, Furnkranz A, Perrotta L, et al. High rate of durable pulmonary vein

- isolation after second-generation cryoballoon ablation: analysis of repeat procedures. *Europace* 2015;17: 725–31
57. Callans DJ, Gerstenfeld EP, Dixit S, et al. Efficacy of repeat pulmonary vein isolation procedures in patients with recurrent atrial fibrillation. *J Cardiovasc Electrophysiol* 2004;15:1050–5
  58. Cappato R, Negroni S, Pecora D, et al. Prospective assessment of late conduction recurrence across radiofrequency lesions producing electrical disconnection at the pulmonary vein ostium in patients with atrial fibrillation. *Circulation* 2003;108:1599–604.
  59. Heeger CH, Wissner E, Mathew S, et al. Once isolated, always isolated? Incidence and characteristics of pulmonary vein reconnection after second-generation cryoballoon-based pulmonary vein isolation. *Circ Arrhythm Electrophysiol* 2015; 8:1088–94.
  60. Jiang RH, Po SS, Tung R, et al. Incidence of pulmonary vein conduction recovery in patients without clinical recurrence after ablation of paroxysmal atrial fibrillation: mechanistic implications. *Heart Rhythm* 2014;11:969–76.
  61. Buist TJ, Adiyaman A, Smit JJJ, Ramdat Misier AR, Elvan A. Arrhythmia-free survival and pulmonary vein reconnection patterns after second-generation cryoballoon and contact-force radiofrequency pulmonary vein isolation. *Clin Res Cardiol* 2018;107:498–506.
  62. Shah S, Barakat AF, Saliba WI, et al. Recurrent atrial fibrillation after initial long-term ablation success: electrophysiological findings and outcomes of repeat ablation procedures. *Circ Arrhythm Electrophysiol* 2018;11:e005785
  63. Das M, Wynn GJ, Saeed Y, et al. Pulmonary vein re-isolation as a routine strategy regardless of symptoms: the PRESSURE Randomized Controlled Trial. *J Am Coll Cardiol EP* 2017;3:602–11.
  64. Neuzil P, Reddy VY, Kautzner J, et al. Electrical reconnection after pulmonary vein isolation is contingent on contact force during initial treatment: results from the EFFICAS I study. *Circ Arrhythm Electrophysiol* 2013;6:327–33.
  65. Nery PB, Belliveau D, Nair GM, et al. Relationship between pulmonary vein reconnection and atrial fibrillation recurrence: a systematic review and meta-analysis. *J Am Coll Cardiol EP* 2016;2: 474–83.
  66. Duytschaever M, Taghji P, Tavernier R. Towards durable pulmonary vein isolation: we are closing the gap. *Europace* 2015;17:1164–5.
  67. Aizer A, Cheng AV, Wu PB, Qiu JK, Barbhuiya CR, Fowler SJ et al. Pacing mediated heart rate acceleration improves catheter stability and enhances markers for lesion delivery in human atria during atrial fibrillation ablation. *JACC Clin Electrophysiol* 2018;4:483–90.
  68. Kottkamp H, Hindricks G, Eitel C, Müller K, Siedziako A, Koch J et al. Deep sedation for catheter ablation of atrial fibrillation: a prospective study in 650 consecutive patients. *J Cardiovasc Electrophysiol* 2011;22:1339–43.
  69. Murakami T, Yamaji H, Numa K, Kawamura H, Murakami M, Higashiya S et al. Adaptive-servo ventilation combined with deep sedation is an effective strategy during pulmonary vein isolation. *Europace* 2013;15:951–6.
  70. Di Biase, Conti S, Mohanty P, Bai R, Sanchez J, Walton D et al. General anesthesia reduces the prevalence of pulmonary vein reconnection during repeat ablation when compared with conscious sedation: results from a randomized study. *Heart Rhythm* 2011;8:368–72.
  71. Martin CA, Curtain JP, Gajendragadkar PR, Begley DA, Fynn SP, Grace AA et al. Improved outcome and cost effectiveness in ablation of persistent atrial fibrillation under general anaesthetic. *Europace* 2018;20:935–42.

72. Hutchinson MD, Garcia FC, Mandel JE, Elkassabany N, Zado ES, Riley MP et al. Efforts to enhance catheter stability improve atrial fibrillation ablation outcome. *Heart Rhythm* 2013;10:347–53.
73. Piorkowski C, Eitel C, Rolf S, Bode K, Sommer P, Gaspar T et al. Steerable versus nonsteerable sheath technology in atrial fibrillation ablation. *Circ Arrhythm Electrophysiol* 2011;4:157–65.
74. Matsuo S, Yamane T, Tokuda M, Date T, Hioki M, Narui R et al. Prospective randomized comparison of a steerable versus a non-steerable sheath for typical atrial flutter ablation. *Europace* 2010;12:402–9.
75. Winkle RA, Moskovitz R, Hardwin Mead R, Engel G, Kong MH, Fleming W et al. Atrial fibrillation ablation using very short duration 50 W ablations and contact force sensing catheters. *J Interv Card Electrophysiol* 2018;52:1–8.
76. Bhaskaran A, Chik W, Pouliopoulos J, Nalliah C, Qian P, Barry T et al. Five seconds of 50–60 W radio frequency atrial ablations were transmural and safe: an n vitro mechanistic assessment and force-controlled in vivo validation. *Europace* 2017;19:874–80.
77. Hocini M, Condie C, Stewart MT, Kirchhof N, Foell JD. Predictability of lesion durability for AF ablation using phased radiofrequency: power, temperature, and duration impact creation of transmural lesions. *Heart Rhythm* 2016;13:1521–6.
78. Ho SY, Sanchez-Quintana D, Cabrera J. A, Anderson RH. Anatomy of the left atrium: implications for radiofrequency ablation of atrial fibrillation. *J Cardiovasc Electrophysiol* 1999;10:1525–33.
79. Cabrera JA, Ho SY, Climent V, Sa´nchez-Quintana D. The architecture of the left lateral atrial wall: a particular anatomic region with implications for ablation of atrial fibrillation. *Eur Heart J* 2008;29:356–62.
80. Wittkamp FHM, Nakagawa H. RF catheter ablation: lessons on lesions. *Pacing Clin Electrophysiol*. 2006;29(11):1285 - 1297.
81. Winkle RA, Mohanty S, Patrawala RA, et al. Low complication rates using high power (45 - 50 W) for short duration for atrial fibrillation ablations. *Heart Rhythm*. 2019;16(2):165 - 169.
82. Barkagan M, Contreras - Valdes FM, Leshem E, Buxton AE, Nakagawa H, Anter E. High - power and short - duration ablation for pulmonary vein isolation: safety, efficacy, and long - term durability. *J Cardiovasc Electrophysiol*. 2018;29(9):1287 - 1296.
83. Dhillon G, Ahsan S, Honarbakhsh S, et al. A multicentered evaluation of ablation at higher power guided by ablation index: establishing ablation targets for pulmonary vein isolation. *J Cardiovasc Electrophysiol*. 2019;30:357-365.
84. Kanj MH, Wazni O, Fahmy T, et al. Pulmonary vein antral isolation using an open irrigation ablation catheter for the treatment of atrial fibrillation: a randomized pilot study. *J Am Coll Cardiol*. 2007;49(15): 1634 - 1641.
85. Calkins H, Hindricks G, Cappato R, et al. 2017 HRS/EHRA/ECAS/APHRS/SOLAECE expert consensus statement on catheter and surgical ablation of atrial fibrillation. *Heart Rhythm* 2017;14:e275–e444.
86. Di Biase L, Saenz LC, Burkhardt DJ, et al. Esophageal capsule endoscopy after radiofrequency catheter ablation for atrial fibrillation: documented higher risk of luminal esophageal damage with general anesthesia as compared with conscious sedation. *Circ Arrhythm Electrophysiol* 2009;2:108–112.



87. Muller P, Dietrich JW, Halbfass P, et al. Higher incidence of esophageal lesions after ablation of atrial fibrillation related to the use of esophageal temperature probes. *Heart Rhythm* 2015;12:1464–1469.
88. Halbfass P, Muller P, Nentwich K, et al. Incidence of asymptomatic oesophageal lesions after atrial fibrillation ablation using an oesophageal temperature probe with insulated thermocouples: a comparative controlled study. *Europace* 2016; 19:385–391.
89. Halbfass P, Pavlov B, Müller P, et al. Progression from esophageal thermal asymptomatic lesion to perforation complicating atrial fibrillation ablation: a single-center registry. *Circ Arrhythm Electrophysiol* 2017;10(8):e005233.
90. Hansen BJ, Csepe TA, Zhao J, Ignozzi AJ, Hummel JD, Fedorov VV. Maintenance of atrial fibrillation: Are reentrant drivers with spatial stability the key? *Circulation. Arrhythmia and electrophysiology*. 2016;9
91. Honarbakhsh S, Schilling RJ, Dhillon G, Ullah W, Keating E, Providencia R, Chow A, Earley MJ, Hunter RJ. A novel mapping system for panoramic mapping of the left atrium: Application to detect and characterize localized sources maintaining atrial fibrillation. *JACC. Clinical electrophysiology*. 2018;4:124-134
92. Lim HS, Hocini M, Dubois R, Denis A, Derval N, Zellerhoff S, Yamashita S, Berte B, Mahida S, Komatsu Y, Daly M, Jesel L, Pomier C, Meillet V, Amraoui S, Shah AJ, Cochet H, Sacher F, Jais P, Haissaguerre M. Complexity and distribution of drivers in relation to duration of persistent atrial fibrillation. *Journal of the American College of Cardiology*. 2017;69:1257-1269
93. Knecht S., Sohal M., Arentz T., et al. (2017) Noninvasive mapping prior to ablation for persistent atrial fibrillation: The AFACART multicenter study. *Europace* 2017 Aug 1;19(8):1302-1309
94. Umapathy K, Nair K, Masse S, Krishnan S, Rogers J, Nash MP, Nanthakumar K. Phase mapping of cardiac fibrillation. *Circulation. Arrhythmia and electrophysiology*. 2010;3:105-114
95. Benharash P, Buch E, Frank P, et al. Quantitative analysis of localized sources identified by focal impulse and rotor modulation mapping in atrial fibrillation. *Circ Arrhythm Electrophysiol*. 2015;8:554-561.
96. Nattel S, Xiong F, Aguilar M. Demystifying rotors and their place in clinical translation of atrial fibrillation mechanisms. *Nat Rev Cardiol*. 2017;14:509-520.
97. Verma A, Sarkozy A, Skanes A, et al. Characterization and significance of localized sources identified by a novel automated algorithm during mapping of human persistent atrial fibrillation. *J Cardiovasc Electrophysiol*. 2018;29:1480-1488.
98. Daoud EG, Zeidan Z, Hummel JD, et al. Identification of repetitive activation patterns using novel computational analysis of multielectrode recordings during atrial fibrillation and flutter in humans. *JACC Clin Electrophysiol*. 2017;3:207-216
99. Honarbakhsh S, Schilling RJ, Dhillon G, et al. A novel mapping system for panoramic mapping of the left atrium: application to detect and characterize localized sources maintaining atrial fibrillation. *JACC Clin Electrophysiol*. 2018;4:124-134.
100. Honarbakhsh S, Schilling RJ, Providencia R, et al. Characterization of drivers maintaining atrial fibrillation: Correlation with markers of rapidity and organization on spectral analysis. *Heart Rhythm*. 2018;15:1296-1303.
101. Brooks AG, Stiles MK, Laborderie J, et al. Outcomes of long-standing persistent atrial fibrillation ablation: a systematic review. *Heart Rhythm*. 2010;7:835-846.

102. Anter E, McElderry TH, Contreras-Valdes FM, Li J, Tung P, Leshem E, Haffajee CI, Nakagawa H, Josephson ME. Evaluation of a novel high-resolution mapping technology for ablation of recurrent scar related atrial tachycardias. *Heart Rhythm*. 2016;13:2048–2055.
103. Anter E, Tschabrunn CM, Josephson ME. High-resolution mapping of scar-related atrial arrhythmias using smaller electrodes with closer interelectrode spacing. *Circ Arrhythm Electrophysiol*. 2015;8:537–545.
104. Pathik B, Lee G, Nalliah C, et al. Entrainment and high-density three-dimensional mapping in right atrial macroreentry provide critical complementary information: Entrainment may unmask “visual reentry” as passive. *Heart Rhythm* 2017; 14:1541-353 1549
105. Waldo AL. From bedside to bench: Entrainment and other stories. *Heart Rhythm* 2004;372 1:94-106
106. Linton NWF, Wilton SB, Scherr D, et al. A practical criterion for the rapid detection of single-loop and double-loop reentry tachycardias. *J Cardiovasc Electrophysiol* 2013;24:544–552.

## CURRICULUM VITAE ET STUDIORUM

### Personal information

**Family name:** Strisciuglio  
**First name:** Teresa

**Date and place of birth** September 21, 1987 –Naples, (Italy)

**Business address** Department of Advanced Biomedical Sciences,  
Section of Cardiology  
University of Naples “Federico II”  
S. Pansini 5, 80131, Naples, Italy  
Tel: 0039 0817462228  
Fax: 0039 081746228  
E-mail: [teresastri@hotmail.it](mailto:teresastri@hotmail.it)

**Residence address** Via Posillipo, 70  
80121, Naples, Italy  
Tel: 0039 081.415469  
Cell: 0039 3293238130

**Languages** Italian (mother tongue), English (written and spoken)

### Current position

Assistant Professor Division of Cardiology at the University of Naples Federico II

## Education

2006-2012	Medical School, University of Naples “Federico II”
July 2012	Doctor of Medicine, MD (Experimental thesis in Cardiology, University of Naples Federico II). Graduated with full marks with honors (110 /110 cum laude)
2013-2018	Residency in Cardiology at the University of Naples “Federico II” and trainee in: <ul style="list-style-type: none"><li>• Echocardiography Laboratory</li><li>• Catheterization Laboratory</li><li>• Electrophysiology Laboratory</li><li>• Intensive care unit and cardiology ward</li><li>• Cardiomyopathies, Heart failure, Hypertension, Valvular diseases Ambulatories</li></ul>

## Research and clinical appointments

2011-2013	Research activity in the Molecular Cardiology Laboratory of the Department of Advanced Biomedical Sciences, Division of Cardiology, at the University of Naples Federico II
2012-2013	Research activity in the Molecular Cardiology Laboratory (Supervisor Prof. A. Baldini) at the National Research Center (CNR) in Naples
2013-2018	Residency in Cardiology: Clinical research
2015-to date 2015-2018	Reviewer for Cardiovascular Translational Research Journal Sub-Investigator in the large multicentric trial POPular Genetics: Cost-effectiveness of CYP2C19 genotype guided treatment with antiplatelet drugs in patients with ST-segment-elevation myocardial infarction undergoing immediate percutaneous coronary intervention with stent implantation: optimization of treatment
2015-2016	Sub-Investigator in the large multicentric trial PARAGON-HF: Prospective comparison of ARni with Arb Global Outcomes in heart failure with preserved ejection fraction
Sep- Dec 2016	Research Fellow at the OLV Cardiovascular Center of Aalst, Belgium

2017- May 2019 Clinical and Research Fellow in Electrophysiology, Division of Cardiology, AZ Sint-Jan Bruges, Belgium

## Research

### Main Research Topics

- 1) Cardiac arrhythmias
- 2) Cardiac pacing

### Other topics

- a. Cardiovascular pathophysiology
- b. Platelets and anti-platelets therapy
- c. Endothelial dysfunction
- d. Genetic polymorphism in cardiovascular disease
- e. Atrial fibrillation
- f. Heart failure
- g. Percutaneous coronary intervention

### Membership of Scientific Societies

- Italian Society for Cardiology (SIC)
- European Society of Cardiology (ESC)
- European Heart Rhythm Association (EHRA)

### Grants and Awards

**2016** Co-proponent of the project "Influence of rs5065 atrial natriuretic peptide gene variant on preeclampsia" funded by the University of Naples Federico II

- 2016** Grant from the Short Term Mobility Programme funded by the University of Naples Federico II
- 2017** Grant from the STAR programme

### **Poster and oral communication**

Poster presentation at the European Society of Cardiology Congress 2015 (title: A loading dose of Aspirin plus Clopidogrel is able to offset platelet reactivity in CAD patients undergoing elective PCI carrying eNOS Glu298Asp polymorphism) at the European Society of Cardiology Congress 2015

Oral Communication at the Italian Society of Cardiology Congress 2015 (title: A Loading dose of Aspirin plus Clopidogrel is able to offset platelet reactivity in CAD patients undergoing elective PCI carrying eNOS Glu298Asp polymorphism)

Oral Communication at the Italian Society of Cardiology Congress 2015 (title: Intracoronary Adenosine Dose–Response Relationship With Hyperemia)

Oral Communication and travel grant at the Italian Society of Arterial Hypertension Congress 2015 (title: Relative difficulty of left ventricular hypertrophy regression during Antihypertensive treatment in a real-world context: The Campania Salute Network)

Oral Communication at the Italian Society of Arterial Hypertension Congress 2015 (title: A Loading dose of Aspirin plus Clopidogrel is able to offset platelet reactivity in CAD patients undergoing elective PCI carrying eNOS Glu298Asp polymorphism)

Oral Communication at the Italian Society of Cardiology Congress 2016 (title: Influence of the genetic variant rs5065 of the atrial natriuretic peptide on platelet reactivity after a loading dose of aspirin plus clopidogrel in patients undergoing elective PCI)

Oral Communication at the Italian Society of Arterial Hypertension Congress 2016 (title: Influence of the genetic variant rs5065 of the atrial natriuretic peptide on platelet reactivity after a loading dose of aspirin plus clopidogrel in patients undergoing elective PCI)

Poster at the Heart Rhythm Society's 38th Annual Scientific Sessions (HRS) ( title: Ablation Efficiency with Contact Force Stability and Ablation Index in Paroxysmal Atrial Fibrillation)

Poster at the EHRA EUROPACE-CARDIOSTIM 2017 ( title: Left atrial volume computed by three-dimensional rotational angiography best predicts atrial fibrillation recurrence after pulmonary vein isolation)

Poster at the Heart Rhythm Society's 39th Annual Scientific Sessions (HRS) ( title: Paroxysmal AF with high vs low arrhythmia burden: atrial remodeling and ablation outcome)

Best Poster award at the 12th Belgian Heart Rhythm Meeting 2018 (title: Clinical, echocardiographic and electro-anatomical determinants of the duration of paroxysmal AF episodes)

### Original Articles, Reviews, Editorials

1. **Strisciuglio T**, El Haddad M, Debonnaire P, De Pooter J, Demolder A, Wolf M, Philips T, Kyriakopoulou M, Almorad A, Knecht S, Tavernier R, Vandekerckhove Y, Duytschaever M. Paroxysmal atrial fibrillation with high vs. low arrhythmia burden: atrial remodelling and ablation outcome *Europace*. 2020 Aug 1;22(8):1189-1196.
2. Canciello G, Mancusi C, Izzo R, Morisco C, **Strisciuglio T**, Barbato E, Trimarco B, Luca N, de Simone G, Losi MA. Determinants of aortic root dilatation over time in patients with essential hypertension: The Campania Salute Network *Eur J Prev Cardiol*. 2020 Jun 12:2047487320931630
3. Stabile G, Lepillier A, De Ruvo E, Scaglione M, Anselmino M, Sebag F, Pecora D, Gallagher M, Rillo M, Viola G, Rossi L, De Santis V, Landolina M, Castro A, Grimaldi M, Badenco N, Del Greco M, De Simone A, Pisanò E, Abbey S, Lamberti F, Pani A, Zucchelli G, Sgarito G, Dugo D, Bertaglia E, **Strisciuglio T**, Solimene F. Reproducibility of Pulmonary Vein Isolation Guided by the Ablation Index: 1-year Outcome of the AIR Registry. *J Cardiovasc Electrophysiol*. 2020 May 5.
4. Kyriakopoulou M, Wielandts JY, **Strisciuglio T**, El Haddad M, Pooter J, Almorad A, Hilfiker G, Philips T, Unger P, Lycke M, Vandekerckhove Y, Tavernier R, Duytschaever M, Knecht S. Evaluation of Higher Power Delivery During RF Pulmonary Vein Isolation Using Optimized and Contiguous Lesions *J Cardiovasc Electrophysiol*. 2020 May;31(5):1091-1098.
5. **Strisciuglio T**, Ammirati G, Pergola V, Imparato L, Carella C, Koci E, Chiappetti R, Abbate FG, La Fazia VM, Viggiano A, Trimarco B, Rapacciuolo A. Contrast-induced nephropathy after cardiac resynchronization therapy implant impairs the recovery of ejection fraction in responders. *ESC Heart Fail*. 2019 Dec 12. doi: 10.1002/ehf2.12523.
6. Duytschaever M, De Pooter J, Demolder A, El Haddad M, Philips T, **Strisciuglio T**, Debonnaire P, Wolf M, Vandekerckhove Y, Knecht S, Tavernier R. [Long-term impact of catheter ablation on arrhythmia burden in low-risk patients with](#)

- [paroxysmal atrial fibrillation: the CLOSE to CURE study](#). Heart Rhythm. 2019 Nov 7. pii: S1547-5271(19)30997-X.
7. De Potter T, Hunter TD, Boo LM, Chatzikiyriakou S, **Strisciuglio T**, Silva E, Geelen P. [The industrialization of ablation: a highly standardized and reproducible workflow for radiofrequency ablation of atrial fibrillation](#). J Interv Card Electrophysiol. 2019 Oct 17.
  8. Wolf M, Tavernier R, Zeidan Z, El Haddad M, Vandekerckhove Y, Pooter J, Philips T, **Strisciuglio T**, Almorad A, Kyriakopoulou M, Lycke M, Duytschaever M, Knecht S. [Identification of repetitive atrial activation patterns in persistent atrial fibrillation by direct contact high-density electrogram mapping](#). J Cardiovasc Electrophysiol. 2019 Oct 6.
  9. Vandersickel N, Van Nieuwenhuysse E, Van Cleemput N, Goedgebeur J, El Haddad M, De Neve J, Demolder A, **Strisciuglio T**, Duytschaever M, Panfilov AV. [Directed Networks as a Novel Way to Describe and Analyze Cardiac Excitation: Directed Graph Mapping](#). Front Physiol. 2019 Sep 10;10:1138
  10. **Strisciuglio T**, Vandersickel N, Lorenzo G, Van Nieuwenhuysse E, El Haddad M, De Pooter J, Kyriakopoulou M, Almorad A, Lycke M, Vandekerckhove Y, Tavernier R, Duytschaever M, Knecht S. [Prospective evaluation of entrainment mapping as an adjunct to new-generation high-density activation mapping systems of left atrial tachycardias](#). Heart Rhythm. 2019 Sep 14. pii: S1547-5271(19)30835-5.
  11. Colaïori I, Izzo R, Barbato E, Franco D, Di Gioia G, Rapacciuolo A, Bartunek J, Mancusi C, Losi MA, **Strisciuglio T**, Manzi MV, de Simone G, Trimarco B, Morisco [Severity of Coronary Atherosclerosis and Risk of Diabetes Mellitus](#). C. J Clin Med. 2019 Jul 21;8(7).
  12. Andreozzi M, Giugliano FP, **Strisciuglio T**, Pirozzi E, Papparella A, Caprio AM, Miele E, Strisciuglio C, Perrone Filardi P. [The Role of Inflammation in the Endothelial Dysfunction in a Cohort of Pediatric Patients With Inflammatory Bowel Disease](#). J Pediatr Gastroenterol Nutr. 2019 Sep;69(3):330-335.
  13. Rapacciuolo A, Mancusi C, Canciello G, Izzo R, **Strisciuglio T**, de Luca N, Ammirati G, de Simone G, Trimarco B, Losi MA. [CHA<sub>2</sub>DS<sub>2</sub>-VASc score and left atrial volume dilatation synergistically predict incident atrial fibrillation in hypertension: an observational study from the Campania Salute Network registry](#).
    - a. Sci Rep. 2019 May 27;9(1):7888.



14. Kyriakopoulou M, **Strisciuglio T**, El Haddad M, De Pooter J, Almorad A, Van Beeumen K, Unger P, Vandekerckhove Y, Tavernier R, Duytschaever M, Knecht S. [Evaluation of a simple technique aiming at optimizing point-by-point isolation of the left pulmonary veins: a randomized study](#). *Europace*. 2019 May 5
15. De Pooter J, **Strisciuglio T**, El Haddad M, Wolf M, Philips T, Vandekerckhove Y, Tavernier R, Knecht S, Duytschaever M. [Pulmonary Vein Reconnection No Longer Occurs in the Majority of Patients After a Single Pulmonary Vein Isolation Procedure](#). *JACC Clin Electrophysiol*. 2019 Mar;5(3):295-305.
16. Wolf M, El Haddad M, De Wilde V, Philips T, De Pooter J, Almorad A, **Strisciuglio T**, Vandekerckhove Y, Tavernier R, Crijns HJ, Knecht S, Duytschaever M. [Endoscopic evaluation of the esophagus after catheter ablation of atrial fibrillation using contiguous and optimized radiofrequency applications](#). *Heart Rhythm*. 2019 Jul;16(7):1013-1020.
17. Stroobandt RX, Duytschaever MF, **Strisciuglio T**, Van Heuverswyn FE, Timmers L, De Pooter J, Knecht S, Vandekerckhove YR, Kucher A, Tavernier RH. [Failure to detect life-threatening arrhythmias in ICDs using single-chamber detection criteria](#). *Pacing Clin Electrophysiol*. 2019 Jun;42(6):583-594.
18. **Strisciuglio T**, Franco D, Di Gioia G, De Biase C, Morisco C, Trimarco B, Barbato E. [Impact of genetic polymorphisms on platelet function and response to anti platelet drugs](#). *Cardiovasc Diagn Ther*. 2018 Oct;8(5):610-620.
19. Anter E, Duytschaever M, Shen C, **Strisciuglio T**, Leshem E, Contreras-Valdes FM, Waks JW, Zimetbaum PJ, Kumar K, Spector PS, Lee A, Gerstenfeld EP, Nakar E, Bar-Tal M, Buxton AE. [Activation Mapping With Integration of Vector and Velocity Information Improves the Ability to Identify the Mechanism and Location of Complex Scar-Related Atrial Tachycardias](#). *Circ Arrhythm Electrophysiol*. 2018 Aug;11(8):e006536.
20. Fournier S, Toth GG, De Bruyne B, Johnson NP, Ciccarelli G, Xaplanteris P, Milkas A, **Strisciuglio T**, Bartunek J, Vanderheyden M, Wyffels E, Casselman F, Van Praet F, Stockman B, Degrieck I, Barbato E. [Six-Year Follow-Up of Fractional Flow Reserve-Guided Versus Angiography-Guided Coronary Artery Bypass Graft Surgery](#). *Circ Cardiovasc Interv*. 2018 Jun;11(6):e006368.

21. Xaplanteris P, Ntalianis A, De Bruyne B, **Strisciuglio T**, Pellicano M, Ciccarelli G, Milkas A, Barbato E. [Coronary lesion progression as assessed by fractional flow reserve \(FFR\) and angiography](#). EuroIntervention. 2018 Oct 20;14(8):907-914.
22. Fedida J, **Strisciuglio T**, Sohal M, Wolf M, Van Beeumen K, Neyrinck A, Taghji P, Lepiece C, Almorad A, Vandekerckhove Y, Tavernier R, Duytschaever M, Knecht S. [Efficacy of advanced pace-mapping technology for idiopathic premature ventricular complexes ablation](#). J Interv Card Electrophysiol. 2018 Apr;51(3):271-277.
23. Wolf M, El Haddad M, Fedida J, Taghji P, Van Beeumen K, **Strisciuglio T**, De Pooter J, Lepièce C, Vandekerckhove Y, Tavernier R, Duytschaever M, Knecht S. [Evaluation of left atrial linear ablation using contiguous and optimized radiofrequency lesions: the ALINE study](#). Europace. 2018 Nov 1;20(FI\_3):f401-f409
24. **Strisciuglio T**, Barbato E, De Biase C, Di Gioia G, Cotugno M, Stanzione R, Trimarco B, Sciarretta S, Volpe M, Wijns W, Delrue L, Rubattu S. [T2238C Atrial Natriuretic Peptide Gene Variant and the Response to Antiplatelet Therapy in Stable Ischemic Heart Disease Patients](#). J Cardiovasc Transl Res. 2018 Feb;11(1):36-41.
25. **Strisciuglio T**, Di Gioia G, Chatzikyriakou S, Silva Garcia E, Barbato E, Geelen P, De Potter T. [Left atrial volume computed by 3D rotational angiography best predicts atrial fibrillation recurrence after circumferential pulmonary vein isolation](#). Int J Cardiovasc Imaging. 2018 Mar;34(3):337-342.
26. Carnevale R, Pignatelli P, Frati G, Nocella C, Stanzione R, Pastori D, Marchitti S, Valenti V, Santulli M, Barbato E, **Strisciuglio T**, Schirone L, Vecchione C, Violi F, Volpe M, Rubattu S, Sciarretta S. C2238 ANP gene variant promotes increased platelet aggregation through the activation of Nox2 and the reduction of cAMP. Sci Rep. 2017 Jun 19;7(1):3797.
27. Di Gioia G, Scarsini R, **Strisciuglio T**, De Biase C, Zivelonghi C, Franco D, De Bruyne B, Ribichini F, Barbato E. Correlation between Angiographic and Physiologic Evaluation of Coronary Artery Narrowings in Patients With Aortic Valve Stenosis. Am J Cardiol. 2017 Jul 1;120(1):106-110.
28. **Strisciuglio T**, Di Gioia G, Mangiacapra F, De Biase C, Delrue L, Pellicano M, Bartunek J, Vanderheyden M, Izzo R, Trimarco B, Wijns W, Barbato E. Platelet reactivity in patients carrying the e-NOS G894T polymorphism after a loading dose of aspirin plus clopidogrel. Thromb Res. 2017 Mar;151:72-73.

29. **Strisciuglio T**, Barbato E. The fractional flow reserve gray zone has never been so narrow. *J Thorac Dis.* 2016 Nov;8(11):E1537-E1539.
30. **Strisciuglio T**, Barbato E. Rotational atherectomy: you will never regret using it but you often regret not having used it! *EuroIntervention.* 2016 Dec 20;12(12):1441-1442.
31. Ferrara A, Di Gioia G, **Strisciuglio T**, Wijns W, Barbato E. Overview of the clinical trials on bioresorbable vascular scaffold. *Minerva Cardioangiol.* 2016 Aug;64(4):473-80. PMID: 27195662
32. Losi MA, Izzo R, Canciello G, Giamundo A, Manzi MV, **Strisciuglio T**, Stabile E, De Luca N, de Simone G, Trimarco B. Atrial Dilatation Development in Hypertensive Treated Patients: The Campania-Salute Network. *Am J Hypertens.* 2016 May 11.
33. Giamundo A, Canciello G, Rapacciuolo A, Musella F, Savarese G, **Strisciuglio T**, Stabile E, Izzo R, Trimarco B, Losi MA. *Int J Cardiol.* Comparison of linear versus cubic assessment of left atrial size in the prediction of atrial fibrillation development in hypertrophic cardiomyopathy. *Int J Cardiol.* 2016 Jun 1;212:198-200.
34. Losi MA, **Strisciuglio T**, Stabile E, Castellano G, de Amicis V, Saccenti A, Maresca G, Santoro C, Izzo R, Barbato E, Esposito G, Trimarco B, Rapacciuolo A. Iatrogenic atrial septal defect (iASD) after MitraClip system delivery: The key role of PaO<sub>2</sub>/FiO<sub>2</sub> ratio in guiding post-procedural iASD closure. *Int J Cardiol.* 2015 Oct 15;197:85-6.
35. **Strisciuglio T**, Di Gioia G, De Biase C, Esposito M, Franco D, Trimarco B, Barbato E. Genetically Determined Platelet Reactivity and Related Clinical Implications. *High Blood Press Cardiovasc Prev.* 2015 Sep;22(3):257-64.
36. Galasso G, De Servi S, Savonitto S, **Strisciuglio T**, Piccolo R, Morici N, Murena E, Cavallini C, Petronio AS, Piscione F. Effect of an invasive strategy on outcome in patients  $\geq 75$  years of age with non-ST-elevation acute coronary syndrome. *Am J Cardiol.* 2015 Mar 1;115(5):576-80.
37. Piccolo R, Niglio T, Spinelli L, Capuano E, **Strisciuglio T**, D'Anna C, De Luca S, Leosco D, Rapacciuolo A, Cirillo P, Stabile E, Esposito G, Trimarco B, Piscione F, Galasso G. Reperfusion correlates and clinical outcomes of right ventricular dysfunction in patients with inferior ST-segment elevation myocardial infarction undergoing percutaneous coronary intervention. *Am J Cardiol.* 2014 Jul 15;114(2):243-9.

38. **Strisciuglio T**, De Luca S, Capuano E, Luciano R, Niglio T, Trimarco B, Galasso G. Endothelial dysfunction: its clinical value and methods of assessment. *Curr Atheroscler Rep*. 2014 Jun;16(6):417.
39. Niglio T, Galasso G, Piccolo R, Di Gioia G, **Strisciuglio T**, Esposito G, Trimarco B, Piscione F. New perspectives for transcatheter aortic valve implantation: more than a "simple" alternative to surgery. *Minerva Cardioangiol*. 2014 Apr;62(2):193-203. Review.
40. **Strisciuglio T**, Galasso G, Leosco D, De Rosa R, Di Gioia G, Parisi V, De Luca S, Niglio T, De Biase C, Luciano R, Rengo G, Trimarco B, Piscione F. Adipokines and coronary artery disease. *Monaldi Arch Chest Dis*. 2012 Sep;78(3):120-8.
41. Piccolo R, Niglio T, Di Gioia G, D'Anna C, De Rosa R, **Strisciuglio T**, Trimarco B, Piscione F, Galasso G. Adenosine-induced torsade de pointes complicating a fractional flow reserve measurement in a right coronary artery intermediate stenosis. *Cardiovasc Revasc Med*. 2013 Mar-Apr;14(2):118-20.
42. Galasso G, De Rosa R, Ciccarelli M, Sorriento D, Del Giudice C, **Strisciuglio T**, De Biase C, Luciano R, Piccolo R, Pierri A, Di Gioia G, Prevete N, Trimarco B, Piscione F, Iaccarino G.  $\beta$ 2-Adrenergic receptor stimulation improves endothelial progenitor cell-mediated ischemic neoangiogenesis. *Circ Res*. 2013 Mar 29;112(7):1026-34.
43. Di Gioia G, Piccolo R, Niglio T, D'Anna C, De Rosa R, **Strisciuglio T**, Galasso G, Piscione F, Trimarco B. Mortality reduction with transradial approach in patients with ST-segment elevation myocardial infarction: is the randomized evidence conclusive? *Int J Cardiol*. 2013 Sep 30;168(2):1578-9.
44. Galasso G, Schiekofer S, D'Anna C, Gioia GD, Piccolo R, Niglio T, Rosa RD, **Strisciuglio T**, Cirillo P, Piscione F, Trimarco B. No-reflow phenomenon: pathophysiology, diagnosis, prevention, and treatment. A review of the current literature and future perspectives. *Angiology*. 2014 Mar;65(3):180-9.
45. Piccolo R, Di Gioia G, Niglio T, D'Anna C, De Rosa R, **Strisciuglio T**, Bevilacqua M, Piscione F, Cirillo P, Galasso G. Pharmacotherapeutic considerations for the use of prasugrel and ticagrelor to reduce stent thrombosis in patients with acute coronary syndrome. *Angiology*. 2014 Feb;65(2):130-6.